



UNIVERSITA' DEGLI STUDI DI PADOVA
DIPARTIMENTO DI PEDIATRIA

SCUOLA DI DOTTORATO DI RICERCA IN
MEDICINA DELLO SVILUPPO E SCIENZE DELLA
PROGRAMMAZIONE
INDIRIZZO: MALATTIE RARE
XXII CICLO

TESI DI DOTTORATO

**AMNIOTIC FLUID STEM CELLS AND KIDNEY
REGENERATION**

Direttore della Scuola: Ch.mo Prof. GIUSEPPE BASSO

Coordinatore d'indirizzo: Ch.mo Prof. GIORGIO PERILONGO

Supervisore: Ch.mo Prof. PIERGIORGIO GAMBA

Dottorando: STEFANO GIULIANI

*Alla mia famiglia per l'amore costante sempre dimostratomi...
A Laura Perin per l'amicizia, la grande passione per la ricerca e
l'insegnamento*

INDEX

ABSTRACT	9
ABSTRACT IN ITALIAN	11
INTRODUCTION:	19
1. ESRD, causes and outcomes	19
• Acute Kidney Disease Therapy	
• Chronic Kidney Disease Therapy	
2. Regenerative Medicine and Kidney regeneration	33
• Tissue Engineering for Kidney regeneration	
• Stem Cells:	
▪ <i>Embryonic Stem Cells</i>	
▪ <i>Primordial Germ Cells</i>	
▪ <i>Adult Stem Cells</i>	
▪ <i>Somatic Cell Nuclear Transfer</i>	
• Stem Cells and Kidney Regeneration	
3. Amniotic Fluid: Stem Cells and Progenitors	39
OBJECTIVES	41
MATERIALS AND METHODS	43
1. Expansion of human Amniotic Fluid Total Cell Population	43
2. Characterization of Amniotic Fluid Cells	43
• Analysis and characterization by RT-PCR	
• Analysis and characterization by Real Time PCR	
• Analysis and characterization by Western Blotting	
3. Ex Vivo whole embryonic kidney culture	53
4. Selection of Amniotic Fluid Stem Cells (AFSC)	55
5. In vitro model for the renal differentiation of hAFSC	56
• Microinjection of hAFSC and co-culture	
• Live Imaging	
• Histology, Chromogenic in situ hybridization	
• Reverse transcriptase-polymerase chain reaction	
6. In vivo experiment with a model of Acute Tubular Necrosis	59
• ATN induction and injection of hAFSC	

- Tissue processing
- Labeling of the AFSC with luciferase and bioluminescence
- Immunostaining
- Blood collection, creatinine and BUN measurement
- Morphological studies
- Cytokine analysis

7. Selection and characterization of Metanephric Mesenchyme Derived Cells (MMDC) and Kidney Progenitor Cells (AKPC) from the whole Amniotic Fluid: 66

- Immunoseparation from whole Amniotic Fluid
- Analysis and characterization by RT-PCR
- Analysis and characterization by Real Time PCR

RESULTS 69

1. Characterization of Amniotic Fluid cells by expression of markers for the three germ layers and progenitor cells 69

- Amniotic Fluid Total Cell Population Culture
- Analysis and characterization by RT-PCR
- Analysis and characterization by Western Blotting
- Analysis and characterization by Real Time PCR

2. Long term ex-vivo whole embryonic kidney culture 72

3. Selection of Amniotic Fluid Stem Cells 73

4. In vitro renal differentiation of hAFSC 74

- Ureteric Bud induces hAFSC to form tubular structures
- Evidence of hAFSC integration into embryonic kidneys
- Molecular evidence of primordial kidney differentiation

5. Protective effect of hAFSC in Acute Tubular Necrosis 76

- Acute Tubulonecrosis mouse model
- Histology, Period Acid Schiff staining (PAS), TUNEL
- In vivo detection of hAFSC by bioluminescence
- Detection of hAFSC by immunohistochemistry and gene expression
- Creatinine and Blood Urea Nitrogen (BUN) measurements
- Morphological studies
- Immuno-Cytokine characterization

6. Selection and characterization of Metanephric Mesenchyme derived cells (MMDC) and Kidney Progenitor cells (AKPC) from the whole Amniotic Fluid	80
• Immunoseparation from the whole Amniotic Fluid	
• Analysis and characterization by RT-PCR	
• Analysis and characterization by Real Time PCR	
DISCUSSION	83
1. hAFSC differentiation in renal parenchyma in vitro and in vivo	88
2. Characterization and isolation of Metanephric Mesenchyme Derived cells (MMDC) and Amniotic Fluid Kidney Progenitor Cells (AKPC)	96
CONCLUSIONS	109
REFERENCES	113
FIGURES AND TABLES	125

ABSTRACT

Acute Kidney Disease (CKD) is a major public health problem that affects some 3-7% of patients admitted to the hospital and approximately 25-30% of patients in the intensive care unit. None of the existing therapies are exempt from side effects and kidney physiological functionality is never restored. Transplantation has been reported as the preferred cure for CKD management but organ shortage and risks due to the immunosuppressive therapy makes it far from being the perfect treatment for ESRD. In this study we have focused our attention on finding novel strategies, in vitro and in vivo, to obtain kidney regeneration in case of acute and chronic kidney damage.

First we have demonstrated the ability of hAFSCs to survive, proliferate and integrate into the embryonic kidney, while it undergoes organ development, in an in vitro culture system. We observed the presence of hAFSCs within kidney primordial, including tubules and developing nephrons. Thus, hAFSCs seem to have the capacity to undergo the expected mesenchymal to epithelial transition that occurs in normal renal development and are induced to express important early kidney markers such as GDNF, ZO-1 and Claudin. Moreover, hAFSCs do not appear to require prior genetic modification or exogenous production of kidney proteins for their differentiation to occur. This is a very important advantage that hAFSCs have for potential future regenerative or bioengineering application.

With the in vivo experiments, we have demonstrated that early direct injection of hAFSCs into the kidney strongly ameliorates ATN injury as reflected by more rapid resolution of tubular structural damage and by normalization of creatinine and BUN levels. In addition, our data show evidence of immunomodulatory and antiinflammatory effect of hAFSCs, at an early time point, comparable in magnitude to endogenous cytokine production. Understanding how donor and host cells combine to attenuate

tubular damage may lead eventually to the application of hAFSCs for therapeutic purposes in acute kidney diseases.

Nonetheless, beside the presence of a small number (1%) of cells with pluripotent characteristics, the composition of the other 99% of Amniotic Fluid cells is diverse, with a great amount of cells exhibiting commitment to a defined germ line or cellular endpoint.

There seems to be clear evidence for the existence of progenitor cells in Amniotic Fluid, which can give rise to different cell types of mature organs. By 17 weeks of gestation is notable an increase tissue specific cellular presence and this data may indicate that the choice of the time point for cell selection is fundamental. In addition, we demonstrated in the amniotic fluid, the presence of a renal population with specific traits of commitment. In particular, the presence of podocytes at both undifferentiated and almost mature stages could favour their use for kidney regeneration *in vitro* and *in vivo* animal models. The presence and identification of specific renal progenitor cells in the Amniotic Fluid, committed to different compartments of the kidney environment, could represent a valuable new tool for regenerative purposes with regards to the treatment of a broad range of renal diseases.

The discovery of renal specific progenitor cells within Amniotic Fluid could bring a breakthrough in the study for novel and more selective approaches in the renal therapy. However, the real pluripotential capability of these progenitors cells, in particular the kidney progenitors presenting more differentiation characteristics, has to be established. Moreover, their potential for survival, proliferation, integration, and differentiation needs to be assessed in *in vivo* models involving different types of renal damage.

ABSTRACT IN ITALIAN

L'insufficienza renale terminale ha raggiunto ormai proporzioni epidemiche in tutto il mondo e, tutt'oggi, non sono ancora state trovate terapie sostitutive o rigenerative efficaci a lungo termine. Attualmente la terapia dialitica e il trapianto allogenico rimangono le uniche alternative valide da utilizzare in questi pazienti nonostante se ne conoscano i numerosi limiti e complicanze. Recenti dati epidemiologici, in America e in Europa, mostrano che l'insufficienza renale colpisce circa l'8% della popolazione. [1] L'aumentata domanda di organi, in aggiunta all'insufficiente disponibilità di donatori, sta spingendo sempre più i ricercatori di tutto il mondo a sviluppare nuove alternative terapeutiche per la sostituzione dei reni non funzionanti. [2] La creazione di organi bio-artificiali, attraverso l'utilizzo delle tecniche di ingegneria tissutale, ha finora dimostrato grandi difficoltà specialmente nel riprodurre quegli organi e tessuti la cui struttura e funzione risultino particolarmente complesse, come nel caso dei reni. Storicamente gli ingegneri tissutali che si sono cimentati in questo campo hanno potuto utilizzare esclusivamente linee cellulari adulte dando origine a costrutti bidimensionali caratterizzati da limitata funzione e difficile applicabilità *in vivo*. [3]

Nell'ultima decade le cellule staminali stanno ricevendo sempre maggiore attenzione scientifica grazie al loro crescente impiego nella medicina rigenerativa per la ricostruzione e rigenerazione di tessuti bio-artificiali ed organi. Le cellule Staminali Embrionali (SE), derivate dalla blastocisti, hanno come caratteristiche peculiari il fatto che si replicano ampiamente e che siano capaci di formare aggregati (corpi embrioidi) che possono dar luogo ad una varietà di cellule specializzate come, ad esempio, cellule neurali, cardiache e pancreatiche. [3, 4] Il reclutamento di questo tipo di cellule staminali, tuttavia, comporta la distruzione di embrioni umani creando spinosi problemi etici e morali che portano, in molti Paesi, a vietarne l'utilizzo e il progresso scientifico. Per evitare questo tipo di controversie ricercatori di varie discipline hanno identificato potenziali fonti

di cellule staminali alternative. [4, 5] E' ormai ben noto che in molti tessuti adulti esistono cellule progenitrici con il compito di rigenerare o riparare l'organo a seguito dei fisiologici processi di senescenza o in caso di danno. [6, 7] Ci sono sempre piu' evidenze che questi progenitori d'organo abbiano caratteristiche di plasticità piu' elevate di quanto si pensasse originariamente. Parallelamente molti ricercatori credono che la rigenerazione di organi adulti derivi principalmente dalla mobilitazione di cellule staminali provenienti dal midollo osseo. E' stato dimostrato che cellule staminali del midollo osseo possono attraversare la barriera endoteliale e dar luogo a differenti linee cellulari differenziate, trasformando cellule circolanti in fegato, cervello, pancreas, pelle, intestino e anche rene. [27, 29]

Il liquido amniotico e' stato usato per anni come uno strumento sicuro e valido per la ricerca di malattie genetiche e congenite del feto. Tuttavia, il liquido amniotico contiene un grande numero di cellule progenitrici che possono avere un importante ruolo nelle applicazioni della bioingegneria tissutale. Streubel et al. [8] hanno riportato l'utilizzo di cellule non emopoietiche per la conversione di amniociti in miociti. Recentemente una popolazione di cellule staminali c-Kit⁺, isolate nel liquido amniotico umano e murino, e' stata caratterizzata e differenziata in tessuti originati dai tre foglietti embrionali: muscolare, neuronale, adipocitario, epatico, osseo ed endoteliale [9]

Nel laboratorio diretto dal dr. R.E. De Filippo, Assistant Professor presso il Childrens Hospital di Los Angeles, abbiamo ampiamente studiato e utilizzato questa nuova popolazione di cellule staminali derivate dal liquido amniotico focalizzando le nostre ricerche sul loro utilizzo nella rigenerazione renale. Abbiamo dimostrato che questa popolazione totipotente di cellule mesenchimali e' capace di riprodurre alcune tappe essenziali della nefrogenesi dopo essere state iniettate in reni embrionali. Tuttavia, le cellule staminali da liquido amniotico rappresentano meno dell'1% dell'intera popolazione cellulare e forse esistono altri progenitori cellulari, nel liquido stesso, gia' orientati e piu' pronti alla differenziazione di

particolari linee cellulari renali che possano essere utilizzate per gli stessi scopi rigenerativi ma con risultati migliori.

Il volume e la composizione del liquido amniotico cambia durante la gravidanza e dall'ottava settimana di gestazione i reni fetali iniziano a produrre liquido che rapidamente aumenta di volume durante il secondo trimestre. [10] Il contatto tra il liquido amniotico e i diversi tessuti fetali sembra giustificare la presenza dei differenti tipi cellulari disciolti nel liquido stesso. La presenza di cellule mature derivanti dai tre foglietti germinali e' stata gia' dimostrata in passato come pure la presenza di progenitori cellulari di origine mesenchimale ed emopoietica prima della 12^{ma} settimana gestazionale nell'uomo. [11,12,13] Cellule esprimenti proteine e markers genetici tipici di tessuti diversi come cervello, cuore, e pancreas sono state ritrovate nel liquido amniotico ma ulteriori indagini sono necessarie per completare la caratterizzazione dei diversi tipi cellulari presenti alle diverse eta' gestazionali. [14, 15, 16]

Lo sviluppo renale e' un complesso processo di attivazione genica, interazioni cellulari ed extracellulari che devono aver luogo secondo un ordine spazio-temporale preciso e nella quantita' adeguata. Durante l'embriogenesi, il rene metanefrico origina dall'invasione da parte della gemma ureterale, derivata dal dotto epiteliale di Wolffian, nel mesenchima metanefrico. [17] La gemma ureterale inizia la sua arborizzazione all'interno del mesenchima e portera' alla formazione dell'intero sistema escretore, dall'uretere ai dotti collettori, mentre il mesenchima metanefrico dara' luogo alle strutture epiteliali costituenti i nefroni (dal tubulo distale alla capsula di Bowman). CD-24 e Caderina 11 sono due markers di superficie che vengono usati per identificare cellule staminali ancora indifferenziate ma presenti nel mesenchima metanefrico prima di ricevere l'induzione da parte della gemma ureterale. [18] In aggiunta, altri markers di superficie che identificano una sottopopolazione di cellule appartenenti al mesenchima metanefrico nei vari stadi dell'induzione verso la nefrogenesi sono stati recentemente descritti in letteratura: Caderine E, PDGFR α , PDGFR β , e NGFR ad alta affinita'. [19]

Cellule Staminali derivate da liquido amniotico e differenziazione renale in vitro e in vivo

Negli ultimi sette anni il gruppo di ricerca di cui ho fatto parte per due anni negli Stati Uniti (University of Southern California - Childrens Hospital Los Angeles) sta studiando una popolazione di cellule staminali ricavate da liquido amniotico (Amniotic Fluid Stem Cells, AFSC), umano e murino. Caratteristiche peculiari di questa popolazione cellulare sono: l'espressione di geni e marcatori di superficie comuni a cellule staminali di origine embrionale e mesenchimale; propagazione *in vitro* senza necessita' di feeder-layer; mantenimento della lunghezza dei telomeri; capacit  di differenziarsi *in vitro* e *in vivo* in molti tipi differenti di cellule e tessuti provenienti da tutti e tre i foglietti embrionali. [7] In particolare, negli ultimi 4 anni, il nostro gruppo si e' concentrato sull'utilizzo di questa particolare popolazione di cellule staminali derivate da liquido amniotico nella rigenerazione renale *in vitro* e *in vivo*. [20, 21]

Brevemente, siamo stati in grado di dimostrare, basandoci su un sistema *in vitro*, come le hAFSC abbiano la capacit  di differenziarsi in parenchima renale dopo iniezione diretta in reni embrionici (12.5-16 giorni di gestazione) coltivati in vitro fino a 10 giorni. Le cellule staminali da liquido amniotico erano state precedentemente transfettate con il gene codificante una proteina fluorescente verde (GFP) e un secondo gene codificante per il Lac-Z. Mediante queste transfezioni siamo stati in grado di distinguere le cellule iniettate e dopo aver coltivato gli organi, anche a lungo termine (10 giorni), e' stato possibile dimostrare la loro integrazione ed assimilazione nelle differenti tappe dello sviluppo renale. Analisi istologica dei reni iniettati con le staminali ha rivelato quanto questa popolazione di cellule sia capace di contribuire alle strutture primordiali del rene a partire dalla vescicola renale fino alle ultime fasi della nefrogenesi (tubuli e glomeruli). Mediante RT-PCR abbiamo quindi dimostrato la neoespressione, da parte delle AFSC iniettate, di geni attivi nelle diverse fasi dello sviluppo embrionale del nefrone. [20]

Dopo aver dimostrato questa abilit  di integrazione nel tessuto renale in via di sviluppo e la compartecipazione a tutte le tappe utili alla formazione

del nefrone maturo *in vitro*, la nostra idea e' stata quella di procedere all'applicazione *in vivo* delle cellule staminali da liquido amniotico. L'obiettivo e' stato quello di dimostrare la loro reale capacita' di sopravvivere, replicarsi ed integrarsi attivamente nei reni danneggiati di un modello di topo immunodepresso. Cellule staminali da liquido amniotico di topo (mouse Amniotic Fluid Stem Cells, mAFSC), esperimenti Lac-z e Luciferasi come marcatori, sono quindi state iniettate per via endovenosa (vena della coda) in un modello di topi immunodepressi con tubulonecrosi acuta. Il nostro ultimo obiettivo e' stato quello di dimostrare se le cellule staminali venissero utilizzate dai reni danneggiati per riparare il danno e quindi fossero in grado di velocizzare la ripresa funzionale dell'organo. I risultati di tali esperimenti hanno dimostrato che le AFSC hanno una buona capacita', anche *in vivo*, di integrarsi e partecipare attivamente alla riparazione del danno. Esse hanno iniziato ad esprimere GDNF, un fattore di trascrizione precoce presente nello sviluppo renale e in particolare nella formazione tubulare e glomerulare, e diversi altri markers tubulari quali Acquaporina-2, Agglutinina P, Agglutinina DB.

Dagli esperimenti *in vivo* e' quindi emerso che la popolazione di cellule staminali totipotenti, derivata da liquido amniotico (hAFSC), e' capace di differenziarsi in diversi tipi cellulari appartenenti sia a strutture glomerulari (capsula di Bowman) che tubulari (tubulo distale e prossimale) senza dimostrare una chiara specificita' per una delle due strutture. [9] In accordo con recenti pubblicazioni, abbiamo dimostrato un effetto immunomodulatorio delle cellule staminali. Lo studio approfondito delle citochine, endogene ed esogene (prodotte dalle hAFSC iniettate), e il loro effetto nel migliorare la porzione infiammatoria del danno renale sono il passo successivo delle nostre ricerche.

Un limite potenziale all'utilizzo terapeutico di questa popolazione cellulare totipotente risiede nel fatto che la maggior parte delle malattie renali che portano ad insufficienza renale terminale, colpiscono primariamente le strutture tubulari o quelle glomerulari, ma difficilmente entrambe contemporaneamente. Utilizzando dunque cellule staminali troppo indifferenziate, e quindi totipotenti, si rischierebbe di perdere efficacia

terapeutica a causa del fatto che esse riceverebbero troppi segnali contemporaneamente in senso differenziativo e sarebbero indotte a seguire patterns riparativi non mirati e meno efficaci nella riparazione del danno principale. Se infatti avessimo bisogno di trattare selettivamente un danno tubulare piuttosto che uno glomerulare, l'utilizzo di cellule staminali totipotenti non sarebbe così ottimale come invece l'utilizzo di progenitori tubulo specifici opportunamente espansi ed eventualmente modificati. Questo concetto insieme al fatto che il liquido amniotico è composto da differenti popolazioni cellulari ha spinto a considerare la possibilità che ci possano essere linee cellulari maggiormente orientate in senso renale (progenitori organo specifici) che possano essere utilizzate in modo più vantaggioso per la rigenerazione di strutture renali specifiche (id. cellule tubulari prossimali o distali, podociti, cellule mesangiali, cellule endoteliali e altro)

Caratterizzazione cellulare del liquido amniotico e ricerca di progenitori renali specifici o già parzialmente differenziati

L'ultima parte della tesi si è concentrata nello studiare ed identificare le varie popolazioni cellulari presenti nel liquido amniotico a diverse settimane di gestazione. I campioni, di età compresa tra le 15 e le 20 settimane di gestazione, sono stati ottenuti tramite amniocentesi, tecnica usata per studiare il cariotipo del feto durante lo sviluppo. Sono stati valutati differenti terreni di coltura, indagando proliferazione e conservazione della morfologia nei campioni ottenuti. L'analisi e la caratterizzazione della popolazione totale presente nel liquido amniotico è stata effettuata utilizzando RT-PCR, Real Time PCR e Western Blotting, analizzando l'espressione specifica di geni che sono coinvolti nel mantenimento della pluripotenzialità, geni che identificano specificamente i tre foglietti embrionali ed infine geni che identificano progenitori organo-specifici. Sono state inoltre identificate popolazioni specifiche renali, tramite immunoseparazione con biglie magnetiche (MASC). L'espressione di marcatori per i foglietti embrionali endoderma e mesoderma è più alta in campioni più giovani rispetto a campioni con

tempo di gestazione maggiore mentre, per l'ectoderma, rimane pressoché invariata nel tempo. La presenza di cellule pluripotenti è costante così come le cellule staminali mesenchimali mentre le cellule progenitrici ematopoietiche, investigate tramite CD34, fanno la loro comparsa successivamente alle 17 settimane di gestazione.

La presenza di progenitori tessuto specifici già "committed" è evidente nei campioni di gestazione più avanzata sia per quantità che per specificità dell'organo preso in esame.

È stata approfondita l'analisi di cellule progenitrici renali, utilizzando un ampio pannello di marcatori che identificano sia la componente tubulare che quella glomerulare del nefrone, struttura fondamentale per la filtrazione renale. I risultati ottenuti confermano la presenza di cellule progenitrici renali dopo le 18 settimane di gestazione.

È stata identificata e studiata una popolazione esprimente CD24 e Cadherin 11 isolata da campioni di liquido amniotico di 18 o più settimane. CD24 e OB-cadherin sono stati identificati nel topo come co-espressi *in vivo* nel mesenchima metanefrico. Dal mesenchima metanefrico ha origine il nefrone ed è una delle due strutture embrionali fondamentali per lo sviluppo del rene. Da questa popolazione principale sono state ottenute 4 nuove sottopopolazioni che identificano sottocompartimenti del glomerulo, come per esempio le cellule corticali stromogeniche (tramite selezione per la Tyrosin Kinase, TrKA), i podociti (selezionati per la Nefrina), le cellule del mesangio (con selezione positiva per PDGFR Alpha) e le cellule in transizione mesenchima-epitelio (con selezione per la Cadherina-E). Tramite PCR e Real Time PCR è stata dimostrata la forte specificità di ogni singola linea cellulare.

È necessario uno studio approfondito che preveda per le AKPC differenziazioni *in vitro* ed *in vivo*, utilizzando fattori di crescita nefro-specifici e diversi modelli di danno renale acuto e cronico, in modo tale da confermare la loro possibile completa differenziazione in cellule renali mature.

Un approfondimento sul meccanismo d'azione e sulle migliori tempistiche di somministrazione, infine, sono i punti fondamentali da chiarire per comprendere il meccanismo d'azione delle hAFSC *in vivo*.

Queste ricerche sono una base fondamentale per future applicazioni cliniche in pazienti che soffrono di nefropatie acute e croniche.

INTRODUCTION

1. ESRD, causes and outcomes

End Stage Renal Disease (ESRD) is a condition of chronic and progressive injury of the kidney, leading to a complete failure of the renal system. ESRD usually occurs when renal functionality is less than 10% of normal activity [1].

According to the 2007 US renal data system, the number of United States patients in treatment for ESRD was 400.000, with more than 20.000 waiting for organ transplantation. Predictions for the year 2020 are showing an increase in patients undergoing dialysis and in need of kidney replacement.

Progression to ESRD can be simplified within two major processes known as Acute Kidney Failure and Chronic Kidney Disease.

Acute Kidney Failure (AKF) is characterized by sudden and fast kidney function deterioration. Pathological kidney functionality is characterized by a decrease in filtration rate, starting from previously called pre-renal acute kidney injury and up to unresponsiveness. In the acute setting, the two most significant threats to renal perfusion pressure are systemic arterial hypotension and increased intra-abdominal pressure and about 4% of all critically ill patients with acute kidney injury will require dialysis. Kidney stones, infections, cancer or drugs intoxication can be causes for AKF [2-3].

Chronic Kidney Disease (CKD) is recognized as a major health problem affecting approximately 13% of the United States population. Numbers of prevalent CKD patients will continue to rise, reflecting the growing elderly population [4].

CKD is defined as the presence of kidney damage, manifested by abnormal albumin excretion or decreased kidney function that persists for more than 3 months.

Typically, kidney function is quantified by glomerular filtration rate (GFR). The glomerular filtration rate (GFR) is the rate at which an ultrafiltrate of

plasma is produced by glomeruli per unit of time. It is the best estimate of the number of functioning nephrons or functional renal mass. To obtain the GFR it's required to measure the renal clearance of molecules with a steady blood concentration, in order to minimize errors in the evaluation. In the current clinical practice GFR value is established considering many factors such as age, weight, race and most frequently estimated using equations that incorporate serum creatinine along with demographic data [5].

To facilitate assessment of CKD severity, the National Kidney Foundation developed criteria as part of its Kidney Disease Outcomes Quality Initiative (NKF K/DOQI) to stratify CKD patients:

- Stage 1: normal eGFR ≥ 90 mL/min per 1.73 m² and persistent albuminuria
- Stage 2: eGFR between 60 to 89 mL/min per 1.73 m²
- Stage 3: eGFR between 30 to 59 mL/min per 1.73 m²
- Stage 4: eGFR between 15 to 29 mL/min per 1.73 m²
- Stage 5: eGFR < 15 mL/min per 1.73 m² or end-stage renal disease

The prevalence of these stages of CKD in the United States population is as follows: 1.8% for stage 1, 3.2% for stage 2, 7.7% for stage 3, and 0.35 % for stages 4 and 5. Patients with stage 3 or 4 disease progress to End-Stage Renal Disease or stage 5 at a rate of 1.5% per year. Stage 1 or 2 CKD patients progress to more advanced stages at approximately 0.5% per year [6].

The early stages of CKD (stages 1 and 2) are manifested by kidney damage and are generally asymptomatic: the kidney functions normally but the risk for progressive disease is significant.

As kidney disease worsens, renal function begins to deteriorate (stages 3 and 4 CKD). Eventually, kidney failure (stage 5) occurs and kidney replacement therapy is required [7].

Common origins for CKD are pathologies affecting the kidney compartment like analgesic nephropathy, glomerulonephritis, kidney

stones, obstructive uropathy and reflux nephropathy, lupus, and polycystic kidney disease, genetic malformations or diseases affecting other organs like diabetes and hypertension [8].

Nearly 45% of incident kidney failure is attributed to diabetes and another 20% is attributed to chronic hypertension. More than 10 million Americans are diabetic and 40 to 50 million American adults have hypertension, constituting an enormous at-risk population for kidney disease [9].

Complications derived from CKD are various. In chronic renal failure the loss of function is usually coupled with an increase of fibrosis, amyloid deposition and glomeruli destruction. Major sequelae of CKD include continued progression of CKD and development of kidney failure requiring kidney replacement therapy, development and/or progression of cardiovascular disease, anemia, and bone disease.

Acute Kidney Disease Therapy

Acute renal failure can be treated by inhibiting injury or enhancing repair, or the injury process itself managed by treating the metabolic consequences of acute renal failure [10-13]. These consequences include volume overload, solute overload (hyperkalemia acidosis, uremia, cytokines), endocrine deficiencies (erythropoietin), and the non-renal complications, including sepsis, gastrointestinal (GI) bleeding, delirium, and respiratory failure. The current treatment for ARF is empirical, that is, agents are used indiscriminately without regard to underlying etiology, with the hope that these agents will influence the course of acute renal failure [14]. At the present time, more often than not this hope remains unfulfilled. Many agents are effective in animal models; however, most of these agents are effective only if started before injury. Since clinicians are generally not present at the time of injury, it is important that any pharmaceutical agents are effective when started after the injury has occurred [15-18].

Diuretics and mannitol (hemodynamic paradigm)

Furosemide is a loop diuretic and a vasodilator; it may decrease the metabolic work of the thick ascending limb and may flush obstructing casts from the nephron. In addition, furosemide may decrease the concentration of toxins such as myoglobin or hemoglobin in the tubules. Based on the hemodynamic paradigm, furosemide should prevent ARF. In normal patients, furosemide does cause a large diuresis. In some patients with ARF, furosemide may convert oliguric ARF to non-oliguric ARF. However, there is no solid evidence that furosemide alters the natural history of human acute renal failure. The single randomized controlled trial did not show any change in azotemia or mortality. Indeed, furosemide may worsen radiocontrast-induced acute renal failure [19]. Conversion of oliguric ARF to non-oliguric ARF simplifies the patient management because the patient can receive a more liberal fluid intake and it is easier to administer parenteral nutrition. However, the conversion does not alter the natural history of the disease, but instead supplies prognostic information that the patient had less severe ARF. Large doses of furosemide are ototoxic, and the large infusion volume can cause pulmonary edema. Thus, it is reasonable to give a single trial of furosemide in escalating doses. If the patient does not respond to furosemide, the agent should not be readministered.

Mannitol is a diuretic that also may scavenge extracellular free hydroxyl radicals, although the importance of this effect on ARF is unknown. Use of mannitol in ARF has been comprehensively reviewed recently. Mannitol is beneficial when added to organ preservation solutions during renal transplantation. Mannitol may also protect against ARF caused by crush injury involving myoglobinuria, but only if given extremely early. Other than these limited uses, mannitol has not been shown to be useful in prevention or treatment of ARF. In contrast, mannitol aggravates radiocontrast induced ARF.

Renal low dose dopamine (hemodynamic paradigm)

Dopamine is a selective renal vasodilator that causes profound natriuresis and increases urine output. It is widely used despite little clinical data supporting its use. The renal selective dose of dopamine is about 1 μ g/kg/min and not 3 to 5 μ g/kg/min as routinely used. The use of dopamine was examined in the placebo group of a recent randomized control trial of atrial natriuretic peptide. Dopamine did not improve survival or delay dialysis. A recent review by Denton, Chertow and Brady concludes that "the routine use of dopamine should be discouraged until it is shown to be effective".

Atrial natriuretic peptide (hemodynamic paradigm)

Atrial natriuretic peptide (ANP) vasodilates the afferent arteriole and constricts the efferent arteriole, resulting in an increase in GFR. ANP also inhibits tubular sodium absorption. The net effect is dramatic increase in urine output. ANP is very effective in animal models even if first started two days after the ischemic or nephrotoxic insult. Because of these dramatic effects in animal studies, an open label trial of ANP was performed at the University of Colorado [20-23]. Fifty-three patients were selected based on a rise in creatinine of 0.7 mg% per day for three days. ANP had dramatic effects: it doubled the GFR and reduced the need for dialysis by almost 50%. Based on these positive results, a multicenter, randomized, double-blind, placebo-controlled trial in 504 critically ill patients with intrinsic acute renal failure was initiated. Patients were included if they had an increase of creatinine greater than 1 mg over 48 hours. Many of the patients were critically ill; 85% of the patients were in the ICU; 50% of the patients were intubated. Patients were excluded if they were hypotensive despite pressors. The trial had an excellent balanced randomization, which was probably aided by the large size of the trial. However, ANP had no effect on 21-day dialysis-free survival, mortality, or change in plasma creatinine. A pre-specified subgroup analysis suggested that ANP improved dialysis-free survival in oliguric patients (baseline creatinine clearance 4 ml/min), but not in non-oliguric

patients (baseline creatinine clearance 13 ml/min). It was hypothesized that ANP was ineffective in non-oliguric patients because the ANP induced hypotension and caused fresh ischemic injury. While the oliguric group was also hypotensive, their kidneys were already injured and evidently not subject to additional hypotensive ischemic injury. Of note, if ANP converted oliguric acute renal failure to non-oliguric acute renal failure, the outcome was improved. A follow-up randomized controlled clinical trial of ANP in oliguric patients with acute renal failure was initiated, but halted after an interim analysis showed that the trial was unlikely to find any therapeutic benefit [24].

Insulin-like growth factor-1 (cell fate paradigm)

Insulin-like growth factor-1 (IGF-1) is made in high concentrations by the developing kidney, where it induces cell proliferation and differentiation. It was hypothesized that IGF-1 might potentiate renal repair mechanisms after renal injury, since the cell fate paradigm states that repair recapitulates renal development. In animal models of renal injury, IGF-1 enhanced repair following renal ischemia even when started 24 hours after injury, and it may prevent renal injury following renal transplantation in dogs. IGF-1 also has direct hemodynamic effects. This agent was tested in two clinical trials. The first trial, performed at Washington University in St. Louis, was a randomized, double-blind, placebo-controlled trial of 58 patients undergoing vascular repair of the renal arteries or aorta. The surgeries are associated with a relatively high rate of acute renal failure, often approaching 25%. IGF-1 was started post-operatively just as the patient entered the Intensive Care Unit. IGF-1 was well tolerated with no notable side effects. IGF-1 produced a modest (\approx 8 ml/min) increase in creatinine clearance, whereas the placebo group had a slight fall in creatinine clearance. Thus, IGF-1 prevented the decline of GFR. There was no effect on morbidity, mortality, or length of stay. However, no patient needed dialysis in either group. Evidently the surgeons did not inflict very much renal injury during the operation. IGF-1 was also tested in a multicenter, randomized, double-blind, placebo-controlled trial. The study

enrolled 72 ICU patients with acute renal failure caused by surgery, trauma, hypertension, sepsis, or drugs of less than six days duration. Initial iothalamate GFR on randomization was 6.4 ml/min in the IGF-1 group and 8.6 ml/min in the placebo group. These patients had severe renal injury. Unfortunately, there was no difference in post-treatment GFR, need for dialysis, or morbidity. On the basis of this trial, testing of IGF-1 to treat or prevent acute renal failure was discontinued. IGF-1 is still being tested for use as an adjunct to nutritional supplementation in a variety of wasting disorders, including acute and chronic renal failure, and is being tested in kidney transplantation [20-23, 25].

Nutritional support

Nitrogen balance is extremely negative in patients with ARF, and protein catabolic rate (PCR) is very high. Nutritional supplementation increases azotemia, which increases the need for renal replacement therapy, so that nutritional support is frequently delayed in these patients to obviate the need for dialysis. Initial studies showed the benefit of essential amino acid supplementation, but subsequent studies have been conflicting reviewed in. However, these studies were performed before the recent advances in parenteral nutrition and dialysis techniques. Most nephrologists recommend that nutritional supplementation should not be withheld to minimize azotemia [24,25].

Nephrologic consultation

Only one non-dialytic intervention has been successful in improving the morbidity and mortality of acute renal failure. There is new evidence that early consultation with a nephrologist improves the outcome of patients with ARF. Mehta *et al* showed that nephrologic consultation was delayed in 28% of ICU patients with ARF in the ICU. Delay in consultation was associated with higher mortality, longer ICU length of stay, and increased number of organ systems failing at the time of consultation. Delay in nephrologic consultation was likely if the degree of ARF was underestimated because of low creatinine (4.5 mg%) or high urine output (400 ml/day). The lower creatinine was often a consequence of volume

overload that diluted the plasma creatinine, or severe malnutrition that decreased creatinine generation. While delay in consultation may have occurred in sicker patients and thus may be a proxy for severity of illness, this study demonstrates that interventions early in the course of ARF may influence outcome.

The role of hemodialysis in ARF has been reviewed recently. Dialysis is required in about 85% of patients with oliguric ARF, and 30% of patients with non-oliguric ARF. Retrospective studies have shown that dialysis is better than no dialysis, but establishing a dose-response relationship has been very difficult. Dialysis is a risky procedure, with risks of bleeding and hemorrhage from the site of vascular access. Hypotension and arrhythmias are frequently produced as a consequence of rapid changes in compartment volumes. Finally, recent studies reviewed below have suggested that dialysis itself may delay the recovery of renal function with ARF. This may be caused by hypotension or activation of the inflammatory cascades by the blood-dialyzer interface. Hypotension occurs frequently during the dialysis of sick ARF patients and can cause recurrent ischemic renal injury. Animal studies have shown that kidneys with ARF have impaired renal autoregulation, and frequently have increased vasoconstriction because of injury to the vascular endothelium, that results in increased sensitivity to vasoconstrictors and a decreased release of vasodilators. Thus, hypotension in the setting of ARF causes additional ischemic injury because of impaired autoregulatory response to hypotension.

Hemodialysis with biocompatible membranes

Dialysis with a bio-incompatible membrane elicits an inflammatory response consisting of complement activation and subsequent neutrophil activation. The amount of the response can be easily measured by a transient neutropenia, as the activated neutrophils are removed from the circulation by the lungs. Animal studies have shown that activated neutrophils are also deposited in the kidneys, where they either infiltrate into the organs or block small blood vessels and cause renal injury.

Recent prospective randomized studies by Schiffli *et al* and Hakim, Wingard and Parker have shown that dialysis with biocompatible membranes shortens the course of non-oliguric ARF, reduces hospitalization, and increases survival. Dialysis with biocompatible membranes resulted in less complement generation, better survival from sepsis, and fewer dialysis sessions. The results in the Hakim trials were more striking in the non-oliguric patients than the oliguric patients. Non-oliguric patients have higher renal blood flow and GFR, which may render the kidney more susceptible to ischemic injury. A similar selective deleterious effect of hypotension was also seen in the ANP trial. The biocompatible membrane trials have been criticized because the criteria for dialysis was not defined, and the decision was left to the discretion of the nephrologist. However, subsequent analysis showed that the two groups had similar blood chemistries at the time of initiation and discontinuation of dialysis. The hypothesis is also supported by data showing that biocompatible membranes preserve residual function in patients on chronic hemodialysis, and that bioincompatible membranes are associated with a higher rate of infections [20, 21].

These positive results have not been reproduced in ARF after renal transplantation nor in several studies published recently in abstract form. A recent abstract by Mehta *et al* of a non-randomized study showed that the effect of dialyzer membrane on mortality and renal recovery was not significant when patients were stratified for APACHE III scores; however, a more accurate scale such as the Liano or Cleveland Clinical Severity of Illness Score was not used. Finally, recent animal studies did not find any differences between dialysis membranes and recovery of renal function. Unlike the study by Schulman *et al*, the rats received hemodialysis rather than injection of complement activated plasma. On the other hand, the exposure to dialysis membranes was short, and only after the renal injury was established. Thus, the issue remains very controversial. Nevertheless, the published randomized trials do show impressive effects.

Does more dialysis enhance survival?

Retrospective trials have shown that dialysis used to keep BUN below 150 mg% improves survival, when compared to no dialysis. However, establishing whether more dialysis is beneficial has been extremely difficult. Conger performed a paired (not randomized) trial during the Vietnam war, and found that sufficient dialysis to keep the pre-dialysis BUN below 150 mg% caused an 80% mortality, while more dialysis to keep the pre-dialysis BUN below 70 was associated with a 36% mortality. Unfortunately, because of the small size of the trial (8 to 10 patients per group), the difference was not statistically significant. In a prospective trial by Gillum *et al* that included a better randomized design, the more intensive dialysis (defined to keep BUN below 60 mg%) had less GI bleeding, but the mortality in the intensive dialysis group was higher (59%) than in the non-intensive group (47%) dialyzed to keep the predialysis BUN below 100 mg%.

Paganini *et al* recently showed a link between dialysis therapy and outcome in ICU patients with ARF; however, this link was only present when the underlying comorbidity was taken into account using the Cleveland Clinic Severity of Illness Score. This severity of illness score incorporates male gender, intubation/mechanical ventilation, platelet and leukocyte count, bilirubin level, number of organ failures, change in BUN since admission, and serum creatinine. This index shares some similar variables (intubation, bilirubin) with the Liano index, although there are differences of which the gender is most notable. Without factoring for comorbidity, dialysis had no effect on survival. When comorbidity was taken into account, dialysis had no effect at the two ends of the spectrum: mortality of 0% in patients with very low (<4) severity of illness scores and nearly 100% at high (>15) scores. However, the dose of dialysis did affect outcome in patients with an intermediate score. Higher delivery of dialysis (URR 58%, Kt/V 1, TAC urea 45 mg%) was associated with significant reduction in morbidity when compared to low dose delivery in the same severity of illness quartile. Whereas the underlying patient morbidity has a

significant effect on survival in ARF, the dose of dialysis also plays a major role in patients with intermediate severity of illness [19-21].

Schiffl *et al* have recently reported the preliminary results of a trial in 72 critically ill patients with ARF who were randomized to either daily or alternative day dialysis using biocompatible high-flux dialyzers. The two groups were well matched in age, severity of ARF, APACHE II scores, and prescribed dialysis techniques. Overall mortality was significantly improved in the daily dialysis group (21% vs. 47% for the alternative day group). When analyzed in terms of delivered dialysis dose (Kt/V), mortality was 16% in the group receiving a weekly Kt/V greater than 6, which was significantly less than the 57% mortality in patients receiving underdialysis (weekly Kt/V < 3). This is the first study to show that the amount of dialysis is an independent determinant of mortality in critically ill patients with acute renal failure. Why did this trial have a positive result that was not seen in previous trials? Unlike previous dosing trials, this trial used biocompatible synthetic membranes, which may have allowed an effect of dialysis dose to be seen for the reasons discussed above. The study also suggests that the alternative day dialysis typically prescribed for acute renal failure is 'grossly inadequate.' More studies are needed to define how to measure dialysis dose in patients with acute renal failure. Recent studies in chronic renal failure have found that equilibrated or 'double pool' Kt/V is more accurate than the traditional single pool Kt/V. Whether reliance on equilibrated kinetics is also more accurate in acute renal failure is unknown [16, 22-24].

Mode of renal replacement therapy

In the past, intermittent hemodialysis (IHD) has been the therapy of choice for ARF, since peritoneal dialysis does not remove sufficient solute or volume. However, IHD is associated with wide swings in body wt, blood pressure, ventricular filling pressures, and solute concentrations (BUN, potassium, and bicarbonate). Because of the concern that recurrent hypotension perpetuates renal injury and lengthens recovery from ARF, newer modes of dialysis therapy have been developed that minimize

hypotension. Continuous renal replacement therapy (CRRT) removes fluid and solutes at a slow and controlled rate, thus minimizing hypotension reviewed in. Because it is more complicated to perform, CRRT is usually reserved for hemodynamically unstable patients (including those with sepsis, burns, and multiple organ dysfunction syndrome) in the ICU who often cannot tolerate the hemodynamic effects of intermittent hemodialysis. The solute clearance of CRRT may be larger than IHD with four treatments a week. The CRRT dialysis membrane has large pores that may allow removal of inflammatory cytokines. CRRT also allows for easier drug dosing. Because of its theoretical advantages, it was hoped this would lead to improved patients survival or recovery from renal failure.

IHD and CRRT have been compared in many non-randomized or retrospective studies reviewed in. Prospective randomized trials are difficult to perform because the hemodynamically unstable patients cannot tolerate hemodialysis, while it may be ethically problematic to confine a hemodynamically stable patient to bed while receiving CRRT. A recent prospective trial from Barcelona failed to find any difference in survival. Mehta *et al* recently completed a multi-center prospective randomized trial of CRRT versus IHD in IHD patients with ARF. One hundred and sixty-six patients were randomized to receive either IHD or CRRT (which was performed as CAVH or CAVHD). The total mortality was only 50%, which was less than that expected from historical studies. An intention to treat analysis found that the mortality was higher in the patients randomized to CRRT (65.5%) than IHD (47.6%). Unfortunately, the randomization did not balance the groups very well; for example, the APACHE III scores were significantly different (85 for IHD vs. 102 for CRRT). Attempts to control for the unbalanced randomization using the APACHE scores still led to the same conclusion. Mehta *et al* have not reported their results using either the Liaño or Paganini severity of illness scales, which are more appropriate for renal patients. Subgroup analyses suggest a beneficial effect of CRRT, since patients who crossed over from IHD to CRRT had a higher mortality than those who crossed over from CRRT to IHD. Also,

despite the higher mortality in the CRRT group, patients initially treated with CRRT had higher rates of recovery of renal function. At the present time, it appears that intermittent hemodialysis and chronic renal replacement therapy are roughly equivalent methods for treatment of ARF.

Chronic Kidney Disease Therapy

Many are the therapeutic and pharmacological tools used by clinicians to slow the progression and symptoms of ESRD but the only effective treatments are dialysis and transplantation.

In the treatment of patients with impaired kidney functionality, it is important to recognize that the major risk for patients with Chronic Kidney Disease is death from cardiovascular disease or diabetic complications.

Currently CKD drug therapy in the early stages is limited to administration of antihypertensive medication to decrease blood pressure, and consequentially decrease the risk of injury provoked by high blood pressure, and limit proteinuria. The use of a particular class of antihypertensives, called Angiotensin-Converting Enzyme (ACE) inhibitors, was reported to give additional renoprotection.

Generally, two major mechanisms have been implicated to explain the additional effects of ACE inhibitors: (i) suppression of angiotensin II formation (ii) increase of kinin concentration via inhibition of bradykinin degradation. Both pathways can cause a decrease in glomerular capillary pressure, proteinuria, or growth of renal cells, accompanied by increased degradation of extracellular matrix.

Treatments with pharmaceuticals are a good start point to treat kidney disease but at long term are not effective because they interfere with very specific pathways. Mechanisms that lead to ESRD are multiple and very complex and the administration of one or more medicine is not enough to treat and cure the CKD.

Even if on pharmacological therapy many patients eventually require renal replacement therapy, or dialysis. Dialysis is a clinical procedure that

substitutes the loss function of the kidney for what concerns the blood purification. The use of external hemodialyzer or “inside the body” dialysate administration is the current therapy for dialysis.

Although either intermittent or continuous current artificial renal replacement therapies can administer substantive small- and middle-molecule solute and fluid clearance, dialysis is not a complete replacement therapy. In addition to its major role in maintaining the constant extracellular environment, the kidney has many other roles. It is regarded as an endocrine organ, responsible for the secretion of hormones that are critical in maintaining hemodynamics (renin, angiotension II, prostaglandins, nitric oxide, endothelin, and bradykinin), red blood cell production (erythropoietin), bone metabolism (1,25-dihydroxyvitamin D₃ or calcitriol). The traditional renal replacement therapies, based on diffusion, convection, or absorption, provide only filtration; they do not replace these lost homeostatic, regulatory, metabolic, and endocrine functions of the kidney.

In addition, although life-sustaining, dialysis does not provide a high quality of life to most patients and several side effects may occur during dialysis such as hypotension, arrhythmia, and complications of vascular access placement. Plus, some studies highlighted concerns regarding an increased risk of slowing the recovery of renal function and developing ESRD by dialysis treatment [26-30]

Several studies reported that a kidney transplant from a live donor should be promoted as the first choice for eligible patients who require renal replacement therapy. Outcomes with deceased donor kidneys are also significantly better than with dialysis [31].

Since the first kidney transplants were performed in the 1950s, there have been major advances in both transplantation and dialysis and the risks and benefits for both options have changed. Kidney transplantation has lifestyle advantages and is cheaper than dialysis and this makes transplantation the first choice treatment for ESRD patients [32].

Nonetheless, availability of donor kidneys is very limited. Many adults on the deceased donor waiting list will die on dialysis before they receive an

organ. Unrelated kidney transplantation is increasing due to organ shortages [33]

Increase of risk factors such as age, obesity and hypertension is raising the demand for organs and by now is possible to transplant not well matched organs, thanks to the use of immunosuppressive drugs. At first, kidney transplant regimens relied on steroids and azathioprine to prevent rejection with some success, but the real success was the introduction of cyclosporin over 30 years ago [34]. More recently, new and potent immunosuppressive drugs have been introduced including tacrolimus, mycophenolate and sirolimus. As might be expected with better immunosuppressive regimens, acute rejection rates fell over the decades. However, immunosuppression takes its toll in both the short and long term. In the short term, infection is a particular concern, especially with viruses such as cytomegalovirus. However, in the long term, the incidence of most cancers is increased in patients who are immunosuppressed [35]. The risk of cancer incidence in patients now under the novel, more aggressive immunosuppressive therapies, may be higher than expected.

2. Regenerative Medicine and Kidney regeneration

In order to overcome the limits of current therapies, scientist and clinician have looked for alternative approaches for CKD management.

In the last years Regenerative Medicine has grown as an alternative for many diseases.

Regenerative Medicine defines a wide field of both research and clinical therapy involving the improvement of healing and reconstruction of tissues and/or organs. The main goal of regenerative medicine is the complete replacement of a damaged organ through the regeneration *in situ* or the transplantation of a bio-engineered and functional organ reconstructed *in vitro* [36]. In the last two decades regenerative medicine has been increasing the efforts of the scientific community toward the discovery of new clinical tools for treatment of acute, chronic and genetic kidney disorders.

Tissue Engineering for Kidney regeneration

Tissue Engineering, that combines natural or biodegradable polymers with cells and growth factors, has contributed to the field of kidney regeneration in recent years. The perfect implantable device needs to mimic main physiological function of the native kidney and it needs to operate incessantly to remove solutes. It will be optimum to design perfect membrane that has the same filtration capability as the nephron.

Humes et al showed the creation of membrane that has both pore selectivity and at the same time hydraulic permeability as the native kidney [37]. The creation of better bioartificial hemofilters is important to overcome the problem of loss of filtration due to thrombotic occlusion and protein deposition and that exclude the use of anticoagulant in the extracorporeal units that very often results in bleeding for the patient [38].

Few experiments have been conducted where renal cells were cultured *in vitro*, seeded into a polyglycolic acid polymer scaffold and subsequently implanted into athimic mice [39]. Over time, formation of nephron-like structures was observed within the polymer. These preliminary results when improved could easily be used to produce three-dimensional functional renal structures that can be used in *ex-vivo* or *in vivo* filtering units. This approach is called cell-based tissue-engineering as it refers to the use of scaffolds (natural or synthetic) and cells mixed together to recreate a tissue that mimics the physiological one by size and functionality.

Nonetheless since adult cells are completely differentiated and their response to growth factors can be absent or different from cells in the developing kidney, the seeding, the integration and the interaction *in vitro* or *in vivo* systems can fail or be partial. Therefore a great improvement came from the discovery of stem cells and their pluripotential capability.

Stem Cells

In recent past, the potential use of stem cells and the advancement in stem cell research for regenerative medicine and in particular for repairing kidney injury is considered as an alternative therapeutic strategy.

The interest about stem cells has been increasing over the past years, since their discovery in the early '90s. Stem Cells might be a promising tool for regenerative purposes because of their capability to become almost any cell of an adult organism. The definition of stem cell is not yet clear, but it is universally accepted that a stem cell possesses two fundamental characteristics: long term self-renewal and pluripotentiality.

Self renewal describes the unique capability of these cells to reproduce itself indefinitely while producing also cell progeny that mature into more specialized, - organ specific cells. In this process, called asymmetric division, a stem cells divide into another stem cell and a cell that is going to differentiate and divide symmetrically. Pluripotentiality of stem cells is defined as the ability of a stem cell to give rise to different tissues. The fertilized oocyte is totipotent, able to differentiate into all the embryonic and extraembryonic tissues. Pluripotent stem cells are defined by the ability to differentiate, under certain stimuli from the surrounding environment, into many different mature cells of all the three germ layers and germ cells. A cell is defined as multipotent if can give rise to more than one cell type and unipotent if it can differentiate into one cell type. Based on their capability to differentiate into different cell types, stem cells are divided into different categories.

Embryonic Stem Cells

Embryonic Stem Cells (ESC) are collected from the Inner Cell Mass (ICM) of the blastocyst at five days from the fertilization of the egg. The blastocyst includes three structures: the trophoblast, which is the layer of cells that surrounds the blastocyst; the blastocoel, which is the hollow cavity inside the blastocyst; and the inner cell mass, which is a group of approximately 30 cells at one end of the blastocoel. ESCs are defined as

pluripotent, meaning they have the capability to give rise to cells derived from all the three germ layers (endoderm, ectoderm and mesoderm). For this reason ESCs have been widely investigated for their wide capability to differentiate into any cell line of the body, being a plastic and reliable tool for therapeutic applications.

Primordial Germ Cells

Primordial Germ Cells (PGC) are retrieved from the embryo at 5-9 weeks of gestation. The germ cell lineage is discriminated from somatic cell lineage during development and repression of the somatic cell fate is therefore a key event during germ cell specification. The specification is initiated by signals provided by the Extraembryonic Ectoderm (ExE), and the Visceral Endoderm (VE) that surrounds the epiblast cells and instructs a small number of epiblast cells to become PGCs. Since PGCs are retrieved at a later time where the original ESCs have started to commit to a specific pathway of differentiation, they present limited plastic properties if compared with ESCs. More hopes are coming from the study of Adult Stem Cells (ASC)

Adult Stem Cells

Adult Stem Cells (ASC) are located within the tissues of the adult body. Their function is, under specific stimulation, to undergo differentiation and replace the loss of cells in an injured/ compartment. A specific organ localization called niche is thought to harbor the stem cells in an environment that protect cells from differentiation. One example of Adult Stem Cells is hematopoietic stem cells (HSCs). HSCs, localized within the bone marrow, are the most important adult stem cell line, discovered over 30 years ago. HSCs are commonly used for transplant for the treatment of leukemia diseases and are, by now, the only stem cell line currently used in therapy. In bone marrow another population called bone marrow stromal stem cells (MSC) show to differentiate into mesenchymal lineages. *In vivo* they support hematopoietic events establishing a microenvironment with function of stem cell niche. MSC where shown capable to differentiate *in*

vitro into adipocytes, chondrocytes, muscular cells, tendons, osteoblasts and endothelial cells. Many ASC were localized within the kidney compartment.

Somatic Cell Nuclear Transfer and Induced Pluripotent Stem Cells

In the most recent years many studies were published regarding the retrieval or the discovery of stem cells populations. Scientific knowledge allows us to modify cell genetic background and gene expression and creating in the laboratory different types of exogenous stem cells like. Somatic Cell Nuclear Transfer (SCNT) cells were derived from the injection of an endogenous somatic cell nucleus within an oocyte. The result was the creation of a pluripotent cell, capable of being implanted in utero or used to retrieve new stem cell lineages. Induced Pluripotent Stem Cells (iPS) were obtained with insertion of pluripotent genes within the DNA of a somatic cell. Retroviral introduction of transcription factors OCT-4, SOX-2, KLF4 and MYC induced pluripotency within somatic cells. Recent studies have shown that OCT-4 and SOX-2 could be combined with other genes to produce iPS cells. IPS cells were able to participate to the embryonic development when injected in a blastocyst.

Stem Cells and Kidney Regeneration

In the last few years some important scientific publications have shown evidence that stem cells, mainly mesenchymal stem cells derived from bone marrow, or of kidney-specific progenitors [40, 41], have the capability to ameliorate renal injury. Transplanted bone marrow stem cells were found integrated into damaged kidney [42, 43]. Morigi *et al* [44, 45] and Herrera *et al*. [46] demonstrated that MSC are capable of integrating into damaged tubules and speculate that exogenous MSC from bone marrow have the ability to differentiate into renal epithelial cells. Yokoo *et al*. [47] injected MSC from bone marrow into kidneys during development and confirmed their integration into various compartments of the kidney, suggesting engraftment of these cells within nephron structures. However,

whether there is any physiologic benefit of incorporation of these cells within damaged tubules of the kidney is still unclear. In contrast, there have been other groups, who have shown that MSC have a role in restoring function to damaged kidneys through some other mechanism other than incorporation and replication [48-50]. Bonventre *et al.*[51] underscored the importance of MSC in renal repair and raised the possibility that MSC may mediate their reparative effect by affecting the inflammatory response following acute renal injury.

With the possibility to choose from so many different pluripotential cell lineages, each one with different characteristics such as differentiation potential, committed status that could increase tissue specificity, autologous source and easiness of collection, stem cells have been the center of interest for scientists, clinicians and patients.

Despite the discoveries and the promising results, many are the controversies raised by stem cells. ESCs are strongly opposed by many for ethical reasons regarding their source and because of their ability to form teratomas *in vivo*. PGCs present a more limited pluripotentiality and share the same ethical issues as ESCs, making them even less attractive for clinical purposes. Free from moral argumentations are ASCs but their yet partially committed state makes them less reliable for a wide broad use for many applications. In fact, HSCs are broadly used in leukemia and some types of anemia therapy with discrete success.

A different problem is presented by SCNT where the incomplete technical knowledge and the know-how are still the major opposition for their therapeutic use as well as for iPS, where safety concerns for the use of retroviral infection are debated in the scientific community.

Feasibility of stem cells for human therapeutic use is regulated by many requirements such as safety, accessibility to a source that can provide an adequate amount of cells for *in vitro* expansion, absence of ethical issues and repeatability of the results.

3. Amniotic Fluid as an alternative source of Stem Cells and Progenitors

To overcome all the above described concerns we and others are investigating new sources of pluripotent cells with low risk for their use, easy access to the source and capacity of giving rise to many mature cells through a safe and specific pathway.

Amniotic Fluid (AF) derives mostly from fetal urine and lung secretions, with minor contribution from the amnion [52]. Due to its contact with the developing fetus along the gestation, many cells are present within AF. In the last years many are the studies performed about the cells populating AF. Pluripotent cells were found within AF based on the expression of pluripotency marker OCT-4 [53] and is demonstrated the presence of mesenchymal and hematopoietic cells with pluripotent or multipotent characteristics. But mostly the AF cell population is still poorly known.

In 2007 Atala [54] widely described a pluripotent population characterized by the expression of C-kit, a surface marker expressed by stem cells of mesenchymal origin. The c-kit receptor is a protein-tyrosine kinase that is specific for stem cell factor. This complex has been suggested to be involved in embryogenesis as well as carcinogenesis.

The stem cells population was about 0.8%-1% of the entire AF population and was shown a fibroblast-like morphology. AFSCs express some surface markers and transcription factors distinctive of Embryonic Stem Cells such as OCT-4 and SSEA-4 indicating they can actually, possess some important characteristics that also Embryonic Stem Cells have, showing their pluripotential capability. In addition, they stained positively for a number of surface markers characteristic of mesenchymal and/or neural stem cells, including CD29, CD44 (hyaluronan receptor), CD73, CD90 and CD105 [54]. The cells were positive for Class I major histocompatibility (MHC) antigens (HLA-ABC), and some were weakly positive for MHC Class II (HLA-DR). The AFS cells were negative for markers of the hematopoietic lineage (CD45) and of hematopoietic stem cells (CD34, CD133). AFSC have a very high proliferative capacity

exceeding Hayflick's limit and the doubling time is around 36 hours with some variation between samples. Over the population doublings the cells maintain a normal karyotype, and also they present normal regulation of the control checkpoints of the cell cycle, in particular the G1 and G2, in preparation for chromosomes replication and entrance into mitosis. When injected into a blastocyst AFSC were able to integrate and participate to the development of several embryonic organs. *In vitro* C-Kit⁺ cells were able to differentiate into adipocytes, myocytes, neurons, and bone [54].

in this thesis we show the capability of AFSC to participate *in vitro* to the development of embryonic kidneys [55]. AFSC labeled with CM-Dil were integrating within the developing structures of the kidney. Integration of AFSC into the metanephric structures was additionally confirmed by the migration of the injected cells from the site of injection, the center of the embryonic kidney, to the periphery, strongly correlates to the centrifugal pattern of induction, morphogenesis and differentiation of the metanephros, proceeding from the center to the periphery of the embryonic organ [55].

In 2008 Carraro *et al* demonstrated *in vivo* integration and differentiation of AFSC into murine injured lungs [56]. Since safety of stem cells is essential for a human therapeutic application tumorigenicity was tested and AFSC were not showing any carcinogenic potentiality when injected *in vivo*. This preliminary work sustains the possible capability of using AFSC in therapeutic applications, especially for Kidney regeneration.

OBJECTIVES

Acute Kidney Disease (CKD) is a major public health problem that affects some 3-7% of patients admitted to the hospital and approximately 25-30% of patients in the intensive care unit. None of the existing therapies are exempt from side effects and kidney physiological functionality is never restored. Transplantation has been reported as the preferred cure for CKD management but organ shortage and risks due to the immunosuppressive therapy makes it far from being the perfect treatment for ESRD.

In this study we have focused our attention on finding novel strategies, *in vitro* and *in vivo*, to obtain kidney regeneration in case of acute and chronic kidney damage.

1. In order to establish a model for *in vitro* kidney regeneration and investigate the pluripotential capacity of hAFSC, we combine technologies of tissue engineering with those of developmental and stem cell biology, based on the principle that stem cells will develop more appropriately in an embryonic tissue environment. An *in vitro* system of renal organogenesis is established to demonstrate this concept and to assist in differentiating hAFSC down to a kidney lineage: hAFSC are injected and cultured into mouse embryonic kidneys, at E12.5-E18 day gestation, to determine their ability to survive, replicate and contribute to the formation of primordial renal structures during organ development *in vitro*.

2. We evaluate the function of hAFSC to rescue damaged kidneys in an *in vivo* mouse model. In kidneys with acute tubulonecrosis, caused by glycerol-induced rhabdomyolysis, hAFSC are studied for their ability to integrate, replicate and differentiate into kidney structures. Moreover, we characterize the cytokine immuno-modulatory response and the capability, of this stem cells population, in restoring the kidney function.

3. It is known that by 8 weeks of gestation Amniotic Fluid derives for the most part by fetal urination, and it could represent a repository of cells with kidney commitment and these progenitors (for example podocytes-like cells) may be a potential source of cells for kidney regeneration. Beside the well known population of AFSC, corresponding to 1% of the total cell population, the most part of the cells within Amniotic Fluid are poorly characterized. To better identify and select a renal population from Amniotic Fluid we performed a wide characterization of the cells present in the liquid, ranging from cells derived from all the three germ layers and organ specific progenitors, from multipotent to unipotent cells. In addition, we focus our research in the molecular characterization of several specific kidney progenitor cells present in the amniotic fluid. We want to obtain a selection of progenitor cells to be specific in the repair of the different damaged cells in the nephropathy (glomerular, stromal, or tubular oriented progenitor stem cells).

MATERIALS AND METHODS

1. Expansion of human Amniotic Fluid Total Cell Population

Under Institutional Review Board approval of Children's Hospital Los Angeles, 28 human amniotic samples were obtained from discarded amniocentesis fluid between 15 and 20 weeks of gestation. Samples with normal male karyotype and normal fetal ultrasound were collected from discarded cultures from Genzyme (Pasadena, CA). Cells were expanded in Tissue Culture Dishes (BD Falcon, Franklin Lakes, NJ) with three different culture media (Figure 1).

1. Chang's media (α -MEM, 20% Chang B and 2% Chang C) (Irvine Scientific, Santa Ana, CA), L-Glutamine 20% of ES-FBS (Gibco/Invitrogen, Carlsbad, CA) and 1% of antibiotic (Pen/Strep, Gibco/Invitrogen, Carlsbad, CA).

2. Amniomax II was added as supplied (Gibco).

3. DMEM was supplemented with 10% FBS (Gibco/Invitrogen, Carlsbad, CA) and 1% antibiotic.(Gibco/Invitrogen, Carlsbad, CA)

Cells were trypsinized using trypsin 0.25% EDTA (Gibco/Invitrogen, Carlsbad, CA).

Cells were cultured at 37° Celsius and 5% CO₂ for 50 passages.

2. Characterization of Amniotic Fluid Cells

16 samples of AF cells were analyzed with RT-PCR for a wide panel of markers for all the three germ layers, early progenitor cells from different organs and pluripotent cells (see Table below).

12 samples were analyzed by real-time PCR to determine the quantitative variation in the expression of the different markers at different gestational ages.

Analysis and characterization by RT-PCR

Between passages 4 and 5 and after trypsinization, cells were collected for RT-PCR.

Total RNA was isolated using the RNeasy Mini Kit (Invitrogen, Carlsbad, CA) as described on the data sheet. Briefly, with the use of silica-gel columns RNA is separated from DNA through centrifugation after lysis and homogenization of the samples. Ethanol addition allows RNA to bind the silica-gel before the centrifugation step. The RNA solution obtained was then processed with DNase treatment (DNase I, Invitrogen, Carlsbad, CA) to avoid any possible genomic contamination. One microgram of total RNA was reverse transcribed using SuperScript II reverse transcriptase (Invitrogen, Carlsbad, CA). The cDNA was amplified with Taq Polymerase (Invitrogen, Carlsbad, CA) in the presence of gene specific primers (Operon, Huntsville, AL). Amplification conditions were as follows: 94°C, 3 minutes; 94° C, 45 seconds; annealing temperature specific for each primer between 55° and 62° C, 30 seconds; 72°C, 1:30 minutes in a total of 36 cycles followed by 10 minutes at 72°C. RT-PCR products were separated in a 1.0% agarose/ethidium bromide gel and visualized using Blue/Orange Loading Dye (Promega, San Luis Obispo, CA).

Gene	Primer Sequence (5'→3')	Size (bp)	Annealing Temperature	Function
AFP	AGCTTGGTGGTGGATGAAAC CCCTCTTCAGCAAAGCAGAC	248	56.2	Early expressed by the visceral yolk sac and, later, by the visceral endoderm
GOOSECOID	AGGAGAAAGTGGAGGTCTGGTT TACAGCTCCTCGTTCCTCTTTC	299	58.6	Transcription factor expressed in the definitive endoderm.

				Essential for normal embryo development.
SOX-17	AGCGCCCTTCACGTGTACTA CTTGACACACGAAGTGCAGAT	216	56.2	Extraembryonic visceral and definitive endoderm. Leading cells toward a pathway of endodermal differentiation
CXCR-4	TGAGAAGCATGACGGACAAG GACGCCAACATAGACCACCT	275	56.2	Chemokine Receptor 4, expressed by pre lymphocytes B cells. Involved in haematopoiesis
E-Cadherin	TGCCCAGAAAATGAAAAAGG GTGTATGTGGCAATGCGTTC	200	58.8	Cell adhesion molecule expressed in the primitive ectoderm and down regulated in cells of primordial germ layer origin. Is also expressed by cells going through Mesenchymal to Epithelial Transition (MET)
FGF-5	AAAGAGGAAAAGCCAAACGAG CCAAAGCGAAACTTGAGTCTG	223	54.7	Structurally related mitogen that promotes neural

				development
NCAM	GGAGGACTTCTACCCGGAAC CTTTGGGGCATATTGCACTT	200	58.8	In nerves, regulates interactions between neurons and muscle; stimulates tyrosine kinase activity of receptor to induce neurite outgrowth. Contributes to cell-cell or cell-matrix adhesion during development.
TAL-1	CTCCCTATGTTCCACCACCAAC CTCATTCTTGCTGAGCTTCTTGT	208	56.9	Transcription factor that plays many important roles in embryo growth, including the development of the putative hemangioblast
BRACHYURY	ACCCAGTTCATAGCGGTGAC ATGAGGATTTGCAGGTGGAC	216	56.2	Required for the development of the posterior mesoderm in mice. The absence of this molecule leads to death of the embryo
FLK-1	GTGACCAACATGGAGTCGTG TGCTTCACAGAAGACCATGC	218	56.2	Migration of haematopoietic and endothelial

				cell progenitors to the yolk sac and also for generation of definitive haematopoietic precursors. Its absence is followed by death of the embryo because of defects in vascular development
PDX-1	GATGAAGTCTACCAAAGCTCACG CTTGACCGAGAGACACATCAAGAT	211	57.6	Homeodomain transcription factor essential for pancreas development, insulin production, and glucose homeostasis
TTF-1	ACAAGAAAGTGGGCATGGAG GCTGTTCTCATGGTGCCT	251	56.2	Transcription factor whose expression has been showed in thyroid, lung and some specific regions of the forebrain
CEBPG	CATGGATCGAAACAGTGACG ACGTTGTCTGCAAGGTTGTG	228	58.8	Transcription factor of the family of the CCAAT/enhancer-

				binding protein and is expressed in the fetal liver at the onset of definitive haematopoiesis
NKX2.5	ACATCCTAACCTGGAGCAGCAG CCAAGTGTGCGTCTGCCTTTC	300	58.8	Encodes a homeodomain-containing transcription factor with major role in heart development. It's the earliest marker for pre cardiac differentiation
GDNF	TATGGGATGTCGTGGCTGT ACACCTTTTAGCGGAATGCTT	624	58.2	Essential for nephrogenesis. Involved in stimulating UB branching. The highest expression of GDNF is found in the developing kidney while is not present in the adult organ
β -actin	AGAAAATCTGGCACCACACC CTCCTTAATGTCACGCACGA		55.4	Housekeeping Gene

Table 1A - Panel of markers used for the characterization of human AF populations for the three germ layers and organ progenitor cells by RT-PCR

Gene	Primer Sequence (5'→3')	Size (bp)	Annealing Temperature	Function
CD24	ACCCAGCATCCTGCTAGAC CTTAAGAGTAGAGATGCAGAA	286	59	Sialoglycoprotein anchored to the cell external surface and is usually expressed by hematopoietic cells
OB CADHERIN	CACTGTCTTTGCAGCAGAAATC TACAATGACCAAGGAGAATGACG	437	55.6	Cadherin 11 is a cell surface glycoprotein and seems to be involved in dendritic spine morphogenic
LIM1	TCAGGAGFCGAAGTAGGAAC AAGAGCGAGGATGAAGATGG	627	59.3	Transcription factor widely expressed in the renal compartment during development and

				evidences of its presence are shown in developing tubules, UB branches, S and comma shaped bodies
PAX-2	AGGATGAGGGACCAACTGC AACGACAGAACCCGACTATGTT	738	59.5	Transcription factor known to be a WT1 inducer and a key ruler of mesenchymal to epithelial transition
OCCL	GCCCTCGCAACCCAAATTTTA TCATTCACCTTTGCCATTGGA	425	58.2	Protein present on tight junctions with the role of sealing tight junctions between cells in a cell layer
AQP1	CACCTCCTCCCTGACTGG GGTTGCTGAAGTTGTGTGTGA	290	58.8	Water channel protein, expressed by red blood cells, renal proximal tubules and descending limbs of loop of Henle
TRKA	CCATCGTGAAGAGTGGTCTC GGTGACATTGGCCAGGGTCA	476	61.4	NGF High Affinity Receptor (chained with Tyrosin Kynase,

				TrKA) is expressed in the stromogenic compartment
PGFR <input type="checkbox"/>	TGGAAGAAATCAAAGTCCCATCC GGATCAGCATTAAATTTGCAACG	720 63		<input type="checkbox"/> isoform of the Platelet Derived Growth Factor, shown to be expressed in cells of the nephrogenic mesenchyme
Nephrin	ACACGGAGCACACATACCAC GGATTGGAGAGGAGCAGAAG	568 59.8		Essential transmembrane protein expressed by podocytes at the slit between foot processes
ZO-1	GCTGGTTTTGCTGTTGTTGA AGGAGAGGTGTTCCGTGTTG	773 59.9		Involved in the assembly and function of various tight junctions. Expressed by podocytes with the slit diaphragm

Table 1C - Panel of markers used for the characterization of human AF populations and derived subpopulations for kidney commitment by RT-PCR.

Analysis and characterization by Real Time PCR

Total RNA was isolated from cell cultured for 4 to 5 passages and retrotranscribed as previously stated starting from an RNA concentration equal to 800ng/μL.

Quantitative real-time PCR was carried out using the Roche Light Cycler 480 and the Light Cycler TaqMan Master Mix.

Real Time PCR conditions were as follows: 90°C for 10 minutes, 60°C for 10 seconds, 72°C 1 second with the analysis of the fluorescent emission at 72°C. 35 cycles were performed for each experiment. All primers and probes were designed by Roche.

Analysis and characterization by Western Blotting

Total cell lysates were prepared using the Nuclear Extract Kit (Active Motif). After washing the plate with a phosphatase inhibitor, solution cells were scraped from the plate, collected, and centrifuged at 500 rpm for 5 minutes at 4° C. After incubation on lysis buffer at 4° C for 20 minutes cells were vortexed and successively centrifuged at 14000 rpm, for 20 minutes at 4° C. Supernatant was collected and concentration measured with UV-VIS Spectroscopy. Each sample was prepared with Loading Buffer containing 250 mM Tris HCl (Sigma-Aldrich, St. Louis, MO) pH 6.8, 10% SDS (USBio, Cleveland, OH), 30% Glycerol (Sigma-Aldrich, St. Louis, MO), 5% B-Mercaptoethanol (Sigma-Aldrich, St. Louis, MO), 0,02% Bromophenol blue (Sigma-Aldrich, St. Louis, MO-Aldrich). Equal amounts (20 μl, 1ng/ul) of individual protein solution were separated from each sample, after 1 minute boiling step, by SDS-PAGE with 4%-20% Glycin gels (Individual solutions were then transferred to PVDF 0.45 μm membrane (Millipore, Billerica, MA) and probed with a various range of antibodies at 1:1000 concentration (Table 2). Peroxide conjugation of secondary antibodies was performed (Sigma-Aldrich, St. Louis, MO) with concentrations as follows: 1:10000 for Anti-Mouse, 1:15000 for Anti-Rabbit, 1:8000 anti-Chicken and 1:120000 for anti-Goat secondary antibodies. The blocking steps were performed with 10% Dry Fat Milk (Santa Cruz Biotech., Santa Cruz, CA) in TBS. TBS-T (1% Triton) was

used as washing solution. Detection of antigens was performed using the ECL Western Blotting detection Reagents (Amersham Biosciences/GE Healthcare, Buckinghamshire, UK), impressed on Biomax Light Film (GE Healthcare, Buckinghamshire, UK) with a 1 minute exposure.

Antigen	Company	Host	Antigen	Company	Host
AFP	Santa Cruz	Goat	GDNF	Santa Cruz	Rabbit
GOOSECOID	Santa Cruz	Goat	OCT-4	Abcam	Mouse
SOX-17	Santa Cruz	Goat	CKIT	Santa Cruz	Rabbit
CXCR-4	Abcam	Rabbit	CD24	Abcam	Mouse
E-Cadherin	US Biological	Chicken	OB CADHERIN	Abcam	Mouse
FGF-5	Santa Cruz	Goat	LIM1	Abcam	Rabbit
NCAM	Abcam	Mouse	PAX-2	Abcam	Rabbit
TAL-1	Santa Cruz	Goat	OCCL	Santa CruzG	Goat
BRACHYURY	Santa Cruz	Goat	AQP1	Santa Cruz	Mouse
FLK-1	Abcam	Rabbit	Nephrin	Abcam	Rabbit
PDX-1	Abcam	Rabbit	ZO-1	US Biological	Rabbit
TTF-1	Abcam	Mouse	β -actin	Santa Cruz	Mouse
CEBPG	Abcam	Mouse	CD34	Santa Cruz	Rabbit
NKX2.5	Santa Cruz	Goat	CD90	Abcam	Mouse

Table 2 - Panel of markers used for the characterization of human AF populations and derived subpopulations by Western Blotting assay.

3. Ex Vivo whole embryonic kidney culture

To ensure sterile culture conditions: all the solutions and equipment must be sterile; all tissue culture steps are best carried out in a laminar-flow hood; it is recommended to perform surgeries in a hood.

Media and Solutions

The base media used was Leibovitz's L-15 (Gibco/Invitrogen, Carlsbad, CA, USA). This solution is light sensitive, it should be stored in a dark bottle at 4°C. Phosphate-buffered saline (1x PBS), pH 7.4. 1%

penicillin/streptomycin (Gibco/Invitrogen). 2% fetal bovine serum (Gibco/Invitrogen)

Tools for the Organ Dissection

Have on hand the following supplies:

- Microsurgery instruments: straight-tip scissors, No.5 Dumont forceps, plastic pipettes (Fine Science Tools Inc., Foster City, California)
- 0.4 μm pore size Transwell membrane (Corning Incorporated, Acton, MA, USA)
- 8x dissecting microscope
- Ice box

Organ Dissection Procedure

Wild-type C57BL/C6 mice metanephric kidneys were dissected under sterile conditions from timed-pregnant embryonic day 13 to 16 (E13 to E16) under a dissecting microscope (8x). Embryonic staging was verified using the criteria of Theiler. The embryos were placed in a 10-cm plastic Petri dish containing cold 1xPBS, their abdominal walls were carefully dissected and then we peeled out the whole gut to expose the retroperitoneum and kidneys. To transfer the organs in a sterile manner into a culture dish, with sterile media, we used plastic pipets. Perfusion channels were created under direct microscopy with a 10 μm diameter glass needle fashioned manually in the laboratory without conveying subsequent damage to the kidney while permitting homogeneous perfusion and bathing throughout the whole organ. The preparation and dissection of tissues should be done as quickly as possible having care to keep the embryonic organs in a cold medium before placing them on the Transwell membrane. Obtained developing kidneys were placed on a 0.4 μm pore size Transwell membrane (Corning Incorporated, Acton, MA, USA) and cultivated in the medium-gas interphase in a 37°C incubator, fully humidified 5% CO₂ for 4-10 days. Excess medium results in floating of the organ. Media was not changed during the culture but added if needed.

In addition a lower concentration of fetal bovine serum (2%) assisted in slowing and significantly decreased the necrosis process over the time span of the culture.

Fixation and Staining

A pipette with medium was used to detach the organs from the membrane. The kidneys were then washed for 1 minute X 3 with ice-cold 1 X PBS. The kidneys were fixed for 1 hour in 4% paraformaldehyde in PBS. Only fresh paraformaldehyde was used (stored at 4C no longer than 1 week old). Fixation was followed by paraffin embeddin, serial sectioning and staining with hematoxylin and eosin (Sigma-Aldrich).

For immunostaining paraffin slides were placed in Vector Antigen Retrieval solution (Vector Laboratories, Burlingame, California) and chilled. Subsequently slides were processed first with Avidin/Biotin Block solution (Vector laboratories), then with 20% hydrogen peroxide (Sigma-Aldrich) for 1 hour to block exogenous peroxidase and finally with 20% goat serum in PBS block for 1 hour. Sections were incubated overnight with anti-caspase-3 primary antibody (Cell Signaling Technology) followed by incubation with an anti-rabbit secondary antibody (Vector Laboratories)

For immunofluorescent staining sections were blocked with Avidin/Biotin Block after deparaffinization, followed by protein block for 30 minutes using the appropriate 5% goat serum in PBS. The slides were incubated in primary antibody (Santa Cruz Biotechnology, Santa Cruz, California) overnight at 4C. Subsequently the slides were washed in PBS for 5 min X 3, incubated with secondary antibody for a half-hour at room temperature and washed in PBS before development with Fluorescein/Avidin DCS (Vector Laboratories). Finally, slides were mounted using 4',6-diamidino-2-phenylindole mounting medium.

4. Selection of Amniotic Fluid Stem Cells (AFSC)

hAFSCs were collected by amniocentesis from the amniotic fluid of male fetuses (14-20 weeks gestation). The stem cell population was separated

from the general cellular milieu using standard Magnetic Sorting (MACS) techniques (Miltenyi Biotech). Stem cells were cultured in medium containing α -MEM supplemented with 20% Chang B and 2% Chang C solutions, 15% Fetal Bovine Serum, 1% L-Glutamine, and 1% antibiotics (pen-strep) [Gibco/BRL]. hAFSCs were analyzed for embryonic stem cell marker expression, clonality, maintenance of cell cycle control, and preservation of normal karyotype and telomeric length. hAFSCs were differentiated *in vitro* into multiple cell lines derived from all the three germ layers using various conditioned medium. Pluripotentiality was also confirmed by demonstrating the capacity of hAFSCs to participate in the formation of tissue and organs during the process of embryogenesis after injection into mouse blastocysts. Lac-Z and GFP labeled hAFSCs was achieved through infection with a retrovirus construct containing the cytomegalovirus promoter driving Lac-z and GFP sequences. Expression of GFP and Lac-z was seen in the infected cells after 20 hours post-infection. A clonal population was also labeled with a cell surface marker CM- DIL (Molecular Probe) using standard protocols in order to track the cells after injection.

5. In vitro experiment for the renal differentiation of hAFSC

Co-culture system

Kidney rudiments were dissected from timed pregnant C57 mice and sprague dawley rat embryos at E 13.5 days of gestation. The UB was separated from the metanephric mesenchyme by incubating kidney rudiments in trypsin and DNase [Sigma-Aldrich] and by mechanical separation. After suspension in Matrigel (BD Bioscience), the UB was cultured in media conditioned with the following growth factors: Glial-Derived Neurotrophic Factor and Fibroblast Growth Factor-1 (BD Biosciences), FBS (Gibco/BRL), and antibiotics (pen-strep) (Gibco/BRL) in an incubator at 5% CO₂ and 37⁰C. A co-culture system was designed using isolated UB isolated as above placed on top of a polycarbonate filter with a total of 1000 hAFSCs suspended in 50 μ l of media seeded onto the

tip of the branching UB. The entire co-culture apparatus was incubated at 5% CO₂ and 37 °C and cultured up to 10 days.

Microinjection

hAFSC were trypsinized, counted, and loaded into a 15µm diameter transfer tip (Eppendorf AG), guided by a micromanipulator (Eppendorf TransferMan NK2) and a CellTram Oil injector (Eppendorf), at a concentration of 1000 cells/µL of medium with no serum. Immediately before injection, kidneys were placed on a polyethylene terephthalate track-etched membrane (Sterlitech Corporation). Each kidney received a single injection (1-2 µL) and immediately placed on the top of a Transwell filter in the incubator for 2 to 10 days.

Live imaging

A microscope incubator-chamber (Leica®) was used to monitor position, migration, and possible replication of hAFSC within the embryonic kidney environment. Pictures were taken every 4 hours for 4 days using Leica Deblur software.

Histology

Kidneys were fixed in 4% buffered paraformaldehyde [Sigma-Aldrich] for 1 hr, routinely processed, embedded in paraffin, and sectioned at 5 µm. The sections were stained with hematoxylin and eosin (H&E) [Sigma-Aldrich] and toluidine blue [Sigma-Aldrich] using standard histological protocols. For in total organ X-Gal staining, kidneys were fixed in 4% paraformaldehyde [Sigma-Aldrich] in PBS at 4°C for 30 min while rocking, washed twice for 10 min in PBS at 4°C, transferred into freshly prepared X-gal [rpi Research Products International Corp.] solution, and stained at 37°C until a clear precipitate formed [16]. For vibratome [Leica®] sections, samples were embedded in an albumin (300mg/ml)-gelatin (5mg/ml) mix [Sigma-Aldrich], cross-linked with glutaraldehyde (0.6%) [Sigma-Aldrich], and sectioned at 30-40 µm before viewing under light microscopy.

Chromogenic In Situ Hybridization (CISH)

CISH was used to detect the Y-Chromosome of hAFSCs after injection into the embryonic kidney. Formalin-fixed paraffin embedded (FFPE) tissue sections were used for this procedure according to the manufacturer's instructions. Zymed's SPOT-Light CISH (Chromogenic In Situ Hybridization) Centromere Kit detected Zymed SPOT-Light Human Chromosome Y Probes [Zymed Laboratories Inc.]. Briefly, FFPE sections were incubated at 55°C overnight, and the slides deparaffinized in xylene and graded ethanol [Sigma-Aldrich]. Heat pretreatment was carried out in pretreatment buffer at 94-95°C for 5 minutes and after application of Zymed SpotLight Chromosome Y Probe the slides were cover-slipped and the edges sealed with rubber cement. The slides were heated at 95°C for 5 minutes followed by overnight incubation at 37°C using a moisturized chamber. Post-hybridization wash was performed the next day and followed by immunodetection using the CISH polymer detection kit [Zymed Laboratories Inc.]. The CISH signals were detected under light microscopy using a 40x objective.

Reverse transcription (RT)-polymerase chain reaction (PCR)

Total mRNA was extracted from the embryonic kidney, using QIAGEN mini KIT [QIAGEN], and reverse transcribed using SSII RT [Invitrogen] and Random Hexamers as primers for the first strand cDNA synthesis. The amplification of the resulting cDNA was carried out using specific human primers. RealTime PCR thermal cycler [Eppendorf] was employed after an initial denaturation step at 95°C for 10 min. We used a denaturation step at 95°C for 30 seconds, an annealing step at 60°C for 45 seconds, and an extension step at 72°C for 45 seconds for a total of 40 cycles. To rule out the possibility of amplifying genomic DNA, RNA samples were treated with a DNA-free kit [Ambion Inc.]. Detection of the PCR amplification products was performed by size fractionation on 2% agarose gel electrophoresis. As a positive control, amplification of fragments of the human β -actin RNA

was performed. Primer sequences and predicted sizes of amplicons were as follows:

1) epithelial membrane protein-1 (EMP-1):

sense 5'-ATG TCA CTC CTC TTG CTG GTG-3' -3',

antisense 5'-CGC TTC CGT AGG TGG ATG TAG-3'

2) zona occludens-1 (ZO-1):

sense 5'-AGG AGA GGT GTT CCG TGT TG-3'

antisense 5'-GCT GGT TTT GCT GTT GTT GA-3'

3) glial-derived neurotrophic factor (GDNF):

sense 5'-TAT GGG ATG TCG TGG CTG T-3'

antisense 5'-ACA CCT TTT AGC GGA ATG CTT-3'

4) aquaporin-1 (AQP-1): sense 5'-CAC CTC CTC CCT GAC TGG-3'

antisense 5'-GGT TGC TGA AGT TGT GTG TGA-3'

5) aquaporin-2 (AQP-2): sense 5'-GAT CAC GCC AGC AGA CAT C-3'

antisense 5'-GGG CAG GAT TCA TAG AGC AG-3'

6) tamm-horsfall protein (THP): sense 5'-TAG ACG AGG ACT GCA AAT CG-3'

antisense 5'-GTC CCG GTT GTC TCT GTC AT-3'

7) β -actin: sense 5'-AGA AAA TCT GGC ACC ACA CC-3'

antisense 5'-CTC CTT AAT GTC ACG CAC GA-3'

6. In vivo experiment with a mouse model of Acute Tubular Necrosis

Isolation and labelling of hAFSC

Samples of human Amniotic Fluid were obtained, under IRB approval, from discarded amniocentesis. No written or verbal consent was required since information obtained about the samples were limited to karyotype

and fetus health status. The stem cell population was separated from the general human amniotic cellular milieu using standard Magnetic Sorting (MACS) techniques [Miltenyi Biotech] against the cell surface marker, c-kit, as described by Atala *et al.* [54]. Pluripotential characteristics of the clonal and subclonal groups were tested according to protocols also outlined by Atala *et al.* [54] Clones were then cultured in petri dishes in medium containing α -MEM supplemented with 20% Chang B and 2% Chang C solutions, 20% Fetal Bovine Serum, 1% L-Glutamine, and 1% antibiotics (pen-strep) [Gibco/BRL]. hAFSC, used for *in vivo* injection, were karyotyped using standard protocols.

Before injection, a clonal hAFSC population was trypsinized in 0.05M trypsin/EDTA solution and centrifuged at 1500rpm for 5 min, and then labeled with a cell surface marker CM-Dil [Molecular Probe] following the manufacturer's instructions, in order to track the cells after injection. Briefly, the cells were incubated with 1mg/ml of CM Dil for 5 minutes at 37°C followed by an incubation of 15 minutes at 4°C and 3 washes with PBS.

ATN induction and injection of hAFSC

Rhabdomyolysis-related ATN was induced in female *nu/nu* mice [Jackson Laboratories] by intramuscular injection with 50% hypertonic glycerol solution (10 ml/kg body/wt) [Sigma-Aldrich] following deprivation of water for 22 hours. Controlled intramuscular injection of glycerol was performed under anesthesia by surgically exposing the caudal thigh muscle and slowly injecting the glycerol solution prior to delivery of cells. Animal experiments were performed in adherence to the National Institutes of Health Guide for the Care and Use of Laboratory Animals, with institutional Animal Care and Use Committee approval.

The mice were carefully anesthetized using isoflurane inhalation. Once satisfactory anesthesia was achieved, the mice were prepared for surgery using chlorhexidine. A 1 cm dorsal incision was made, both kidneys carefully delivered via the incision, and the hAFSC (1×10^6 diluted in PBS) carefully injected into the renal cortex of both kidneys with a 30-33 gauge

needle using a microinjector Eppendorf TransferMan NK2 Injector [Eppendorf]. The kidneys were then replaced into the retroperitoneum, the incision closed with polypropylene suture and the mice were allowed to recover from anesthesia. The animals were maintained on a heating pad throughout the period of anesthesia. 0.1 mg/kg of buprenorphine was administered subcutaneously and 1 mg/kg bupivacaine (a local anesthetic) along the incision margins just prior to wound closure to provide post-operative pain relief. The animals were sterilely draped to prevent contact of the kidneys with the skin of the animal to reduce risk of peritonitis. Control mice were also injected with PBS.

Tissue processing

At different times points (from 24 hours to 3 weeks), the injected and the control mice were sacrificed. The kidneys were minced and processed in one of the following ways depending on the analysis performed.

1. RNA/DNA extraction. The kidneys were minced in small pieces and the RNA extracted using Qiagen RNeasy kit according to the manufacturer's instructions. Briefly, total mRNA was extracted and reverse transcribed. Amplification of the resulting cDNA was carried out using specific human primers not coding for mouse sequences. A PCR thermal cycler [Eppendorf] was employed after an initial denaturation step at 95°C for 10 minutes. We used a denaturation step at 95°C for 30 seconds, an annealing step at the temperature specific for each primer (ranging from 54°C to 60°C) for 45 seconds, and an extension step at 72°C for 45 seconds for a total of 35 cycles. To rule out the possibility of amplifying genomic DNA, RNA samples were treated with a DNA-free kit [Ambion Inc.]. Detection of the PCR amplification products was performed by size fractionation on 1% agarose gel electrophoresis. As a housekeeping gene, amplification of fragments of the human β -actin RNA was performed. Primer sequences, predicted sizes of amplicons and specific annealing temperatures are shown in Table 1. In order to perform PCR on the genomic DNA to evaluate the presence of the luciferase gene, DNA

extraction was performed following standard protocols of the Qiagen DNeasy kit.

2. Histology. Kidneys were fixed in 4% buffered paraformaldehyde [Sigma-Aldrich] for 8 hours at 4⁰C, dehydrated through a gradual series of alcohol, embedded in paraffin, and sectioned at 4-5 μm . The sections were stained with (H&E) [Sigma-Aldrich], and PAS [Sigma-Aldrich] following standard histological protocols.

In addition, some kidneys were frozen in liquid nitrogen and stored at -20°C. When the antibody required, kidneys were cryosectioned at 5 μm and then used for immuno-histochemistry.

Labeling of the AFSC with luciferase and bioluminescent detection technique

hAFSC were transduced with a lentiviral vector (SMPU-R-MNCU3-LUC based on HIV-1 that transduces the firefly luciferase gene) made by the Vector Facility at Childrens Hospital Los Angeles following standard protocols. Two cycles of transduction were performed by removing old medium and adding new virus supernatant and medium. 24 hours after the initial transduction, cells were thoroughly washed 3 times with PBS before transplantation or *in vitro* analysis. Before *in vivo* injections, a simple *in vitro* test was employed to determine the minimum amount of hAFSC detectable by bioluminescence. Different concentrations of the cells ranging from 5×10^4 to 2×10^6 were evaluated. In addition, it was confirmed that after 20 passages in culture the cells were still expressing the luciferase gene by PCR. 10-week old *nu/nu* mice, obtained from Jackson Laboratories were injected directly into the kidney with luciferase-transduced hAFSC (1×10^6 cells/mouse diluted in PBS) after glycerol damage. *In vivo* optical imaging was performed with a prototype IVIS 3-dimensional bioluminescence/fluorescence optical imaging system [Xenogen] at different time points. Prior to imaging, each mouse was given an intravenous injection of luciferin [Promega] at a dose of 125 mg/kg, as previously described [29]. General anesthesia was then induced with 5% isoflurane and the mouse was placed in the light-tight heated chamber;

anesthesia was continued during the procedure with 2% isoflurane introduced via a nose cone. The imaging system consists of a cooled, back-thinned charge-coupled device (CCD) camera to capture both a visible light photograph of the animal taken with light-emitting diodes and a luminescent image. A rotating mirror and translatable animal stage allowed for images to be acquired over 360°.

Immunostaining

Frozen and paraffin slides were stained for immunofluorescence. Paraffin slides were deparaffinized, placed in 1% Triton for 5 minutes (if the antigen was nuclear) and briefly washed in PBS. The paraffin slides were then placed in Vector Antigen Retrieval Solution [Vector Laboratories] for three cycles. The frozen slides were fixed for 5 minutes in 80% methanol. After Avidin/Biotin blocking [Vector Laboratories] a second block was carried out for 30 minutes using the appropriate 5% normal serum in PBS. The slides were then incubated in primary antibody [Dolicholus Biflorus and Peanut Agglutinin from Vector Laboratories, Luciferase from Promega and Glial Derived Neurotrophic Factor and Aquaporin 2, Santa Cruz] solution for one hour at room temperature or overnight at 4°C. Afterwards, the slides were washed in PBS for 5 minutes for 3 times. Secondary antibodies [Vector Laboratories] were diluted 1:200 in 5% normal serum – slides were incubated in this solution for 1.5 hours at room temperature, followed by 5 minutes for 3 times in PBS. The appropriate fluorescent marker [Texas Red or Fluorescein Avidin DCS from Vector Laboratories] was then applied in a concentration of 1:500 in PBS buffer for 5-10 minutes, followed by a final 5 minutes for 3 times in PBS wash. TUNEL staining [Roche, Applied-Science] was performed to determine the presence of apoptotic cells. Briefly, the cells were incubated at 37°C for one hour with the TUNEL reagent and then washed in PBS. Slides were mounted with Vector DAPI mounting medium [Vector Laboratories]. In the experimental groups, the number of positive apoptotic nuclei was counted per 300 nuclei and hAFSC treated animals were compared to untreated controls.

Values are mean \pm SD. A Leica DM RA fluorescent microscope was used in conjunction with Open Lab 3.1.5 software to image the staining.

Blood Collection, Creatinine and BUN measurements

The facial vein was lanced with a 5mm animal lancet and blood collected using standard protocols approved by the Animal Core Facility at Childrens Hospital of Los Angeles and Saban Research Institute. Animals were divided into different groups as follow:

1. group of 10 animals for measuring baseline creatinine and BUN levels;
2. group of 10 animals that underwent ATN with no injection of hAFSC;
3. group of 10 animals that underwent ATN and intrarenal injection of hAFSC after 2 hours of glycerol injection;
4. group of 10 animals that underwent induction of ATN with glycerol and intrarenal injection of PBS after 2 hours of glycerol injection.

The blood samples (30 μ L) were collected into plasma separation tubes with lithium heparin. They were centrifuged at 13,000-RPM for 3 minutes and the plasma (upper layer) was removed and stored at -80°C until analysis. A maximum of 15% of circulating blood was sampled in a given 14-day period (total blood volume \sim 0.6% of total body weight). Post-damage measurements were obtained every 24 hours. The blood samples were used to monitor renal function, by analyzing creatinine and BUN levels. ELISA was performed according to the manufacture for both creatinine [BioAssay Systems Cat # DUCT-500] and BUN [BioAssay System Cat # DIUR-500] using 30 μ L serum samples loaded into 96-well microplates. Comparison between groups was made using an unpaired *t* test. A value of $p < 0.05$ was considered statistically significant. Analyses were done using GraphPad Prism software. Data are shown as mean \pm SD.

Morphological studies

Kidney sections were prepared at 4 μ m thickness by a routine procedure and stained with PAS reagents as described above. The kidney sections were divided into six main groups:

1. Mice that underwent ATN with no injection of hAFSC at sacrificed at 24 hours;
2. Mice that underwent ATN and injection of hAFSC after 2 hours of glycerol injection sacrificed at 24 hours;
3. Mice that underwent ATN with no injection of hAFSC sacrificed at 48 hours
4. Mice that underwent ATN and injection of hAFSC after 2 hours of glycerol injection sacrificed at 48 hours
5. Mice that underwent ATN with no injection of hAFSC sacrificed at 72 hours;
6. Mice that underwent ATN and injection of hAFSC after 2 hours of glycerol injection sacrificed at 72 hours.

Tubular injury was evaluated based on three major parameters using PAS staining: 1. Disruption of the tubular membrane; 2. Disruption of brush borders 3. Cast formation.

In the experimental groups, the damaged tubules were counted as a fraction of the total number of tubules present in the section using consecutive, non-overlapping fields of PAS-stained specimens. The percentage of damaged tubules was estimated without knowledge of the experimental group Values are mean \pm SD.

Cytokine analysis

To examine pro-inflammatory and anti-inflammatory cytokines that were generated after glycerol-induced ATN (with or without injection of cells), human and mouse cytokines levels were measured in digested mouse kidneys using a multiple cytokine array technique Proteome Profiler Array Kit. Briefly, kidney tissue was homogenized in a cell lysis buffer, and the homogenates were centrifuged at 12,000 rpm for 15 minutes at 4°C. Total protein concentration in each supernatant was determined using a Cytokine Array Kit (for human c# ARY005 and for mouse c# ARY006), as

suggested from the protocol [R&D Systems, Inc.]. The data were analyzed using the Array Vision Program [R&D Systems, Inc.].

7. Selection and characterization of Metanephric Mesenchyme derived cells (MMDC) and kidney progenitor cells (AKPC) from the whole Amniotic Fluid

Immunoseparation of MMDC and AKPC from whole Amniotic Fluid

A positive population from AF for both CD24 and OB-Cadherin (MMDC) was selected incubating the total cell population with these two specific antibodies for 30 minutes at 4° C on a rocking platform, followed by second incubation with immunomagnetic microbeads for 5 minutes at 25° C and then 15 minutes at 4° C followed by immunoseparation by MS columns (Miltenyi Biotech, Germany). Positive and negative (used as a negative control) selected populations were replated on Tissue Culture dishes with Chang's Media for subsequent expansion. A further immunoselection from the MMDC to identify 4 subpopulations of renal progenitors (AKPC) was performed as above described, using anti-Human antibodies for Nephryn, TrKA, PDGFR α and E-Cadherin following the previously described immunoseparation technique. Final subpopulations were obtained after a total of 18 passages from the original samples. Cells were reseeded under the same conditions used for the total AF cell population and the main selection for MMDC cells.

Characterization of MMDC and AKPC by RT-PCR

The CD24+OB-Cadherin+ population (MMDC) was investigated by RT-PCR for early and mature kidney markers.

After the immunoselection, the four subpopulations of AKPC were analyzed according to the same panel of markers in order to investigate differences and common traits between the Nephryn+, TrKA+, PDGFR α +

and E-Cadherin+ AKPC derived populations following the protocol previously described.

Analysis and characterization of MMDC and AKPC by Real Time PCR

MMDC and AKPC were analyzed by Real Time PCR as previously described. Markers analyzed were: GDNF, LIM-1, PAX-2, Nephrin, OCT-4, TrKA, PDGFR α , E-Cadherin, ZO-1 and Occludin. Analysis was performed following the previously described protocol.

RESULTS

1. Characterization of Amniotic Fluid cells by expression of markers for the three germ layers and progenitor cells

Amniotic Fluid Total Cell Population Culture

The morphology of the total cell population is very heterogeneous with a preponderance of fibroblastoid shapes (Figure 1). The expansion of the total population of Amniotic Fluid was possible for up to 10 passages using DMEM. Therefore, after these few passages, the cells stopped growing and started dying. Nevertheless when the cells were cultured in Amniomax II and Chang media they could be expanded for more than 50 passages in culture. The cells cultured with Amniomax II acquired a defined fibroblastoid shape. We therefore chose to culture cells in Chang media for all experiments, since cell morphology did not change significantly over subsequent population doublings.

Analysis and characterization of human Amniotic Fluid cells by RT-PCR

AF Total Cell Population was stratified by week of gestation (from 15 to 20 weeks) and analyzed using RT-PCR. As shown in Figure 2 A-B-C, expression of markers for the three germ layers, for pluripotent cells as well as for mesenchymal, hematopoietic and early progenitor cells of several organs were analyzed.

Expression of genes characteristics of the Endodermal and Mesodermal germ layers was found to decrease over time, while ectodermal markers remained constantly expressed (Figure 2A).

Pluripotent markers were expressed in all samples younger than 19 weeks.

While mesenchymal marker CD90 is expressed at all the time points analyzed, CD34 (Marker for mature haematopoietic lineages) was absent in early gestation samples, but appeared in samples of 18 weeks of gestation or older (Figure 2A).

Early progenitor markers were expressed in 18 weeks and older samples (Figure 2B) as well as specific kidney markers. (Figure 2C)

Analysis and characterization of human Amniotic Fluid cells by Western Blotting

The protein expression of the cells showed a decrease on endodermal and mesodermal layers over the course of gestation while, as seen with the mRNA expression, ectodermal proteins are constantly present along the gestational age investigated in this study. Pluripotent, hematopoietic and mesenchymal markers follow the same trend seen in the RT-PCR analysis. (Figure 3A)

The early proteins of progenitor cells from different organs, as shown in Figure 3B, show increased expression into Amniotic Fluid cells over the course of gestation. Kidney specific proteins were shown to increase around 17-18 weeks of gestation as shown in Figure 3C.

Analysis and characterization of total Amniotic Fluid cell population by Real Time PCR

Four samples for each chosen time points (15-16, 17-18 and 19-20 Gestational Age Weeks) for a total of 12 samples were analyzed. The investigated samples for all the markers analyzed confirmed the same overall trends showed by RT-PCR analysis. However, some of the markers such as Brachyury, Tal-1, Nephric, GDNF, TrKA were not expressed in one or more samples. Goosecoid and PDX-1 were not found in any of the twelve samples analyzed.

The ectodermal marker E-Cadherin increased 15-fold between 15-16 and 17-18 weeks of gestation. In contrary NCAM and FGF5, while confirmed to be present, did not change significantly between 15 and 20 weeks. (Figure 4A). The Endodermal marker CXCR-4 increased 3.5-fold between 15-16 and 19-20 weeks while the other Endodermal markers Sox-17 and AFP tended to decrease. (Figure 4A)

The mesodermal marker Brachyury was expressed at 15-16 weeks in one sample but not later on. TAL-1 appeared to decrease over time, while FLK1 increased 4-fold. (Figure 4A)

Pluripotency marker OCT4 didn't change over the investigated weeks of gestation while C-kit marker increased by 3-fold between 15-16 and 17-18 weeks and disappeared in the older samples. (Figure 4B)

Hematopoietic marker CD34 decreased between the 17-18 and the 19-20 weeks in contrast with mesenchymal marker CD90 that increased 2 fold by 17-18 weeks old samples. (Figure 4B)

Progenitor markers, excluded PDX-1 that showed no expression, generally increased with the progression of the gestation; NKX2.5, early cardiac marker showed a 6-fold increase between 17-18 and 19-20 weeks while lung/Thyroid marker TTF-1 increased 1 fold between 15-16 weeks and 17-18 weeks and an additional 2.5 fold to 19-20 weeks. (Figure 4C)

CEBPG showed a 5 fold increased expression at 17-18 weeks if compared with the 15-16 and 19-20 weeks of gestation. (Figure 4C)

Renal marker GDNF was expressed only in two of the samples, increasing 5 fold between the 15-16 sample and the 19-20 weeks sample. (Figure 4D)

Undifferentiated Metanephric Mesenchyme markers CD24 and Ob-Cadherin increased 1 fold between 15-16 and 17-18 weeks. While CD24 expression remained unchanged between 17-18 weeks and 19-20 weeks, Ob-Cadherin decreased to the previous expression. (Figure 4D)

PAX-2 increased slightly between 15-16 and 19-20 weeks while LIM1 didn't change its expression. (Figure 4D)

One sample for each time period was positive for Nephlin, showing a constant increase over the time with a 1-fold increase between 15-16 weeks and 19-20 weeks of gestation. (Figure 4D)

Zo-1 and Aquaporin-1 marker didn't change significantly overtime while Occludin increased 8-fold between 17-18 weeks and 19-20 weeks. (Figure 4E)

PDGFR- α expression did not change significantly over the progression of the gestation while TrKA expression of the only three positive samples decreased 4 fold between 17-18 and 19-20 weeks. (Figure 4E)

2. Long term ex-vivo whole embryonic kidney culture

Our original protocol made possible what is to our knowledge the longest reported culture time for embryonic kidney (up to 10 days) with the preservation of UB branching and fine tubulogenesis in vitro (Figure 9). Histological examination of the specimens revealed initial distal UB ramification and condensation of MM cells at the branching UB tips. No endothelial elements or primitive capillaries were present at this stage of embryonic gestation (E12 to E13) in the metanephric blastema. By 24 to 48 hours of in vitro culture nephrogenesis had proceeded through the early stages of normal tubular development in the explants (Figure 10). [57]

Reciprocal inductive interactions between the 2 primordia (UB and MM) induced dichotomous branching of the UB, initiating morphogenesis of the collecting duct system. Condensation and aggregation of the metanephric mesenchyma at the tips of the branching ureteral bud formed normal renal vesicle structures. After primordial connection between the MM and UB we noted that kidney growth progressed toward the natural succession of primitive nephron structures, comma-shaped and S-shaped body elements, with final maturation into end structures, including glomeruli, a proximal and distal convoluted tubule, and collecting duct canalization (Figure 11). Glomeruli were formed by a central core of well preserved, elongated epithelial cells and surrounded by a regular shaped capsule of squamous epithelial cells, also lacking in vascularization.

The degree of glomerular epithelial differentiation that occurs in our system is similar to what occurs in vivo. The lower and middle limbs of the S-shaped tubule persisted for 72 to 96 hours of culture. The lower limb of the tubules formed a double lumen hemisphere and the middle limb differentiated into discrete proximal tubules (Figure 11 A and B). The expression of GDNF, an essential inducer of UB, was found in E15

embryonic kidneys after 5 days of culture (Figure 11 C). GDNF expression was localized to the MM adjacent to the tip of the UB and immunofluorescence could be seen in UB cells, which express GDNF receptor. Immunofluorescence staining for Pax-2 was noted on the branching UB and adjacent MM in an E15 embryonic kidney after 5 days of culture (Figure 11 and 12).

The kidney culture environment remained intact and cells survived up to 10 days in culture without signs of necrosis. A clear distinction between the cortex and medulla was maintained, accompanied by good quality glomerular and tubular structures without evidence of apoptosis (Figure 13).

3. Selection of Amniotic Fluid Stem Cells

We have been investigating a novel population of human stem cells derived from amniotic fluid. These hAFSC are magnetically separated from the rest of the cell population to acquire a specific totipotent group of cells that display true embryonic stem cell characteristics (Figure 14). They express embryonic stem cell markers including Oct-4 and SSEA-3. hAFSC were also capable of differentiating into cell lines from all three germ layers both *in vitro* and *in vivo* under specific culture conditions [54].

hAFSC before injection present a fibroblastoid shape as shown in Figure 14. hAFSC were analyzed for the expression of early and late kidney markers before injection. As shown in Figure 14 B, hAFSC were negative for the most important kidney markers, ranging from transcription factors expressed during early kidney development to late differentiation markers. Thus, we confirmed that hAFSC are not specifically committed to kidney progenitor cells when cultured *in vitro*. The cells were then tested to confirm a normal karyotype before *in vivo* applications in order to exclude chromosomal abnormalities that could compromise their pluripotential capability (Figure 14 C).

4. In vitro renal differentiation of hAFSC

Ureteric Bud induces hAFSC to form tubular structures

The ureteric bud (UB) originates from the Wolfian Duct of the embryo and undergoes branching morphogenesis to ultimately partake in the formation of the collecting system and is absolutely essential for normal organ development. We postulate that placement of stem cells into a predominantly embryogenic environment while organogenesis is occurring can be optimal for cell differentiation to take place. To test this hypothesis, we used different culture models designed to recapitulate the developmental pathways of kidney organogenesis starting with the tubular network of the kidney's collecting system. Various conditions were tested to acquire a reliable culture system for hAFSC induction into a tubular network that resembled the primordial branching system of the ureteric bud (UB) (Figure 15). hAFSCs were, therefore, tested for their capacity to form tubular structures in a novel embryonic co-culture system that combined the branching UB with hAFSCs (Figure 15). UB plus metanephric mesenchyme conditioned medium with growth factors GDNF and FGF1 provided the optimum culture environment for hAFSC tubulogenesis to occur (Table 1). GFP⁺ hAFSCs were seeded onto a branching UB microdissected from developing rat metanephros, gestational age 13.5 days (Figure 15), and examined for morphologic changes and gene expression indicative of renal differentiation.

GFP⁺ hAFSCs gave rise to fluorescently labeled tubules by day 5 of co-culture. Lac-Z⁺ (nuclear stained) hAFSC also formed tubular structures when co-cultured next to a branching UB identified under light microscopy (Figure 15). hAFSC renal differentiation was confirmed by reverse transcriptase RT-PCR demonstrating gene expression of aquaporin 1 (AQ1) in the cells, a membrane channel protein specific for the proximal convoluted tubule of the kidney. Undifferentiated hAFSC controls demonstrated no expression of AQ1.

Evidence of hAFSC integration into embryonic kidneys

Under appropriate culture conditions, hAFSCs were capable of assimilating into the developing structures of embryonic kidney after injection of the cells into the middle of the organ and, as a result, participated in organogenesis. hAFSCs were of clonal origin that guaranteed a homogeneous population. Prior to injection, the hAFSCs were infected with a retrovirus coding for both GFP and β -galactosidase (Lac-Z) in order to track the cells *in vitro* (Figure 16). Moreover, cells were also labeled with cell surface marker CM-Dil (Figure 16) for easy identification under stereo microscopy during the injection phase (Figure 16). Histochemical analysis as well as live imaging of the specimens were performed at serial time points. After 4 days of fluoroscopic live imaging of the injected kidney, hAFSCs seem to follow a natural branching pattern during organogenesis of the organ (Figure 17). After 3 days of culture, vibratome sections examined under light microscopy revealed that lac-z⁺ hAFSCs had migrated from the center of the kidney to the periphery of the organ in the exact centrifugal fashion that normally occurs during kidney development in the embryo. No lac-z signal was seen in controls consisting of kidneys cultured in identical conditions as above but with no injected cells (Figure 17). [55]

Light microscopy with H&E counter stain was used to detect Lac-z⁺ cells within important renal precursors to the glomerular and tubular components of the nephron. Four days after injection hAFSCs were amassed within S-shaped bodies of the murine embryonic kidney. This demonstrated their capacity to undergo an obligatory mesenchymal-to-epithelial transition that is normally observed with native metanephric mesenchymal cells and complete an important step in the developmental pathway of the kidney (Figure 18). Formation of nephron structure is predetermined by location on the metanephric mesenchyme by the hAFSCs. After lac-z staining, histologic sections demonstrated that hAFSCs were able to survive and follow the natural branching pattern of the developing kidney, localizing to just around the tip of UB. After 5 days cells injected into E13 kidneys integrated into C and S-shaped structures,

stroma and renal vesicles (Figure 18). No Lac-z⁺ cells were detected in the controls.

hAFSC labeled with a surface marker CM-Dil were identified after injection as having assimilated into developing kidney primordial structures. After 6 days of culture, these cells has integrated into embryonic tubular and glomerular structures which ultimately give rise to mature nephrons (Figure 18).

The presence and the integration of the hAFSC in the injected kidneys were also confirmed using Chromogenic In Situ Hybridization (CISH) (Zymed, San Francisco, CA). The population of hAFSC used in all experiments were derived from male fetuses and, therefore, chromosomally XY. Specimens were incubated with biotinylated probes against the Y chromosome and counterstained with DAB(3,3-diaminobenzidine) in a peroxidase reaction. Positively stained cells were visualized under light microscopy lining the walls of the embryonic kidney tubules (Figure 19). This comprised both medullary and cortical portions of the kidney. No signal was identified in the controls.

Molecular evidence of primordial kidney differentiation

After 9 days of culture, RT-PCR was performed on specimens and expression of several specific human kidney genes in the injected embryonic kidneys were identified. Zo-1, Claudin and GDNF, early markers for kidney differentiation, were detected when compared to controls, which consisted of hAFSCs before injection (Figure 20).

5. In vivo model of acute tubulonecrosis integration

Glycerol induced muscle damage and ATN. Hematoxylin and Eosin (H&E), Period Acid Schiff staining (PAS), TUNEL

Figure 22 A demonstrates the normal morphology of a mouse kidney (*nu/nu*) before any damage. The distinction between the medulla and the cortex is clearly evident, and the tubules are intact as well as the glomeruli. Figure 22D shows the morphology of the kidney 3 days after the

intramuscular injection of glycerol. ATN caused a marked disorganization in the structure so that medulla and cortex are not distinguishable. The normal structure of proximal and distal tubules is lost (with cast formation), while most of the glomeruli remain intact. This type of damage is typical of the injury induced by rhabdomyolysis, where the main structures of the kidneys that undergo failure are the tubules and not the glomeruli. Figure 22 F shows the increase in apoptotic cells (TUNEL staining) when compared with the control, that did not undergo glycerol induced muscle damage (Figure 22 E). The difference in the number of apoptotic cells present in the treated glycerol mice when compared with the untreated control mice was highly significant (Figure 22 F)

In vivo detection of hAFSC by bioluminescence

hAFSC transduced with a lentivirus coding for luciferase showed stable expression of the transgene over many population doublings. Figure 23 A shows control cells that were not infected versus infected cells exposed to luciferin (the luciferase substrate) to confirm the presence of the signal under bioluminescence detection after 20 population doublings. In Figure 23 B it is shown an *in vitro* experiment determining the limit starting point of 1×10^5 cells that exhibits a signal optically detected under bioluminescence.

1.2×10^6 hAFSC injected directly into the right kidney after damage induction (Figure 23 C) were easily detected. The signal is clearly evident and spreads into multiple zones of the body such as the lung over the first few days. The signal for hAFSC in the area of the kidney can be seen at 24 hours after injection (panel 3), was strongest at 48 hours and 72 hours, and persisted for up to 6 days (panels 4-6), after which the signal began to diminish over the next several days (panel 7). However, 21 days after injection, the signal was still evident in the area of the kidney (panel 8).

DNA extraction and PCR were performed at 21 days on injected and non-injected kidneys in order to determine the presence of luciferase. Results show that luciferase and human *ATCB* DNA, was present only in the

injected kidney tissue, as confirmed by the absence of the housekeeping *ATCB* (Figure 23D). DNA was extracted from the entire injected kidney. The results were also confirmed with a positive immunostaining against luciferase as shown in Figure 23

Detection of hAFSC in damaged kidneys by immunohistochemistry and gene expression

The presence of injected hAFSC was evaluated histologically. Frozen sections performed at 1 week after injection confirmed the presence of hAFSC, detected by red fluorescence of the surface marker CM-Dil (Figure 24 A). We were able to observe several instances where the CM-Dil signal from the hAFSC overlapped with the fluorescent-staining of a kidney marker as follows: luciferase positive hAFSC were double stained for Aquaporin2, Peanut Agglutinin as well as Dolichus Biflorus Agglutinin at 3 weeks after injection; indicating that hAFSC are able to differentiate into cells expressing both adult proximal and distal tubular agglutinins (Figure 24 B, D). In some rare cases hAFSC were also found in glomerular structures expressing Glial Derived Neurotrophic Factor (Figure 24 E), indicating that the stem cells were also able to express early glomerular markers of differentiation.

After 21 days, RT-PCR was performed using human specific primers on the harvested kidneys and expression of several human specific kidney genes (early as well as late markers of differentiation) by the hAFSC in the injected kidneys were identified: *NPHS1*, *AQP2*, *PAX2*, and *OCN* when compared to hAFSC before injection (Figure 24 F)

Creatinine and Blood Urea Nitrogen (BUN) measurements

A control group of 10 *nu/nu* mice was used to determine the basal level of serum creatinine before any treatment, which averaged 0.6 mg/dl. After intramuscular injection of glycerol on day 0, creatinine levels increased to as high as 1.10 mg/dl, showing a peak between 48 and 72 hours after injections. Similarly, the level of BUN (basal level of 27mg/dl) increased

after glycerol injection and the peak was detected around 48 and 72 hours. The concentration of both creatinine and BUN returned to normal level after 3 weeks. Further analysis showed no statistical in significant difference in creatinine and BUN levels between the animals that were injected with saline vehicle solution versus no injection following intramuscular glycerol, and therefore these groups were pooled for statistical analysis. In contrast, animals subjected to damage induced with intramuscular glycerol and receiving an intrarenal hAFSC injection demonstrated no increase in levels of creatinine (Figure 25 A) or BUN (Figure 25 B) during the expected acute phase of injury.

Morphological studies

In Figure 26 an increase in the number of damaged tubules is seen from 24 hours to 72 hours in the glycerol-treated animals. By 72 hours the damage is more severe due to the cast formation (arrow, Figure 26 C) within damaged tubules. In Figure 26 (D,E) is evident that in glycerol-injected animals treated with hAFSC the number of damaged tubules increased at 48 hours compared to the animals that were not injected with stem cells, but by 72 hours the number of damaged tubules decreased significantly. Two-factor ANOVA showed a highly significant effect of time ($p= 0.03$) and interaction of time with treatment ($p=0.01$) as shown in Figure 26

Immuno-cytokine profile

Since the salutary effect of hAFSC injection occurred during the acute phase of ATN, we postulated that this protective effect might involve acute changes in the kidney's cytokine milieu. The cytokine profile of human as well as mouse cytokines expressed in the kidney at 24 hours and 48 hours after intramuscular injection of glycerol is compared to undamaged controls and mice with glycerol-injected and intrarenal injection of hAFSC. Cytokine levels are shown as comprehensive suite of sequential bar graphs (Mean and SD) in Figure 27 For relative ease of interpretation, the different cytokines were displayed as four broad functional clusters based

on their principal immunological functions. 1. Anti-inflammatory 2. Pro-inflammatory 3. Chemoattractants and 4. Multiple biological effects. For each individual cytokine, the bars in the figure show from left to right, control cytokine levels, ATN kidney at 24 hours, ATN kidney plus hAFSC injection at 24 hours (shown as the sum of mouse derived plus hAFSC derived human cytokine levels). This order of display is then repeated at 48 hours.

The mouse specific cytokine assay does not cross react with the human cytokine assay. This was confirmed by incubating mouse digested kidneys with membranes specific for human cytokines and conversely incubating hAFSC with membranes specific for mouse cytokines (data not shown).

The mouse tissue is exposed to the activity of both human and mouse cytokines at both time points shown (24 hours and 48 hours). When viewed in this fashion it becomes clear that the major trend of the analyzed combined cytokine levels is a significant increase in the early cytokine response. Thus, 24 and 48 hours following intramuscular injection of glycerol, at the time of peaking kidney damage, mice without hAFSC injection had significant elevation (as much as 5 or 6-fold) of cytokine expression level across all 4 classes of cytokine. However, when glycerol-treated mice were injected with hAFSC, an even greater elevation of cytokine levels was evident, particularly at 24 hours when both mouse and human cytokine levels were combined. However, by 48 hours, this trend in combined cytokine levels is reversed so that the majority of combined cytokine levels are either reduced significantly or no longer elevated relative to the kidneys that did not receive hAFSC. Further, by 48 hours the relative contribution of human versus mouse cytokines is also reversed, with the human component of the cytokine milieu being relatively small.

6. Selection and characterization of Metanephric Mesenchyme derived cells (MMDC) and Kidney Progenitor cells (AKPC) from the whole Amniotic Fluid

Immunoseparation of MMDC and AKPC from whole Amniotic Fluid

A specific cell population positive for CD24 and OB-Cadherin (MMDC) was successfully isolated from whole Amniotic Fluid and cultured under the conditions described above.

MMDC selected cells present a different morphology with typical fibroblast shapes (Figure 29). From the CD24+OB-Cadherin+ population, AKPC subpopulations expressing TrkA, Nephlin, PDGFR- α and E-Cadherin were successfully obtained by immunoseparation. (Figure 7)

Characterization of MMDC and AKPC by RT-PCR

The MMDC population (CD24+ Ob Cadherin+) (Figure 30) and the four derived AKPC subpopulations were characterized by RT-PCR for early and mature kidney markers, as well as pluripotency markers (Figure 31). Expression of renal markers differed in the investigated populations as shown in the figures. The AKPC E-Cadherin+ population expressed E-Cadherin, GDNF and was slightly positive for Nephlin.

AKPC Nephlin+ cells were positive for Nephlin, Aquaporin 1 and Zona-Occludens 1. The population immunoselected for AKPC PDGFR- α + was positive for ZO-1 and PDGFR α while the AKPC TrkA+ population expressed TrkA, ZO-1 and, slightly, PDGFR α . (Figure 8)

Analysis and characterization of MMDC and AKPC by Real Time PCR

The main population MMDC and the four AKPC subpopulations were analyzed by Real Time PCR (Figure 7) for the expression of specific kidney markers. GDNF, Metanephric Mesenchyme specific marker, was expressed by the main population and was almost 12 fold greater in the Nephlin+ subpopulation, but absent in the other subpopulations.

LIM-1 was 11 folds greater in the Nephlin population and increased 9 folds in E-Cadherin population. It was increased in the TRKA+ population. PAX-2 increased 4 fold in Nephlin. Nephlin expression was 2 fold greater in Nephlin population. (Figure 7A)

Pluripotent marker OCT-4 was increased 10 fold in Nephrin+ AKPCs , 15 fold in E-cadherin+ population and 2 fold in TRKA. (Figure 7A) E-Cadherin+ cells showed a 3 fold increase in E-Cadherin expression, decreased in PDGFR α + and slightly in TRKA. (Figure 7B) TRKA showed no increase in TrKA expression if compared with the main population but the other population were negative for TrKA. PDGFR α increased 2 fold in PDGFR α + APKCs, decreased in Nephrin+ and was practically absent in E-cadherin+ APKCs. ZO-1 was increased 7 fold in the Nephrin population but absent or slightly expressed in the other subpopulations. Occludin was 3.5 fold greater in Nephrin+ APKCs, 7 fold greater in E-Cadherin and 1.5 fold greater in PDGFR α + cells. (Figure 7B - 8)

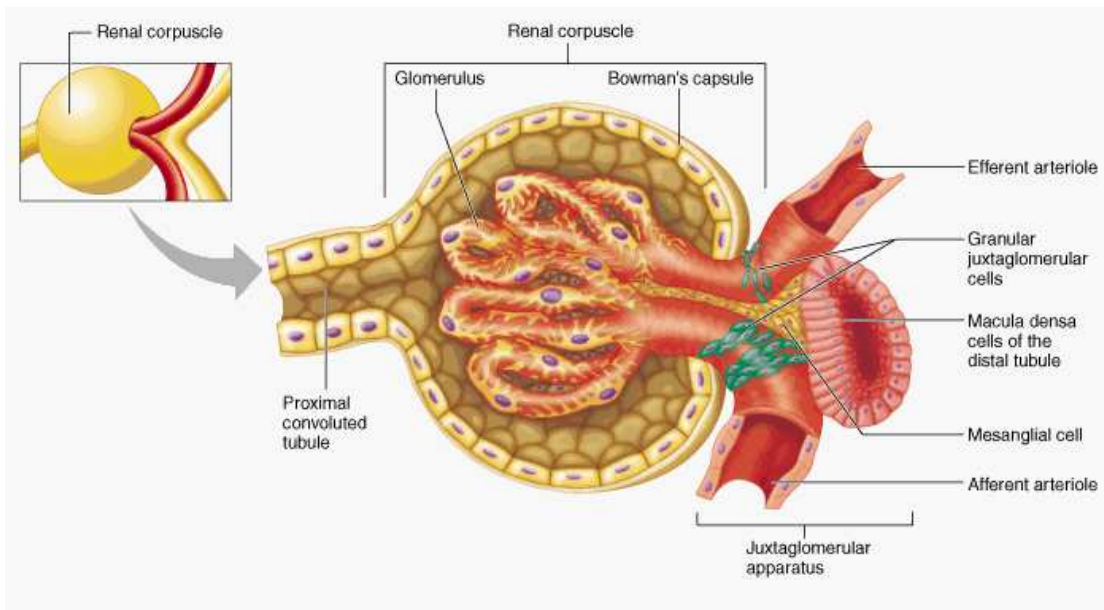
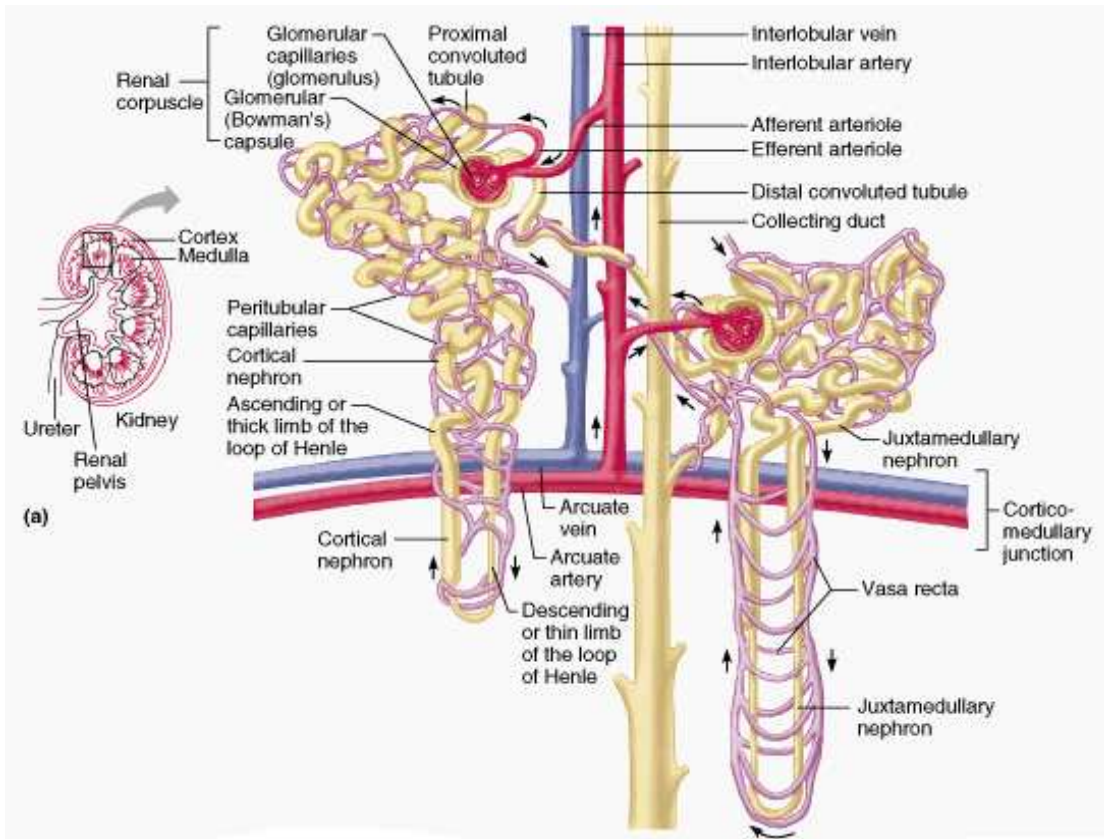
DISCUSSION

The adult kidney is a highly vascularized organ, receiving about 20% of the blood supply of the body. The kidneys filter about 180 liters of fluid per day with an electrolyte composition similar to that of plasma and the nephrons have the responsibility of handling this large volume of filtrate and separating that which must be conserved and that which needs to be excreted. The basic functional unit of the kidney is the nephron, composed of a tubular system and a glomerulus. The tubular system has four components: (a) proximal tubule, (b) loop of Henle, (c) distal tubule, and (d) collecting tubule (see below).

The kidneys filter about 180 liters of fluid per day with an electrolyte composition similar to that of plasma. The role of tubules is the reabsorption of water and electrolytes in order to maintain the body homeostasis and each segment is specialized in a different process of water and electrolytes intake.

In the proximal tubule, water, electrolytes and glucose are reabsorbed from the filtrate. The connection between the proximal tubule and the loop of Henle is called descending loop. In the descending loop, the concentrations inside and outside the tubule are increasing with the current, with the maximum concentration being reached at the bottom of the loop. The increased concentration is the result of the passive diffusion of Na^+ into the tubule and water out of the tubule. When the filtrate reaches the distal tubule, a net loss of Na^+ and water has occurred through the loops of Henle.

In the ascending loop, Na^+ (or any solute) is actively pumped out of the tubule. As flow continues up the loop, the tubular concentration decreases as does the interstitial concentration. Because water is impermeable in the ascending loop, the volume at the bottom of the loop is the same as that



Schematic representation of kidney structure. A General representation of the kidney showing the tubular, glomerular and vascular organization in the renal compartment. **B.** Organization of the glomerulus with the capillary network surrounded by the Bowman's Capsule.

entering the distal tubule. At the bottom of the loop, the tubular and interstitial concentrations are equal. Inside the distal and collecting tubules, the filtrate is either diluted or concentrated to form urine.

But the kidney function is not only to maintain the balance of water and electrolytes. A key role for the kidney is to avoid the loss of any essential molecule from the blood. The glomerulus is the compartment in charge of discriminate what may be discarded and what needs to be preserved.

The glomerulus is a specialized capillaries network of interconnected loops surrounded by Bowman's capsule. The glomerular capillaries have unique characteristics that contribute to its filtering capabilities. The porosity of the endothelial layer increases capillary permeability, the mesh-like structure of the basement membrane provides a barrier to large molecules, and the portal structure allows maintenance of an intracapillary pressure that favors filtration.

The Bowman's capsule is made up of two cell layers: the visceral layer that forms the epithelial layer (podocytes) of the filtration barrier and the parietal cell layer that forms the outer layer of the capsule. The space between the two cell layers, referred to as Bowman's space, collects the filtered fluid and solutes and directs this filtrate toward the proximal tubule.

The glomerular membrane has three layers: (a) endothelial, (b) basement membrane, and (c) epithelial. The endothelium lines the capillary lumen and contains many pores, or fenestrae, that favor the filtration of fluid and small solutes. The glomerular basement membrane (GBM), mainly produced by podocytes, is a matrix of collagen and similar proteins as well as glycosaminoglycans that provides a size and charge barrier to the movement of large particles out of the capillary lumen. The visceral epithelial cells of Bowman's capsule, or the podocytes, have cytoplasmic foot processes that extend over the basement membrane. Spaces between these foot processes are called slit-pores and allow the filtrate into Bowman's space. Mesangial cells are located between the capillary loops of the glomerulus and form a support network within the tuft. The glomerular membrane allows filtration of fluid and small molecules. Large molecules are prevented from entering the filtrate in two ways. First the

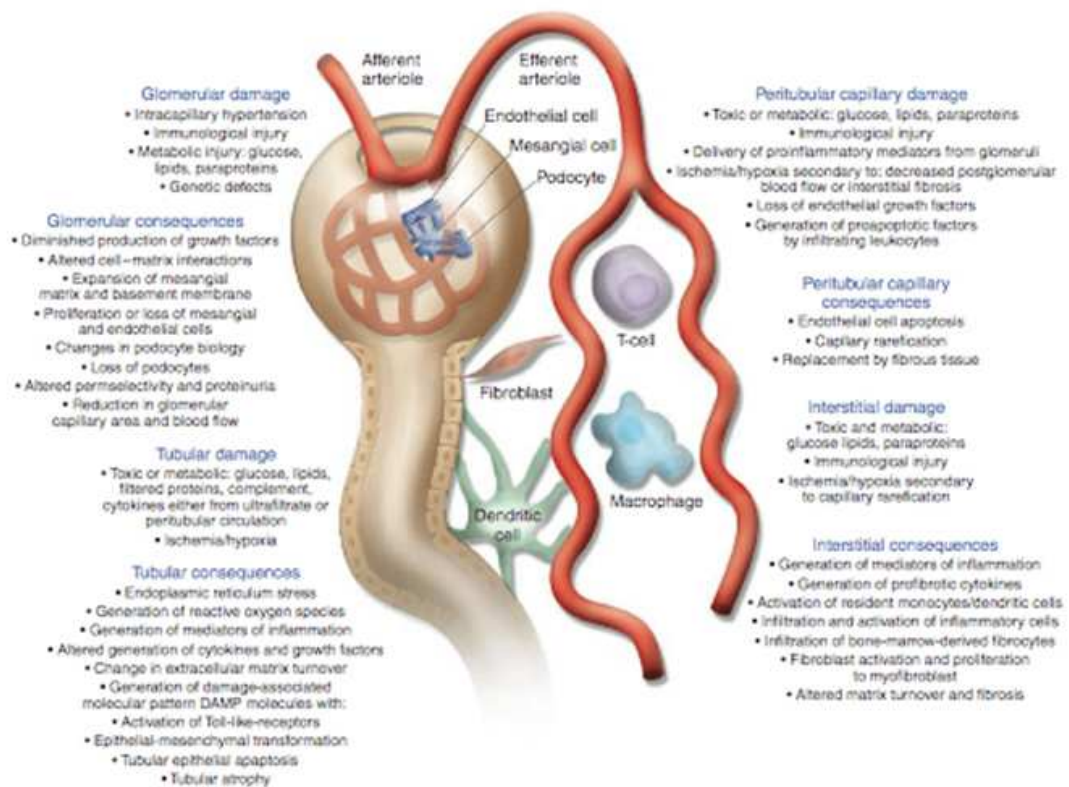
size of the spaces in the glomerular epithelium and basement membrane limits the passage of these larger molecules and cells such as the white and red blood cells and albumin. Second, the podocytes and, to some extent, the GBM have a net negative charge that repels large negatively charged molecules, particularly the plasma proteins. Small anions that easily filter through the pores are not influenced by the negative electrical charge.

Since kidney is in charge of blood purification (ultrafiltration) with maintenance of acid/basic balance, metabolites elimination and blood pressure control, when damage occurs, the effects are notable in many other organs and tissues of the body.

In this work we focus mainly our attention to the Acute Kidney Disease (AKD) but we know it can progress to the more dangerous Chronic Kidney Disease. CKD is often referred as a “silent” disease because no evident symptoms or pain are caused. Nonetheless, many are the chemical changes that origin from CKD injury.

Neuropathies and bone disorders are common in patients with CKD and more than 70% of patients with CKD were reported to undergo hypertension. High blood pressure is well known as involved in cardiac and vascular diseases such as heart enlargement, congestive heart failure, heart attacks and strokes. In addition, hypertension is causing even a faster loss of kidney function.

Since kidney is involved production and release of hormones like erythropoietin, stimulating proliferation and differentiation of erythroid cells, a loss in renal endocrine function can lower levels of red blood cells with subsequent anemia. The loss of proteins (proteinuria), due to the destruction of the tubular system, can worsen the malnutrition caused by absence of appetite, low protein intake and loss of weight that is typical in patients with CKD.



Specific kidney damages and their effects Graphic representation of the most frequent kidney damages and their effect at a cellular and molecular level.

At a cellular and molecular level CKD causes a progressive scarring that ultimately affects all kidney structures leading to fibrosis, activated after the initial injury. Tubular damage can lead to apoptosis of the cells of the tubule, release of toxic substances, excretion of cytokines and other inflammatory molecules and eventually tubular atrophy. Decrease in peritubular capillary density has been proposed as a mechanism for tubulointerstitial fibrosis characterized by an abnormal production of extracellular matrix and maybe infiltration of macrophages.

One important aspect of CKD is the subsequent glomerular damage leading to decrease of growth factors, alterations in the cell-matrix interactions, altered selectivity and permeability of the GBM and a reduction of the blood flow (figure above). All these consequences can

damage the podocytes leading to loss of function and apoptosis. Since podocytes are thought to be the key cell of the glomerular compartment, their malfunctionality induces a cascade of other effects that can lead to ESRD like altered proliferation of mesangial proliferation and changes in microvascular permeability.

As described in the Introduction one of the main challenging in therapeutic treatment of CKD using stem cells and regenerative medicine principles, is to be able to identify a podocyte precursor cell that can rescue the functionality of the glomerolus. In addition, it is fundamental to understand the processes involved in the progression of the fibrosis in order to slow down the progression of the disease.

In this work we have decided to use two different strategies as experimental approaches to cure acute and chronic kidney failure: the differentiation of hAFSC into kidney parenchyma, *in vitro* and *in vivo*, and the isolation, from the amniotic fluid, of specific and already committed kidney progenitor cells (AKPC).

1. Amniotic Fluid Stem Cells differentiation in renal parenchyma in vitro and in vivo

Bioengineering of the kidney with all of its multifaceted function and structure still remains a challenge. However, some progress has been made towards this goal. Both autologous and pluripotential cells have been used to either propagate or, regenerate *de novo*, kidney cell lines under appropriate culture conditions [58-61]. These cells can then be used to create a wide range of filtration devices some with potential life sustaining properties and others with only limited functionality [61, 62]. Extracorporeal perfusion circuits constructed from cell seeded hemofiltration devices are described in the literature but these are only capable of limited perfusion [63-65]. One of the first applications of an artificial renal device implanted *in vivo* was recently reported but only demonstrated limited excretory function [60, 66]. Perhaps the development of immunocompatible tissues or therapies from stem cells can offer

advantages over current methods of allogenic transplantation or dialysis and provide investigators with a better method for regenerating organs like the kidney de novo. The novelty in our approach to this complex field of *in vitro* kidney regeneration strives to match the field of tissue engineering with the fields of developmental and stem cell biology. A combination of utilizing stem cells for tissue regeneration with an understanding of developmental biology and organogenesis is imperative if one chooses to reproduce *in vitro* a normal embryonic niche where cells can interact with their environment for regenerative medicine applications.

Few studies to date have addressed the application of stem cells for kidney differentiation. Jiang et al. report the isolation of a multipotent adult progenitor cell (MAPC) from murine bone marrow and have shown the contribution by these cells to virtually all somatic tissues of a developing embryo after injection [67]. This included several commonly seen cell types in the kidney, such as endothelial and tubular cells. More recently, exogenously derived genetically modified human mesenchymal stem cells (hMSC), in combination with whole-embryo culture, have been shown to differentiate and contribute to functional complex structures of the kidney during embryogenesis *in vitro* [68]. In some cases, entire nephrons were hMSC-derived. Thus, hMSC are reprogrammed for other fates and organ structures, depending on the embryonic environment into which they are placed. Embryonic stem (ES) cells have been also used in cases of direct injection into a mouse embryonic kidney [69] This established a new model system in which patterns of epithelialization within the developing kidney can be studied. Therefore, direct injection of cells provides a useful tool for the evaluation of steps required for epithelial differentiation and tubulogenesis.

Over the past 2 years, we have studied and characterized a new stem cell population isolated from human amniotic fluid [70]. hAFSCs are a novel population of cells that can be used for regenerative medicine applications. They possess many of the same properties as traditional embryonic stem cell lines. Namely, hAFSC are pluripotential and can give rise to many different cells types both *in vitro* and *in vivo*. hAFSC express embryonic

stem cell markers, Oct-4 and SSEA 3 and 4. However, hAFSC possesses many important advantages over ES cells: They can be easily isolated with no harm to the fetus and are cultured without feeder layers using very simple culture conditions. hAFSC can also be expanded in multiple passages, frozen and thawed to provide an unlimited source of stem cells when required [54].

In this study we investigated the ability of hAFSC to differentiate into renal-like cells [55, 57, 71]. As mentioned above, the kidney is a very complex organ and standard culture protocols available until now were not sufficient to accomplish differentiation of the stem cells into all the various renal cell types. Our novel approach physically placed hAFSCs into a developing embryonic kidney which allowed differentiation to occur by providing the stem cells not only with the necessary growth factors but the appropriate extracellular environment for differentiation. The UB organ culture model, more specifically, highlighted the ability of the hAFSCs to respond to inductive signals and develop into individual kidney structures.

Nigam et al. demonstrated branching of the UB is possible in a gel suspension [72, 73]. Thus during culture, the UB secretes into the extracellular environment all the embryonic co-factors necessary for development. When hAFSCs are physically placed close to these branching UB tips they are in turn influenced by the presence of the embryonic structure and the circulating co-factors to differentiate their morphology and become fully formed tubular structures resembling the branching network observed with the UB. This was demonstrated by lac-z positive hAFSC tubular cells observed close to the branching UB tips as shown in the previous figures. hAFSC not only have the capacity to give rise to specialized cells as observed by structural change but also cells capable of expressing AQ1, a specific kidney cell marker, when induced to differentiate by the embryonic environment of the UB.

The origin of the kidney is from two separate embryonic constituents that ultimately fuse together to form the completed organ: the UB, which forms the collecting system of the kidney, and the metanephric mesenchyme (MM), which gives rise to the glomerular and tubular nephron, or filtration,

portion of the kidney. Bioengineering both constituents separately from a pluripotential stem cell source is a major focus of research in our laboratory in our ultimate pursuit of tissue engineering a viable renal unit for eventual *in vivo* applications for the future. On the one hand, the UB is quite easy to culture which made applying hAFSCs to this culture system straightforward. However, the MM still remains a formidable challenge to culture by itself, and therefore, we needed to employ an entirely different culture system to study the capacity that hAFSCs would have to differentiate into this crucial portion of the developing kidney and obtain an *in vitro* primordial nephron. Therefore, we examine the ability of hAFSCs to form kidney primordial structures in culture after injection directly into the embryonic kidney, essentially the developing MM. We postulated that this embryonic niche surrounded by normal developing kidney structures in close proximity to the injected hAFSCs would provide all the necessary stimuli to differentiate the hAFSCs into kidney specific lineages and structures. The novelty of our work also serendipitously established a protocol for long term organ culture of the embryonic kidney devoid of tissue necrosis never before reported [57]. No previously published reports addressing similar culture systems demonstrated culture of embryonic kidneys for more than 5 days without necrosis [74-77]

We were successful at culturing embryonic kidneys at different stages of gestation (E11.5- E16) without necrosis for 10 days, which was imperative to initiate the differentiation process. In this context we could inject hAFSC with reasonable confidence they would survive and replicate in a normal and well preserved environment. Furthermore, it was possible to follow the proliferation and differentiation of these cells during the entire culture period (10 days). It is well known that the process of induction, morphogenesis, and differentiation of the metanephros occurs in a centrifugal pattern, proceeding from the center to the periphery. This was also observed with our lac-z stained hAFSC where movement of the injected cells from the site of injection, the center of the embryonic kidney, to the periphery was documented by both live imaging and histologic techniques [78-80] Thus, hAFSC put into the differentiating metanephric

mesenchyme follow all the necessary steps of differentiation into a nephron. Further evidence of this fact was conveyed by our histologic data which also demonstrated that hAFSC integrated into the renal vesicle, C- and S-shaped bodies, which are the primordial structures of the kidney that eventually develop into mature glomerular and tubular structures of the kidney. In addition, there was also molecular evidence exhibited by expression of GDNF, ZO-1, and Claudin by the hAFSC toward a renal fate. Expression of late kidney gene markers AQ1 or AQ2, indicating that perhaps they did not go through the entire differentiation process. Possibly more time in the embryonic environment is necessary to complete the differentiation process. Nevertheless, our data suggest that hAFSC complete an initial step essential for commitment to a renal fate and that during organ culture, they further undergo a mesenchymal-to-epithelial transition [55].

Recently published reports have demonstrated that it was possible to obtain kidney cell differentiation from bone marrow derived mesenchymal stem cells only when the cells were induced (genetically modified) to produce GDNF. In this case bone marrow stem cells were driven toward a kidney fate before injection. In our study hAFSC were not induced to express any kidney genes and were not genetically modified prior to injection. This underscores the importance that hAFSC do not appear to need any prior manipulation before installment into this particular culture system. We therefore conclude that hAFSCs appear to possess a greater pluripotentiality than mesenchymal stem cells from bone marrow, since it appears that the signals from the embryonic renal environment are sufficient to induce hAFSC toward the differentiation process into kidney cells and structures.

In the *in vivo* experiments we have demonstrated a protective role of hAFSC when injected directly into kidneys with glycerol-induced ATN [81]. In the last few years, published studies have supported the potential therapeutic role of stem cells, mainly mesenchymal stem cells derived from bone marrow or of kidney-specific progenitors [82, 83] to ameliorate renal injury. Transplanted bone marrow stem cells were found to be

integrated into damaged kidneys [84, 85]. In this study, we have found that in *nu/nu* mice the amount of glycerol required for induction of ATN was 50% higher than the dose needed in wild type mice (data not shown). This suggests that the T-deficient mice are relatively protected as compared to wild type mice against glycerol-rhabdomyolysis-induced ATN [86]. This model of ATN involves a complex sequence of events wherein myoglobin, released from the damaged muscle, damages the epithelial cells of the proximal tubules, causing cast formation, vasoconstriction and decreased glomerular filtration. The high level of apoptotic cells, the increased levels of creatinine and BUN, and the histological analysis confirmed the presence of ATN in our model.

The number of hAFSC that survived after injection is reduced over time as evidenced by the luciferase detection. Nevertheless, injected hAFSC can differentiate into tubule epithelial cells. hAFSC were found within the damaged kidneys three weeks post injection located within damaged tubules, and expressing epithelial markers, as measured by both immunohistochemistry and RT-PCR using specific human antibodies and human primers. These markers were not present in hAFSC *in vitro* prior to injection.

We further found that injected hAFSC are also capable of expressing kidney genes such as *PAX2* and *NPHS1*, indicating that they can be induced to commit toward renal differentiation. Furthermore, in some rare instances, injected hAFSC cells could express Glial Derived Neurotrophic Factor (*GDNF*), which is expressed during very early kidney development; *GDNF* is not usually expressed in the adult kidney.

We also evaluated whether hAFSC can modulate kidney function after damage, as reflected in the serum creatinine and BUN. When hAFSC were injected during the established acute phase of the damage (between 48-72 hours after the injection of the glycerol), the levels of creatinine and BUN did not decrease (data not shown). This implies that injection of hAFSC when damage is already established is too late to attenuate the damage. In contrast, when hAFSC were injected into the kidney on the same day of glycerol injection no peaks in creatinine and BUN levels were

observed, underscoring the potential protective effects of hAFSC. We therefore speculate that hAFSC can, when injected early enough, in this case contemporaneously with the time of injury, attenuate acute renal injury.

Furthermore, the histology analysis demonstrated that by 72 hours after glycerol injection, the kidneys that were injected with the hAFSC show fewer damaged tubules compared with the glycerol-injected kidneys not treated with hAFSC. There was less disruption of tubular membranes and no cast formation in the hAFSC-treated animals. We can speculate that the injection of hAFSC accelerates the proliferation of epithelial tubular cells that were partially damaged and prevents additional apoptosis. This mechanism of protection lead to an overall better maintenance of the tubular structure, thus avoiding the increase in BUN and creatinine typically seen in glycerol-induced ATN.

During acute renal injury the immune-response plays a key role especially in the first 48 hours; damaged kidney endothelial cells attract leukocytes, vasomediators are released with injury, and epithelial cells of the tubule produce proinflammatory and chemotactic cytokines [87].

Bonventre *et al.* [88] and Lin *et al.* [82] have speculated recently that the mechanism by which bone marrow stem cells contribute to renal repair was by attenuating the immune response, rather than through integration or differentiation of the stem cells into the cells of the damaged organ. Togel *et al.* have shown that injection of MSC is protective against ischemic renal injury as early as 24 hours, based on measurement of serum creatinine levels. They also speculated that the protection in these animals was not through integration and differentiation of the injected MSC, because of the very short period of time with which a protective response was observed.

We also observed that the beneficial effect of hAFSC injection occurred early in the course of ATN. Therefore, to further investigate the potential mechanisms by which hAFSC enhance renal protection, we examined intrarenal cytokines in order to determine whether there is a general change in inflammatory cytokine pattern in mice that were treated with

hAFSC compared to untreated mice during the first 48 hours, thus when the immuno-system acts in a very significant manner in determining the course of the acute damage.

In the animals that were subjected only to glycerol injection it was observed a significant increase in kidney cytokine expression when compared with control mice that were not so treated. This demonstrates that in acute ATN the kidney responds with a brisk outpouring of cytokines. When mice were injected with hAFSC, an even greater elevation of cytokine levels was evident, particularly at the earlier (24 hours) time point, when compared with the cytokines levels measured in kidney treated only with glycerol. This suggests to us that an important function of hAFSC may be to augment the kidney cytokine milieu early in the course of ATN. Moreover by 48 hours, this trend in combined cytokine levels is reversed so that the majority of combined cytokine levels are either reduced significantly or no longer elevated relative to the kidneys that did not receive hAFSC. Further, by 48 hours the relative contribution of human versus mouse cytokines is also reversed, with the human component of the cytokine milieu being relatively small.

With a few exceptions, most human cytokines are also active on mouse cells [89-94], so both the human and mouse cytokines likely affect the kidney milieu. We think this is an important concept, since it is likely that the complex interaction of cytokines derived from both the injected human cells as well as the endogenous mouse cytokines are responsible for any protective effects.

Therefore we propose that hAFSC, when injected directly into the kidney in a mouse model of ATN, can be recruited as previously shown by us in two mouse models of lung injury. Thus, hAFSC can home to injury sites, where they protect damaged tissue from further injury and accelerate repair probably through cytokine-mediated paracrine mechanisms. We further propose that in this model the cytokines secreted by hAFSC work in synergy with the endogenous mouse cytokines to promote and maintain overall homeostasis of the tissues and thus interact with the inflammatory

environment favoring damage resolution, thus allowing the prevention of progression of the acute phase in glycerol-induced ATN.

In addition, it is important to observe that at 48n hours after injection of hAFSC into the ATN kidney, the major contribution to the pattern of cytokine expression is from mouse cytokines, when compared with the combined cytokine levels at 24 hours, at which point the relative contribution of human cytokines is very high. This suggests that the human cytokines first play a key role only in the earliest phase of renal response to injury.

In conclusion, we have demonstrated a trophic effect of hAFSC on resident kidney cells that survive a toxic injury, rather than via direct repopulation of the damaged structures, even if they show potential of differentiation into epithelial tubular cells over time. We demonstrated that early direct injection of hAFSC into the kidney strongly ameliorates ATN injury as reflected by more rapid resolution of tubular structural damage and by normalized creatinine and BUN levels. In addition, our data show evidence of immunomodulatory effects of hAFSC at a very early time point, comparable in magnitude to endogenous cytokine production. Understanding how donor and host cells combine to attenuate tubular damage may lead eventually to the application of hAFSC for therapeutic purposes in kidney diseases.

2. Amniotic Fluid Cells characterization and isolation of Metanpehric Mesenchyme Derived cells (MMDC) and Amniotic Fluid Kidney Progenitor Cells (AKPC)

AF is known source of stem cells, but almost 99% of cell population is still poorly investigated. It seems reasonable to speculate that within AF there is a repository of different progenitor cells included, due to its origin, progenitors derived from the renal compartment.

AF fills the amniotic cavity, providing an environment in which floats the developing embryo and later on the fetus. The volume and the composition of the Amniotic Fluid change during pregnancy following the

physiological variations of the developing fetus. During embryogenesis, maternal plasma is the main protagonist of Amniotic Fluid volume increase and water flows osmotically, through fetal membranes, and, later on, through the placental membrane. The composition of AF during the first weeks of gestation is similar to the fetal plasma with a volume of 25 ml at 10 weeks to about 400 ml at 20 weeks [95]. By 8 weeks of gestation the fetal kidney begins fluid production that rapidly increases in volume during the second trimester. The exchange of fluids through the skin is present until keratinisation that occurs between 20 and 24 weeks of gestation. The molecular composition of AF and the presence of nutritive substances have been shown to play a key role, in animals, in the proliferation and differentiation of various intestinal cell types such as epithelial and mucosa cells. AF has been used as a safe and reliable screening tool for genetic and congenital diseases in the fetus for many years and, by now, is being deeply investigated trying to match its molecular composition (or its variation) with preterm delivery, infective processes and embryo diseases. Contact between Amniotic Fluid and compartments of the developing fetus, such as lung and gastrointestinal tract could explain the presence of different cell types in the milieu of the Amniotic Fluid as reported in literature.

The first approach was to characterise more specifically the presence of cells derived from all the three germ layers. The development of the embryo goes through a defined pathway of differentiation that follows specific steps of maturation. From the small cell agglomerate called blastula, derived from the fertilized oocyte, a subsequent separation of the cells in agglomerates gives rise to three layers called germ layers. From this three germ layers (Endoderm, Mesoderm and Ectoderm) are deriving all the cells that originates all the tissues and organs. The cells within each germ layer are multipotent, able to give rise only to some cell lineages. Each germ layer develops along the first phases of the gestation to form different compartments of the fetal body.

In addition to the multipotent cells belonging to the three germ layers were investigated the presence of more committed cells and in particular organ specific progenitor cells focusing on kidney precursors.

Since the composition of Amniotic Fluid changes over time as the fetus develops during pregnancy, we divided samples according to gestational age. Since the identification of a single marker to identify a specific embryological tissue is difficult, do to the frequent co-expression of a gene in many cells at the same or different time, we found the necessity to analyze several markers for each germ layer in order to obtain more precise results. The choice of the markers was made according to gene expression in the early passages of germ layer specification, in order to avoid the chance of false positives. Endodermal marker Sox-17, for example, is expressed in the early stages of endoderm specification but, in the mouse, expression was confirmed in mature lung cells. But since Sox-17 was not revealed before E18 and our human amniotic fluid samples are far from the end of gestation, we can speculate that positive results obtained were not from mature cells derived from lung [95]. On the other hand, AFP was shown to be expressed in endodermal tissues and only at very low levels in the adult as well as Goosecoid [96-97]. Cells from mesodermal lineages were detected through expression of FLK-1, Brachyury and SCL/TAL-1. FLK-1 is expressed broadly and transiently in the mesodermal cells in the embryo but is known to be expressed in adults too [98]. TAL-1 has been shown to be essential for hematopoiesis in the early stages of life, and was shown to be expressed in the adult. But its expression is limited to a short term repopulating cell population, with characteristics of pluripotentiality, confirming that the marker was specific enough for our purposes [99]. Brachyury was shown to be present in adult almost only in pathological situation, becoming a reliable marker for Endodermal specification [100]. The expression of markers from endoderm and mesoderm was higher in samples of Amniotic Fluid of earlier gestational age versus those samples taken from later gestational age. In contrast, ectodermal markers NCAM, FGF-5 and E-Cadherin were

equally expressed in early and later samples of human Amniotic Fluid maybe due to the turnover of the fetal skin cells during the development. (Figure 3A-4A)

The presence of pluripotent cells within Amniotic Fluid is well known since the studies of Prusa but possible information about pluripotent cells variation over the gestational time could give us better data for the best time for their collection. Therefore were analyzed OCT-4, pluripotent marker essential for the development of the embryo, and C-Kit, characterizing a population of mesenchymal stem cells.

Expression of OCT-4 and C-Kit was constant over time, indicating the presence of pluripotent cells in AF in a large number of the samples investigated, with no significant difference in presence between the earlier and the later samples. These data prove that the pluripotent population within AF is maintaining a strong of presence over the time, with no overall difference in the choice of the time for the collection, at least for the time range considered in this study.

We investigated also the presence and variation of markers for mesenchymal and hematopoietic cells through expression of CD90 and CD34.

Results revealed a constant and strong expression of mesenchymal-derived cells, while hematopoietic cells were absent from the most part of AF samples at 15-16 weeks (Figure 3A-4A) and only increased slightly in older samples. Real Time PCR showed an increase number of samples positive for CD34 in older weeks but with a decreased expression of the marker (Figure 5B). Previous studies about AF MSCs [101] confirmed the expression of CD90 in this population. CD34 is a well known marker for hematopoietic lineage [102], even if recent publications are debating the necessity of CD34 expression for cells to undergo hematopoietic differentiation [103].

Interestingly previous studies showed that hematopoietic cells were present before the 12 weeks of gestation but no further characterizations were performed on older samples.

Secretions from the lung, gastrointestinal tract, skin and the urinary system are the origin of a repository of a heterogeneous population of cells within AF that has been demonstrated to be present in the Amniotic Fluid in our study. The development of the human embryo follows a precise pathway and the cells committed to various organs are differentiating at different time points.

Any adult cell follows a specific pathway of gene expression that leads to maturation with specificity.

We investigated, for this analysis, early markers of differentiation to the specific organ cell lineage in order to identify cells committed, but not yet mature, through a precise pathway. The choice of the markers was done looking for an early expression but with a certain specificity that could grant the definitive commitment to a cell lineage or group of cell lineages. Since Nkx2.1 expression is limited to lung, thyroid and certain regions of the forebrain [104] was used for the identification of lung progenitors as well as Nkx2.5, essential for cardiac differentiation, is present at low levels in other organs of the murine embryo [105]

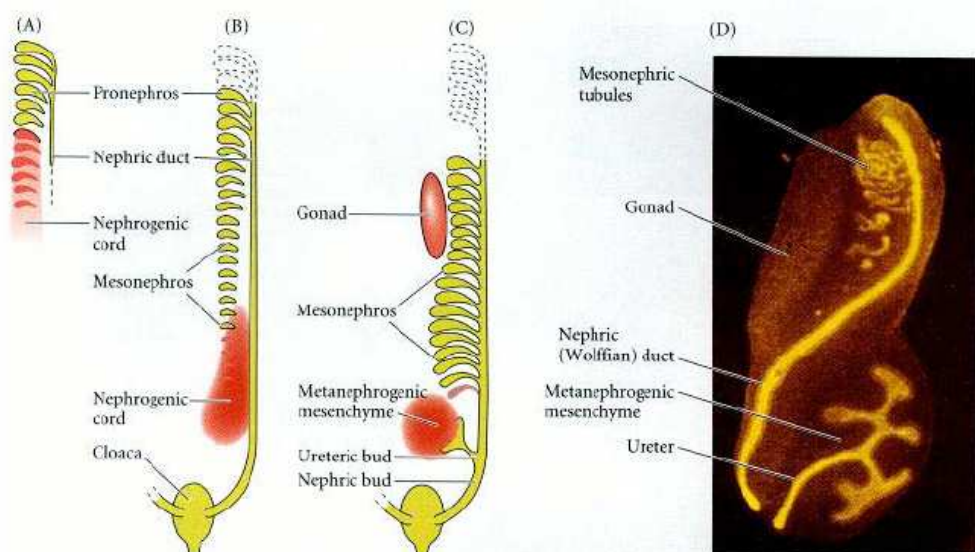
In our study we found the presence of early transcription factors that regulate differentiation processes of pluripotent cells into mature cells including Nkx2.1 (TTF-1, Thyroid Transcription Factor-1) for lung, Nkx2.5 (CSX, Cardiac Specific Homeobox) for cardiomyocytes, CEBPG (CCAAT/enhancer binding protein, gamma) for liver, PDX-1 (pancreatic and duodenal homeobox 1) for pancreas, and GDNF (Glial Cell Line-Derived Neurotrophic Factor) for kidney. As expected, the expression of markers for committed cell populations is increased in the older samples but is weak or absent in samples of earlier weeks of gestation. (Figure 3B-4B) As the fetus develops, pluripotential cells subsequently may then give way to multipotent cells, which in turn become committed to tissue-specific lineages. These data suggest the presence of cells undergoing specific differentiation. A deeper analysis should be performed within these populations to evaluate cell expression paired with other markers that could confirm the cell commitment toward a definitive differentiation.

On the other hand, PDX-1 and GDNF are pretty specific and are identifying populations committed to pancreas and kidney [106], respectively.

Since the major part of the liquid in AF derives from fetal urine, progenitors for the kidney could be floating in the liquid and, therefore, we focused our attention to the isolation and characterization of renal precursor cells from Amniotic Fluid since the overall aim of our research is to identify lineages that may be useful for kidney therapeutic purposes.

Kidney complex development required to select AF cells derived in order to obtain a specific progenitor cell population.

In fact, kidney, unlike other organs, has two different embryological origins. Two different structures derive from the intermediate mesoderm: the Ureteric Bud (UB), an extroflexion of the Wolffian duct and the Metanephric Mesenchyme (MM). The two structures show a common expression of LIM-1, essential for the development from the intermediate mesoderm.



Early kidney development *The picture shows kidney development from the pronephros to the formation of nephric duct and the nephrogenic cord leading to the formation of the metanephros.*

The evolution of the kidney reflects the need of land-adaptive vertebrates to conserve water, excrete waste and maintain electrolyte homeostasis within a variety of challenging environments [107].

Human kidney development starts around E18 and is ending between gestational weeks 32-36 and also after birth; in the mouse is starting around E7.5 and is ending 2 weeks after birth. Kidney develops from the intermediate mesoderm located between the axial, or somitic, mesoderm and the lateral plate mesoderm [106]

The UB gives rise to two transient structures called the pronephros and the mesonephros and extend caudally along the axis with a structure called Nephric Duct. (Figure 14). At the caudal end of the UB is present an agglomerate of cells, called Metanephric blastema, that forms the MM. While the pronephros and the mesonephros degenerates, the metanephros, a structure present only in mammals, goes through an intensification of signals between two structures: the MM and the UB, an outgrowth of the nephric duct.

The invasion of the UB into the MM represents a crucial point for the kidney development. This process is probably guided by signals secreted from the MM, although this has not yet been demonstrated. Inductive signals exchanged between the MM and the UB are pushing the bud to grow and branch while the MM cells replicate themselves prior to condensate around the UB tips.

GDNF (Glial derived neural factor) is secreted by the MM and addressed to the RET receptor expressed on the UB cells surface starting the UB branching. This process is essential to induce the UB branching that stimulates MM condensation through expression of factors such as molecules of the FGF's family. The induced MM at this point starts to express PAX-2, first indicator of the nephrogenic cell lineage (Podocytes, mesangial cells, stromal cells and MET cells) at this stage.

The condensed mesenchymal cells induce the branching of UB giving rise to two new ureteric tips that are going to form pretubular aggregates. These pretubular aggregates undergo a mesenchyme-to epithelial transition and form an epithelial tubule. Kidney tubules develop into nephrons, through several stages of development. First, a tubule first develops into a comma shaped body and then into an S-shaped body. In the S-Shaped stage is possible to retrieve mesangial cell precursors expressing PDGF receptor and podocyte cells precursors beginning to express Nephrin at the cleft of the S-shaped body [108-109]. The most proximal end of the S-Shaped body undergoes angiogenesis [110]. These processes are started by repression of PAX-2 expression, and consequentially the S-Shaped body forms the glomerulus and proximal and distal tubules, which fuse to the UB. The middle part of the tubule develops into the loop of Henle. The proximal tubule and the loop of Henle are the kidney regions that are responsible for most of the reabsorption of essential molecules and salts from urine, before they pass to the collecting duct system. During the branching morphogenesis of the epithelial UB, each tip acts as an inductive center to initiate nephrogenesis, after it has elongated and branched to generate new epithelial tips. The branches of the UB eventually form the collecting-duct system, which collects urine into the renal pelvis and urinary bladder. These stages are repeated to generate ~12,000 nephrons in the mouse kidney and almost 1,000,000 nephrons in the human kidney. In humans, nephrogenesis is complete around 35-37 weeks while in rats and mice it continues postnatally for about 2 weeks.

The understanding of the kidney development helped us to determine which are the more specific genes involved in particular pathway that identify the different cells present in the nephron.

We focus our attention in defining and characterizing a more specific cell population isolated from AF for kidney regenerative purposes, capable of more precise homing, integration and differentiation in the injured glomerular structures.

In order to increase the specificity of a stem cell lineage for the glomerulus compartment, and in particular for the podocytes cell type we investigated reliable markers that could be used to retrieve a progenitor cell population from the Amniotic Fluid.

Since many are the cells constituting the glomeruli, the first necessary step was the identification of markers that allow us to separate the different progenitor cells.

Based on literature review we identified Nephritin as a reliable marker for immature and mature podocytes, PDGFR α for mesangial cell progenitors, TrKA for stromogenic cortical mesenchymal cells and E-Cadherin for epithelial cells of the Bowman's Capsule [107]. It is important to mention that the identification of these particular markers was not granting us the selection of a reliable renal population since their expression is not exclusive of the kidney compartment, but they are expressed also in other organs pathways development. Nephritin, for example, expressed in the differentiating and mature podocytes, has been found in other extrarenal tissues such as brain and pancreas and E-Cadherin, epithelial marker, has been known to be present, beside in the first steps of gastrulation, in many epithelial tissues [111-112].

One important *in vivo* study [113] for our purpose reported that CD24 and OB Cadherin are co-expressed in cells of the undifferentiated MM in a mouse developing kidney.

Since Metanephric Mesenchyme is the fetal structure that gives rise only to the nephron, it was a reliable starting point for our purposes, giving us the capability to select a more specific MM population from which retrieves the more specific progenitor populations. In this way we could exclude the possibility of isolating other progenitors that would eventually give rise to cells with no specific renal fate.

We showed that in the total population of AF is evident the expression of renal markers (Early and mature) such as PAX-2, LIM-1, Nephritin ,

PDGFR α , NGF High Affinity Receptor (chained with Tyrosin Kynase, TrKA) , E- Cadherin, CD24, and OB-Cadherin (Cadherin 11) with a strong increase expression by the end of the 17th week of gestation, when kidney C-Shaped bodies are formed and are turning into S-Shaped bodies (Figure 3C-4C). Real time PCR revealed an increase expression for Nephtrin and GDNF, markers of the MM derived lineages.

After having confirmed that within AF we can identify the expression of renal markers, we focused our attention in isolating the MM lineage using immunoseparation techniques for the CD24 and OB Cadherin. Since the origin of cells within AF is from different organ, as described previously, the first necessary step was to confirm that the MMDC population was sharing with the *in vivo* renal population specific traits of expression patterns. We confirmed that CD24+ OB-Cadherin+ population (MMDC) expresses several kidney markers including AQP1, LIM-1, PAX-2, Nephtrin, GDNF, Occludin and ZO-1 by RT-PCR.

Subsequently we performed specific selection from MMDC population in order to obtain four different subpopulations, called AKPC, expressing for **1.** E-Cadherin (MET cells), **2.** Nephtrin (podocytes), **3.** TrkA (for stromogenic mesenchymal cells) and **4.** PDGFR α (mesangial cells) respectively. In doing this we could be confident that the expression of these markers were not involved in other organs pathways, but very specific for the kidney since the were immunoseparated form and already renal induced population, the MM.

These four subpopulations were then analyzed by the more sensitive Real Time PCR. The expression pattern for the four population confirmed that the four progenitor cell lineages are very distinct populations, with specific and particular roles in the glomeruli structure of the nephron.

Among others, expression of LIM-1 and PAX-2 were evaluated in order to confirm their not complete maturation since the two transcription factors are not present in the renal adult cells.

TrKA⁺ APKC cells showed expression of TrKA, LIM-1, PAX-2 and OCT-4 at important levels and expressed E-Cadherin, Occludin and PDGFR α at low level. No expression of Nephritin or GDNF was shown. TrKA has been shown not to be expressed in other than Stromogenic Cortical Mesenchymal cells and since the expression of this marker has been found only within this selection, we can with high confidence speculate that this population represents the progenitors of the renal stromal cells (PDGFR α AKPC).

Mesangial precursor cells, selected for PDGFR α were positive at different levels for PDGFR α and E-Cadherin (Figure 8A-8B). Expression of E-Cadherin is normally not reported in cells of the mesangium but since is evident the slightly expression of uninduced mesenchyme markers (LIM-1, PAX-2 and OCT-4) and E-Cadherin is expressed in the uninduced mesenchyme it is not unreasonable to think that the differentiation process is still in progress.

E-Cadherin⁺ APKC expressed high levels of OCT-4 and Occludin and high levels of E-Cadherin and LIM-1, both expressed in the uninduced mesenchyme. E-Cadherin⁺ cells expressed low levels of PAX-2 and showed no expression of TrKA, PDGFR α and ZO-1 (Figure 8A-8B). These data may indicate that, since E-Cadherin is expressed in the uninduced mesenchyme, the selection performed was not precise enough to retrieve cells undergoing Mesenchymal to Epithelial Transition but more analysis have to be performed.

As reported by Pavenstadt *et al.* [115] mature podocytes are expressing several markers such as Nephritin and ZO-1 but data are lacking regarding eventual precursors of this visceral epithelial cells. Our Nephritin⁺ APKC populations was highlighted the expression of the pluripotent marker OCT-4 and of LIM-1 and PAX-2, that may let us confirm the traits as a renal precursor that haven't yet committed to glomerulus or proximal/distal tubules, due to the presence of E-Cadherin (Figure 8A-8B). At the same

time, the expression of Nephrin that in the kidney is localized only in the differentiating and mature podocytes may indicate these cells are undergoing through visceral epithelial cell maturation. An additional data in support of this thesis is the expression of Zo-1 that usually co-localized within the podocytes, coupled with Nephrin.

CONCLUSIONS

First we have demonstrated the ability of hAFSCs to survive, proliferate and integrate into the embryonic kidney, while it undergoes organ development, in an in vitro culture system. We observed the presence of hAFSCs within kidney primordial, including tubules and developing nephrons. Thus, hAFSCs seem to have the capacity to undergo the expected mesenchymal to epithelial transition that occurs in normal renal development and are induced to express important early kidney markers such as GDNF, ZO-1 and Claudin. Moreover, hAFSCs do not appear to require prior genetic modification or exogenous production of kidney proteins for their differentiation to occur. This is a very important advantage that hAFSCs have for potential future regenerative or bioengineering application.

With the in vivo experiments, we have demonstrated a trophic effect of hAFSC on resident kidney cells that survive a toxic injury, rather than via direct repopulation of the damaged structures, even if they show potential of differentiation into epithelial tubular cells over time. We demonstrated that early direct injection of hAFSCs into the kidney strongly ameliorates ATN injury as reflected by more rapid resolution of tubular structural damage and by normalization of creatinine and BUN levels. In addition, our data show evidence of immunomodulatory and antiinflammatory effect of hAFSCs, at an early time point, comparable in magnitude to endogenous cytokine production. Understanding how donor and host cells combine to attenuate tubular damage may lead eventually to the application of hAFSCs for therapeutic purposes in acute kidney diseases. Nonetheless, beside the presence of a small number (1%) of cells with pluripotent characteristics, the composition of the other 99% of Amniotic Fluid cells is diverse, with a great amount of cells exhibiting commitment to a defined germ line or cellular endpoint.

There seems to be clear evidence for the existence of progenitor cells in Amniotic Fluid, which can give rise to different cell types of mature organs. By 17 weeks of gestation is notable an increase tissue specific cellular presence and this data may indicate that the choice of the time point for cell selection is fundamental. In addition, we demonstrated in the amniotic fluid, the presence of a renal population with specific traits of commitment. In particular, the presence of podocytes at both undifferentiated and almost mature stages could favour their use for kidney regeneration *in vitro* and *in vivo* animal models. The presence and identification of specific renal progenitor cells in the Amniotic Fluid, committed to different compartments of the kidney environment, could represent a valuable new tool for regenerative purposes with regards to the treatment of a broad range of renal diseases.

The discovery of renal specific progenitor cells within Amniotic Fluid could bring a breakthrough in the study for novel and more selective approaches in the renal therapy. However, the real pluripotential capability of these progenitors cells, in particular the kidney progenitors presenting more differentiation characteristics, has to be established. Moreover, their potential for survival, proliferation, integration, and differentiation needs to be assessed in *in vivo* models involving different types of renal damage.

Future aims of the project are:

1. assessment of the Amniotic Kidney Progenitor Cells differentiative potential, performing *in vitro* and *in vivo* studies, in order to evaluate their specificity for glomerular, stromal or tubular structures. *In vitro* differentiation and functional investigation will be used as a preliminary evaluation of their regenerative capability. *In vivo* studies on AKF, ATN or CKD will be performed to understand their integration, differentiation and immunogenicity. The understanding of AKPC maturation pathways can reveal new tools for the comprehension of kidney development and pathology formation;

2. investigation of AFSCs immunomodulatory mechanisms in Acute and Chronic Kidney Disease models. In addition, the establishment of a more effective administration of the cells, like injection at different timepoint along the progression of the disease or multiple injections, are a priority in order to maximize their beneficial effects.

REFERENCES

1. US Renal Data System. USRDS 2002. Annual Data Report : Atlas of End.-Stage Renal Disease in the United States. Bethesda., MD : National Institute of Health, National Institute of Diabetes and Digestive and Kidney Diseases
2. Lanza, R. P., Chung, H. Y., Yoo, J. J. et al.: Generation of histocompatible tissues using nuclear transplantation. *Nat Biotechnol*, 20: 689, 2002
3. Stocum D.L., 2001. Stem cell in regenerative biology and medicine. *Wound Rep. Reg.* 9: 429-442.
4. Thomson J.A. et al., 1998. Embryonic stem cells derived from human blastocysts. *Science* 282: 1145-1147.
5. Reubinoff B.E. et al. 2000. Embryonic stem cell lines from human blastocytes: somatic differentiation in vitro. *Nature Biotech.* 18: 399-404.
6. Pittenger M.F Pittenger MF, Mackay AM, Beck SC, Jaiswal RK, Douglas R, Mosca JD, Moorman MA, Simonetti DW, Craig S, Marshak DR. 1999. Multilineage potential of adult human mesenchymal stem cells. *Science* 284:143-147.
7. Goodwin HS. et al., 2001. Multilineage differentiation activity by cells isolated from umbelical cord blood: expression of bone, fat and neural markers. *Biology of blood and marrow transplantation*, 7: 581-588.
8. Streubel B, Martucci-Ivessa G, Fleck T, Bittner RE., In vitro transformation of amniotic cells to muscle cells--background and outlook, *Wien Med Wochenschr.*1996;146(9-10):216-7
9. P. De Coppi, G. Bartsch, M. Siddiqui, T. Xu, C. Santos, L. Perin, G. Mostoslavsky, A. Serre, E. Snyder, J. Yoo, M. Furth, S. Soker and A. Atala. Isolation of amniotic stem cell lines with potential for therapy. 2007. *Nature Biotechnology*, 25: 100-106.

10. Anderson, RJ Prevention and management of acute renal failure. *Hospital Practice* 1993 61–75
11. Thadhani, R, Pasqual, M, Bonventre, JV: Medical progress—Acute renal failure. *N Engl J Med* 1996 334: 1448–1460
12. Dubose, TD, JR, Warnock, DG, Mehta, RL Acute renal failure in the 21st century: Recommendations for management and outcomes assessment. *Am J Kidney Dis* 1997 29: 793–799
13. Lieberthal, W: Biology of acute renal failure: Therapeutic implications. *Kidney Int* 1997 52: 1102–1115
14. Mindell, JA, Chertow, GM: A practical approach to acute renal failure. *Med Clin North Am* 1997 81: 731–748,
15. Ronco, C, Bellomo, R, Feriani Critical care nephrology: The time has come. *Kidney Int* 1998 53(Suppl 66): S1–S2
16. Shemesh, O, Golbetz, H, Kriss, JP, Myers, BD: Limitations of creatinine as a filtration marker in glomerulopathic patients. *Kidney Int* 1985 28: 830–838,
17. Moran, SM, Myers, BD: Course of acute renal failure studied by a model of creatinine kinetics. *Kidney Int* 1985 27: 928–937
18. Liano, F, Pasqual, J, MADRID ACUTE RENAL FAILURE STUDY GROUP: Epidemiology of acute renal failure: A prospective, multicenter, community-based study. *Kidney Int* 1996 50:811–818,
19. Hou, SH, Bushinsky, DA, Wish, JB Hospital-acquired renal insufficiency: A prospective study. *Am J Med* 1983 74: 243–248
20. Shusterman, N, Stromb, BL, Murray Risk factors and outcome of hospital acquired acute renal failure: Clinical epidemiologic study. *Am J Med* 1987 83: 65–71
21. Cecka, JM, Cho, YW, Terasakil, PI: Analyses of the UNOS scientific renal transplant registry at three years—Early events affecting transplant success. *Transplantation* 1992 53: 59–64,
22. Troppman, C, Gilligham, KJ, Benedetti, E Delayed graft function, acute rejection, and outcome after cadaver renal transplantation. The multivariate analysis. *Transplantation* 1995 59: 962–968

23. Alexander, JW, Zola, JC: Expanding the donor pool: Use of marginal donors for solid organ transplantation. *Clin Transplant* 1996 10: 1–19
24. Biesenbach, G, Zazgornik, J, Kaiser, W Improvement in prognosis of patients with acute renal failure over a period of 15 years: An analysis of 710 cases in a dialysis center. *Am J Nephrol* 1992 12: 319–325
25. McCarthy, JT: Prognosis of patients with acute renal failure in the intensive-care unit: A tale of two eras. *Mayo Clin Proc* 1996 71: 117–126,
26. Adams PL, Adams PF, Bell PD, Navar LG: Impaired renal blood flow autoregulation in ischemic acute renal failure. *Kidney Int* 1980; 18:68–76.
27. Conger J: The role of blood flow autoregulation in pathophysiology of acute renal failure. *Circ Shock* 1983;11:235–244.
28. Conger JD: Does hemodialysis delay recovery from acute renal failure? *Semin Dial* 1990;3: 146–147.
29. Meier-Kriesche HU, Kaplan B. Waiting time on dialysis as the strongest modifiable risk factor for renal transplant outcomes: a paired donor kidney analysis. *Transplantation* 2002;74:1377-81.
30. Mange KC, Joffe MM, Feldman HI. Effect of the use or nonuse of long-term dialysis on the subsequent survival of renal transplants from living donors. *N Engl J Med* 2001;344:726-31.
31. Wolfe RA, Ashby VB, Milford EL, et al. Comparison of mortality in all patients on dialysis, patients on dialysis awaiting transplantation, and recipients of a first cadaveric transplant. *N Engl J Med* 1999;341:1725-30
32. Murray JE, Merrill JP, Harrison JH. Renal homotransplantation in identical twins. *Surg Forum* (1955) 6:432–36
33. Takahashi K, Takahara S, Uchida K, Yoshimura N, Toma H, Oshima S, et al. Successful results after 5 years of tacrolimus therapy in ABO-incompatible kidney transplantation in Japan. *Transplant Proc* (2005) 37:1800–3

34. Calne RY, White DJ, Thiru S, Evans DB, McMaster P, Dunn DC, et al. Cyclosporin A in patients receiving renal allografts from cadaver donors. *Lancet* (1978) 2:1323–7.
35. Vajdic CM, McDonald SP, McCredie MR, van Leeuwen MT, Stewart JH, Law M, et al. Cancer incidence before and after kidney transplantation. *JAMA* (2006) 296:2823–31.
36. Haseltine A. The Emergence of Regenerative Medicine: A New Field and a New Society *The Journal of Regenerative Medicine* Volume 2—2001 June 7, 2001
37. Humes HD, Buffington DA, MacKay SM, Funke AJ, Weitzel WF. Replacement of renal function in uremic animals with a tissue-engineered kidney. *Nat Biotechnol.* 1999 May;17(5):451-5.
38. Amiel GE, Yoo JJ, Atala A. Renal therapy using tissue-engineered constructs and gene delivery. *World J Urol.* 2000 Feb;18(1):71-9.
39. Amiel GE, Yoo JJ, Atala A. Renal therapy using tissue-engineered constructs and gene delivery. *World J Urol.* 2000 Feb;18(1):71-9.
40. Abkowitz JL, Robinson AE, Kale S, Long MW, Chen J. Mobilization of hematopoietic stem cells during homeostasis and after cytokine exposure. *Blood.* 2003 Aug 15;102(4):1249-53.
41. Sagrinati C, Netti GS, Mazzinghi B, Lazzeri E, Liotta F, Frosali F, Ronconi E, Meini C, Gacci M, Squecco R, Carini M, Gesualdo L, Francini F, Maggi E, Annunziato F, Lasagni L, Serio M, Romagnani S, Romagnani P. Isolation and characterization of multipotent progenitor cells from the Bowman's capsule of adult human kidneys. *J Am Soc Nephrol.* 2006 Sep;17(9):2443-56.
42. Lin F, Cordes K, Li L, Hood L, Couser WG, Shankland SJ, Igarashi P: Hematopoietic stem cells contribute to the regeneration of renal tubules after renal ischemia-reperfusion injury in mice. *J Am Soc Nephrol* 2003;14:1188-1199.
43. Abkowitz JL, Robinson AE, Kale S, Long MW, Chen J. Mobilization of hematopoietic stem cells during homeostasis and after cytokine exposure. *Blood.* 2003 Aug 15;102(4):1249-53.

44. Morigi M, Benigni A, Remuzzi G, Imberti B The regenerative potential of stem cells in acute renal failure. 2006 Cell Transplant 15 Suppl 1:S111-117.
45. Morigi M, Imberti B, Zoja C, Corna D, Tomasoni S, Abbate M, Rottoli D, Angioletti S, Benigni A, Perico N, Alison M, Remuzzi G. Mesenchymal stem cells are renotropic, helping to repair the kidney and improve function in acute renal failure. 2004 J Am Soc Nephrol. Jul;15(7):1794-804.
46. Herrera MB, Bussolati B, Bruno S, Fonsato V, Romanazzi GM, Camussi G Mesenchymal stem cells contribute to the renal repair of acute tubular epithelial injury. 2004 Int J Mol Med 14:1035-1041.
47. Yokoo T, Fukui A, Ohashi T, Miyazaki Y, Utsunomiya Y, Kawamura T, Hosoya T, Okabe M, Kobayashi E Xenobiotic kidney organogenesis from human mesenchymal stem cells using a growing rodent embryo. 2006 J Am Soc Nephrol 17:1026-1034.
48. Duffield JS, Park KM, Hsiao LL, Kelley VR, Scadden DT, Ichimura T, Bonventre JV 2005 Restoration of tubular epithelial cells during repair of the postischemic kidney occurs independently of bone marrow-derived stem cells. J Clin Invest 115:1743-1755.
49. Duffield JS, Bonventre JV Kidney tubular epithelium is restored without replacement with bone marrow-derived cells during repair after ischemic injury. 2005 Kidney Int 68:1956-1961.
50. Lin F, Moran A, Igarashi P Intrarenal cells, not bone marrow-derived cells, are the major source for regeneration in postischemic kidney. 2005 J Clin Invest 115:1756-1764.
51. Humphreys BD, Bonventre JV Mesenchymal Stem Cells in Acute Kidney Injury. 2007 Annu Rev Med.
52. Underwood MA, Gilbert WM, Sherman MP. Amniotic fluid: not just fetal urine anymore. J Perinatol. 2005 May;25(5):341-8. Review
53. Prusa AR, Marton E, Rosner M, Bernaschek G, Hengstschläger M. Oct-4-expressing cells in human amniotic fluid: a new source for stem cell research? Hum Reprod. 2003 Jul;18(7):1489-93

54. De Coppi P, Bartsch G, Jr., Siddiqui MM, et al. Isolation of amniotic stem cell lines with potential for therapy. *Nat Biotechnol.* Jan 2007;25(2):100-106.
55. **Giuliani S**, Perin L, Jin D, Sedrakyan S, Carraro G, Habibian R, et al. Renal differentiation of amniotic fluid stem cells. *Cell Prolif.* 2007 Dec;40(6):936-48.
56. Carraro G, 2008. Human Amniotic Fluid Stem Cells Can Integrate and Differentiate Into Epithelial Lung Lineages. *Stem Cells.* 2008 Aug 28
57. **Giuliani S**, Perin L, Sedrakyan S, Jin D, Parnigotto PP, Warburton D, Zanon GF, De Filippo RE. Ex-vivo whole embryonic kidney culture: a novel method for long term analysis in regeneration and transplantation. 2005 *J Urology* 179:365-370.
58. US Renal Data System. *USRDS 2002. Annual Data Report : Atlas of End.-Stage Renal Disease in the United States.* Bethesda., MD : National Institute of Health, National Institute of Diabetes and Digestive and Kidney Diseases
59. Stocum, D.L. Stem cells in regenerative biology and medicine. *Wound Repair Regen* 9, 429-442 (2001).
60. Lanza, R.P. et al. Generation of histocompatible tissues using nuclear transplantation. *Nat Biotechnol* 20, 689-696 (2002).
61. MacKay, S.M., Funke, A.J., Buffington, D.A. & Humes, H.D. Tissue engineering of a bioartificial renal tubule. *Asaio J* 44, 179-183 (1998).
62. Aebischer, P., Ip, T.K., Panol, G. & Galletti, P.M. The bioartificial kidney: progress towards an ultrafiltration device with renal epithelial cells processing. *Life Support Syst* 5, 159-168 (1987).
63. Amiel, G.E., Yoo, J.J. & Atala, A. Renal therapy using tissue-engineered constructs and gene delivery. *World J Urol* 18, 71-79 (2000).
64. Ip, T.K., Aebischer, P. & Galletti, P.M. Cellular control of membrane permeability. Implications for a bioartificial renal tubule. *ASAIO Trans* 34, 351-355 (1988).

65. Amiel, G.E. & Atala, A. Current and future modalities for functional renal replacement. *Urol Clin North Am* 26, 235-246, xi (1999).
66. Yoo, J.J. & Atala, A. Tissue engineering applications in the genitourinary tract system. *Yonsei Med J* 41, 789-802 (2000).
67. Jiang, Y. et al. Pluripotency of mesenchymal stem cells derived from adult marrow. *Nature* 418, 41-49 (2002).
68. Yokoo, T. et al. Human mesenchymal stem cells in rodent whole-embryo culture are reprogrammed to contribute to kidney tissues. *Proc Natl Acad Sci U S A* 102, 3296-3300 (2005).
69. Steenhard, B.M. et al. Integration of embryonic stem cells in metanephric kidney organ culture. *J Am Soc Nephrol* 16, 1623-1631 (2005).
70. Siddiqui, M.M. & Atala, A. Amniotic Fluid Derived Pluripotential Cells (Ch 16), Vol. Editors: Robert Lanza, Helen Blau, Douglas Melton, Malcolm Moore, E. Donnall Thomas, Catherine Verfaillie, Irving Weissmann, and Michael West. (2004).
71. Perin L, **Giuliani S**, Sedrakyan S, Da Sacco S, De Filippo RE. Stem Cell and regenerative science applications in the development of bioengineering of renal tissue. *Pediatr Res* 2008 63:467-71
72. Qiao, J. et al. Multiple fibroblast growth factors support growth of the ureteric bud but have different effects on branching morphogenesis. *Mech Dev* 109, 123-135 (2001)
73. Qiao, J., Sakurai, H. & Nigam, S.K. Branching morphogenesis independent of mesenchymal-epithelial contact in the developing kidney. *Proc Natl Acad Sci U S A* 96, 7330-7335 (1999).
74. Gupta, I.R., Lapointe, M. & Yu, O.H. Morphogenesis during mouse embryonic kidney explant culture. *Kidney Int* 63, 365-376 (2003).
75. Hardman, P., Klement, B.J. & Spooner, B.S. Growth and morphogenesis of embryonic mouse organs on non-coated and extracellular matrix-coated Biopore membrane. *Dev Growth Differ* 35, 683-690 (1993).
76. Rogers, S.A., Ryan, G. & Hammerman, M.R. Insulin-like growth factors I and II are produced in the metanephros and are required

- for growth and development in vitro. *J Cell Biol* 113, 1447-1453 (1991).
77. Steer, D.L., Bush, K.T., Meyer, T.N., Schwesinger, C. & Nigam, S.K. A strategy for in vitro propagation of rat nephrons. *Kidney Int* 62, 1958-1965 (2002).
78. Evan, A.P., Gattone, V.H., 2nd & Schwartz, G.J. Development of solute transport in rabbit proximal tubule. II. Morphologic segmentation. *Am J Physiol* 245, F391-407 (1983)
79. Evan, A.P., Satlin, L.M., Gattone, V.H., 2nd, Connors, B. & Schwartz, G.J. Postnatal maturation of rabbit renal collecting duct. II. Morphological observations. *Am J Physiol* 261, F91-107 (1991).
80. Potter, E.L. Glomerular development in the kidney as an index of fetal maturity. *J Pediatrics* 22, 695 (1943).
81. Perin L, **Giuliani S**, Sedrakyan S, Da Sacco S, Carraro G, Shiri L, Lemley K, Rosol M, Wu S, Atala A, Warburton D, De Filippo RE. Submitted to Open Access J 2009
82. Lin F. Renal repair: role of bone marrow stem cells. *Pediatr Nephrol*. Nov 9 2007.
83. Al-Awqati Q, Oliver JA. The kidney papilla is a stem cells niche. *Stem Cell Rev*. 2006;2(3):181-184.
84. Gupta S, Verfaillie C, Chmielewski D, Kim Y, Rosenberg ME. A role for extrarenal cells in the regeneration following acute renal failure. *Kidney Int*. Oct 2002;62(4):1285-1290.
85. Poulosom R, Forbes SJ, Hodivala-Dilke K, et al. Bone marrow contributes to renal parenchymal turnover and regeneration. *J Pathol*. Sep 2001;195(2):229-235.
86. Semedo P, Palasio CG, Oliveira CD, Feitoza CQ, Gonçalves GM, Cenedeze MA, Wang PM, Teixeira VP, Reis MA, Pacheco-Silva A, Câmara NO. Early modulation of inflammation by mesenchymal stem cell after acute kidney injury. *Int Immunopharmacol*. 2009 Jun;9(6):677-82.

87. Bonventre JV. Molecular response to cytotoxic injury: role of inflammation, MAP kinases, and endoplasmic reticulum stress response. *Semin Nephrol.* Sep 2003;23(5):439-448.
88. Humphreys BD, Bonventre JV. Mesenchymal Stem Cells in Acute Kidney Injury. *Annu Rev Med.* Feb 18 2008;59:311-325.
89. Maliszewski CR, Schoenborn MA, Cerretti DP, Wignall JM, Picha KS, Cosman D, Tushinski RJ, Gillis S, Baker PE. Bovine GM-CSF: molecular cloning and biological activity of the recombinant protein. *Mol Immunol.* 1988 Sep;25(9):843-50.
90. Hu-Li J, Shevach EM, Mizuguchi J, Ohara J, Mosmann T, Paul WE. B cell stimulatory factor 1 (interleukin 4) is a potent costimulant for normal resting T lymphocytes. *J Exp Med.* 1987 Jan 1;165(1):157-72.
91. Liu C, Bai Y, Ganea D, Hart RP. Species-specific activity of rat recombinant interleukin-1 beta. *J Interferon Cytokine Res.* 1995 Nov;15(11):985-92.
92. Schwabe M, Cox GW, Bosco MC, Prohaska R, Kung HF. Multiple cytokines inhibit interleukin-6-dependent murine hybridoma/plasmacytoma proliferation. *Cell Immunol.* 1996 Feb 25;168(1):117-21.
93. Kennedy J, Rossi DL, Zurawski SM, Vega F Jr, Kastelein RA, Wagner JL, Hannum CH, Zlotnik A. Mouse IL-17: a cytokine preferentially expressed by alpha beta TCR + CD4-CD8-T cells. *J Interferon Cytokine Res.* 1996 Aug;16(8):611-7.
94. De Haan G, Ausema A, Wilkens M, Molineux G, Dontje B. Efficient mobilization of haematopoietic progenitors after a single injection of pegylated recombinant human granulocyte colony-stimulating factor in mouse strains with distinct marrow-cell pool sizes. *Br J Haematol.* 2000 Sep;110(3):638-46.
95. Kwon-Sik Parka, James M. Wellsb, Aaron M. Zornb, Susan E. Werta and Jeffrey A. Whitsetta, Sox17 influences the differentiation of respiratory epithelial cells *Developmental Biology* Volume 294, Issue 1, 1 June 2006, Pages 192-202

96. Jones EA, Clement-Jones M, James O and Wilson D, Differences between human and mouse alpha-fetoprotein expression during early development, *J. Anat.* (2001) 198, pp. 555±559
97. Perea-Gomez, A. et al. Nodal antagonists in the anterior visceral endoderm prevent the formation of multiple primitive streaks. *Dev. Cell* 3, 745–756 (2002)
98. Victoria L Bautch Flk1 expression: promiscuity revealed *Blood*, 1 January 2006, Vol. 107, No. 1, pp. 3-4.
99. Curtis DJ, Hall MA, Van Stekelenburg LJ et al. SCL is required for normal function of short-term repopulating hematopoietic stem cells. *Blood* 2004;103:3342–3348
100. Palena C, Polev D, Tsang K, Fernando R, Litzinger M, Krukovskaya L, Baranova A, Kozlov A, Schlom J . 2007. The human T-box mesodermal transcription factor Brachyury is a candidate target for T-cell-mediated cancer immunotherapy.. *Clinical Cancer Research*. 13:2471-2478
101. Ming-Song Tsai, Jia-Ling Lee, Yu-Jen Chang and Shiao-Min Hwang. Isolation of human multipotent mesenchymal stem cells from second-trimester amniotic fluid using a novel two-stage culture protocol *Human Reproduction*, Vol. 19, No. 6, 1450-1456, June 2004
102. Krause DS, Ito T, Fackler MJ, Smith OM, Collector MI, Sharkis SJ, May WS. Characterization of murine CD34, a marker for hematopoietic progenitor and stem cells. *Blood*. 1994 Aug 1;84(3):691-701
103. Yalin Guo, Michael Lübbert, Monika Engelhardt CD34-Hematopoietic Stem Cells: Current Concepts and Controversies *Stem Cells* 2003;21:15-20
104. Pan Q, Li C, Xiao J, Kimura S, Rubenstein J, Puelles L, Minoo P. In vivo characterization of the Nkx2.1 promoter/enhancer elements in transgenic mice. *Gene*. 2004 Apr 28;331:73-82
105. Hideko Kasahara, Sonia Bartunkova, Martina Schinke, Makoto Tanaka, , Seigo Izumo Cardiac and Extracardiac

- Expression of Csx/Nkx2.5 Homeodomain Protein Circulation Research. 1998;82:936-946.
106. Hideaki Kaneto, Takeshi Miyatsuka, Toshihiko Shiraiwa, Kaoru Yamamoto, Ken Kato, Yoshio Fujitani, Taka-aki Matsuoka Crucial Role of PDX-1 in Pancreas Development, β -Cell Differentiation, and Induction of Surrogate β -Cells Current Medicinal Chemistry, Volume 14, Number 16, July 2007 , pp. 1745-1752
 107. Dressler GR. The cellular basis of kidney development. Annu Rev Cell Dev Biol. 2006;22:509-29. Review
 108. Horster MF, Braun GS, Huber SM. Embryonic renal epithelia: induction, nephrogenesis, and cell differentiation. *Physiol Rev*. 1999 Oct;79(4):1157-91.
 109. Juan Oliver and Qais Al-Awqati Development of vascular elements during renal organogenesis *Kidney International* (2000) 57, 2167–2168;
 110. Pöschl E, Schlötzer-Schrehardt U, Brachvogel B, Saito K, Ninomiya Y, Mayer U. Collagen IV is essential for basement membrane stability but dispensable for initiation of its assembly during early development.
 111. Beltcheva O, Kontusaari S, Fetissov S, Putaala H, Kilpeläinen P, Hökfelt T, Tryggvason K. Alternatively used promoters and distinct elements direct tissue-specific expression of nephrin. *J Am Soc Nephrol*. 2003 Feb;14(2):352-8.
 112. K Boller, D Vestweber and R Kemler Cell-adhesion molecule uvomorulin is localized in the intermediate junctions of adult intestinal epithelial cells *The Journal of Cell Biology*, Vol 100, 327-332
 113. M. Kasper , O. Huber, H. Großmann, B. Rudolph, C. Tränkner and M. Müller Immunocytochemical distribution of E-cadherin in normal and injured lung tissue of the rat *Histochemistry and Cell Biology* Volume 104, Number 5 / November, 1995

114. Challen GA, Bertonecello I, Deane JA, Ricardo SD, Little MH. Kidney side population reveals multilineage potential and renal functional capacity but also cellular heterogeneity. *J Am Soc Nephrol.* 2006 Jul;17(7):1896-912.
115. Pavenstädt H, Kriz W, Kretzler M. Cell biology of the glomerular podocyte. *Physiol Rev.* 2003 Jan;83(1):253-307. Review.

TABLES AND FIGURES

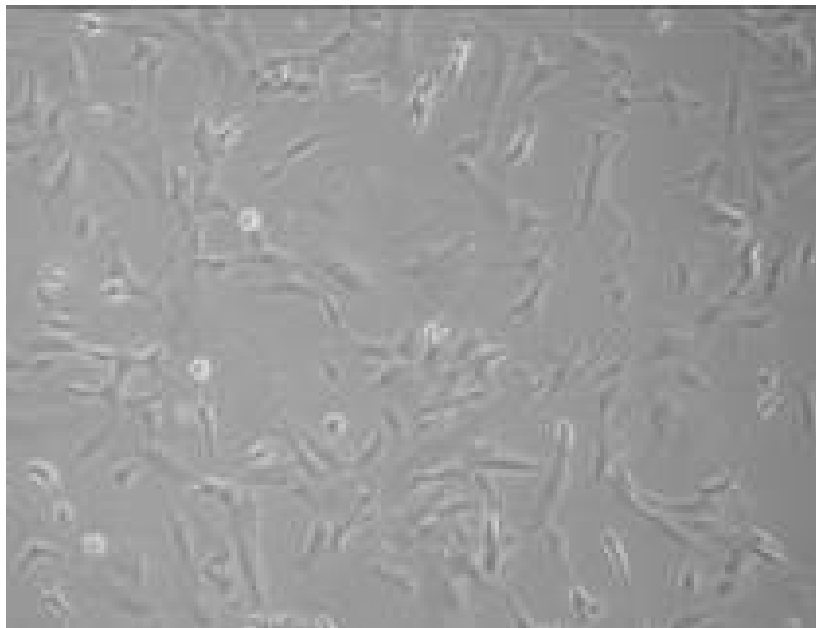
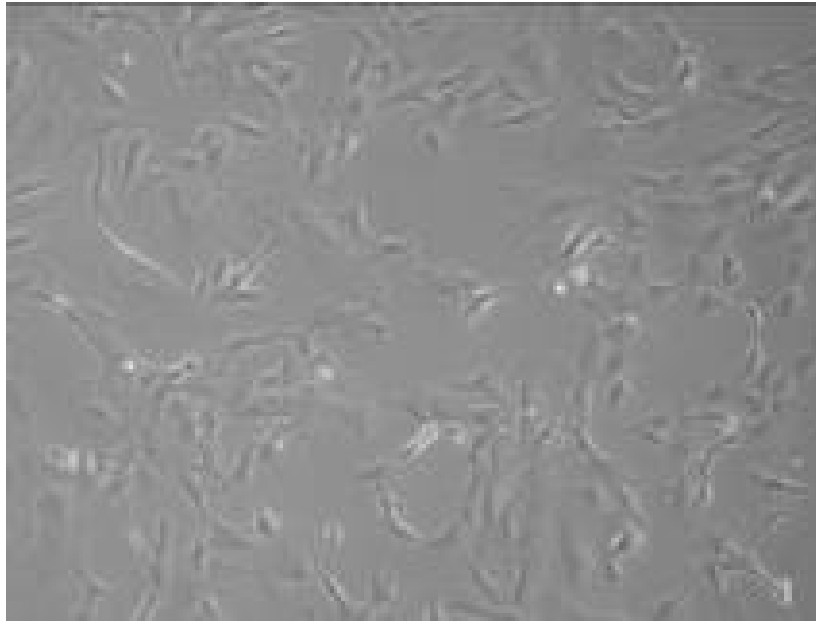


Figure 1 A - B – Morphology of Total amniotic fluid cell population
The morphology of total amniotic fluid populations is various with a prevalence of fibroblastoid shapes. In Chang's medium the morphology is unchanged for at least 50 passages in culture.

	Weeks of Gestation	15	16	16	17	17	17	17	17	18	18	18	18	18	19	20	20
	Sample	A	B	C	D	E	F	G	H	I	J	K	L	M	N	O	P
Pluripotency	CD34										*	*	*	*	*	*	*
	CD90	*	*	*	*	*	*	*	*	*	*	*	*	*	*	*	*
	Clit	*	*	*	*	*	*	*	*	*	*	*	*	*	*	*	*
	OCT-4	*	*	*	*	*	*	*	*	*	*	*	*	*	*	*	*
Ectoderm	NCAM	*	*	*	*	*	*	*	*	*	*	*	*	*	*	*	*
	FGF-5	*	*	*	*	*	*	*	*	*	*	*	*	*	*	*	*
	E-Cadherin	*	*	*	*	*	*	*	*	*	*	*	*	*	*	*	*
Mesoderm	Fli-1	*	*	*	*	*	*	*	*	*	*	*	*	*	*	*	*
	Brachyury	*	*	*	*	*	*	*	*	*	*	*	*	*	*	*	*
	Tal-1	*	*	*	*	*	*	*	*	*	*	*	*	*	*	*	*
Endoderm	Cxcr-4	*	*	*	*	*	*	*	*	*	*	*	*	*	*	*	*
	Sox-17	*	*	*	*	*	*	*	*	*	*	*	*	*	*	*	*
	Goosecoid	*	*	*	*	*	*	*	*	*	*	*	*	*	*	*	*
	AFP	*	*	*	*	*	*	*	*	*	*	*	*	*	*	*	*

	Weeks of Gestation	15	16	16	17	17	17	17	17	18	18	18	18	18	19	20	20
	Sample	A	B	C	D	E	F	G	H	I	J	K	L	M	N	O	P
CEBPG	*	*	*	*	*	*	*	*	*	*	*	*	*	*	*	*	*
GDNF	*									*	*	*	*	*	*	*	*
TTF-1										*	*	*	*	*	*	*	*
NKX2.5			*							*	*	*	*	*	*	*	*
PDX-1					*					*	*	*	*	*	*	*	*

	Weeks of Gestation	15	16	16	17	17	17	17	17	18	18	18	18	18	19	20	20
	Sample	A	B	C	D	E	F	G	H	I	J	K	L	M	N	O	P
OB-Cad										*	*	*	*	*	*	*	*
CD24										*	*	*	*	*	*	*	*
GDNF	*							*	*	*	*	*	*	*	*	*	*
PAX-2		*				*				*	*	*	*	*	*	*	*
NEPHRIN										*	*	*	*	*	*	*	*
LIM1	*	*	*	*	*	*	*	*	*	*	*	*	*	*	*	*	*
OCCLUDIN	*	*	*	*	*	*	*	*	*	*	*	*	*	*	*	*	*
AQP-1	*	*	*	*	*	*	*	*	*	*	*	*	*	*	*	*	*
ZO-1	*	*	*	*	*	*	*	*	*	*	*	*	*	*	*	*	*

Figure 2 A-B-C – Expression of markers for the three germ layers, for progenitor cells and for kidney specific progenitor cells over the time by RT-PCR. Expression of Endodermal and Mesodermal markers decreases in older samples while Ectodermal and pluripotency markers expression is constant over the time (Table 3A). By 17 weeks of gestation it's evident an increase in expression of several progenitor markers (Table 3B) including renal specific proteins (Table 3C).

		Weeks of Gestation															
		15	16	16	17	17	17	17	17	18	18	18	18	18	19	20	20
Sample		A	B	C	D	E	F	G	H	I	J	K	L	M	N	O	P
Pluripotency	CD34										*	*	*	*	*	*	*
	CD90	*	*	*	*	*	*	*	*	*	*	*	*	*	*	*	*
	Clit	*	*	*	*	*	*	*	*	*	*	*	*	*	*	*	*
	OCT-4	*	*	*	*	*	*	*	*	*	*	*	*	*	*	*	*
Ectoderm	NCAM	*	*	*	*	*	*	*	*	*	*	*	*	*	*	*	*
	FGF-5	*	*	*	*	*	*	*	*	*	*	*	*	*	*	*	*
	E-Cadherin	*	*	*	*	*	*	*	*	*	*	*	*	*	*	*	*
Mesoderm	Flk-1	*	*	*	*	*	*	*	*	*	*	*	*	*	*	*	*
	Brachyury	*	*	*	*	*	*	*	*	*	*	*	*	*	*	*	*
	Tal-1	*	*	*	*	*	*	*	*	*	*	*	*	*	*	*	*
Endoderm	Cxcr-4	*	*	*	*	*	*	*	*	*	*	*	*	*	*	*	*
	Sox-17	*	*	*	*	*	*	*	*	*	*	*	*	*	*	*	*
	Goosecoid	*	*	*	*	*	*	*	*	*	*	*	*	*	*	*	*
	AFP	*	*	*	*	*	*	*	*	*	*	*	*	*	*	*	*

		Weeks of Gestation															
		15	16	16	17	17	17	17	17	18	18	18	18	18	19	20	20
Sample		A	B	C	D	E	F	G	H	I	J	K	L	M	N	O	P
	CEBPG	*	*	*	*	*	*	*	*	*	*	*	*	*	*	*	*
	GDNF	*	*	*	*	*	*	*	*	*	*	*	*	*	*	*	*
	TTF-1	*	*	*	*	*	*	*	*	*	*	*	*	*	*	*	*
	NKX2.5	*	*	*	*	*	*	*	*	*	*	*	*	*	*	*	*
	PDX-1	*	*	*	*	*	*	*	*	*	*	*	*	*	*	*	*

		Weeks of Gestation															
		15	16	16	17	17	17	17	17	18	18	18	18	18	19	20	20
Sample		A	B	C	D	E	F	G	H	I	J	K	L	M	N	O	P
	OB-Cad	*	*	*	*	*	*	*	*	*	*	*	*	*	*	*	*
	CD24	*	*	*	*	*	*	*	*	*	*	*	*	*	*	*	*
	GDNF	*	*	*	*	*	*	*	*	*	*	*	*	*	*	*	*
	PAX-2	*	*	*	*	*	*	*	*	*	*	*	*	*	*	*	*
	NEPHRIN	*	*	*	*	*	*	*	*	*	*	*	*	*	*	*	*
	LIM1	*	*	*	*	*	*	*	*	*	*	*	*	*	*	*	*
	OCCLUDIN	*	*	*	*	*	*	*	*	*	*	*	*	*	*	*	*
	AQP-1	*	*	*	*	*	*	*	*	*	*	*	*	*	*	*	*
	ZO-1	*	*	*	*	*	*	*	*	*	*	*	*	*	*	*	*

Figure 3 A-B-C –Western Blotting Analysis of Amniotic Fluid Total Cell Population for markers of all the three germ layers and pluripotency (Figure 4A), tissue specific progenitor cells (Figure 4B) and kidney specific cell markers (Figure 4C). Expression of Endodermal and Mesodermal markers decreases along the gestation while Ectodermal and pluripotency markers expression is preserved in older samples. By 17 weeks of gestation it's evident an increase in expression of several progenitor markers including renal specific proteins.

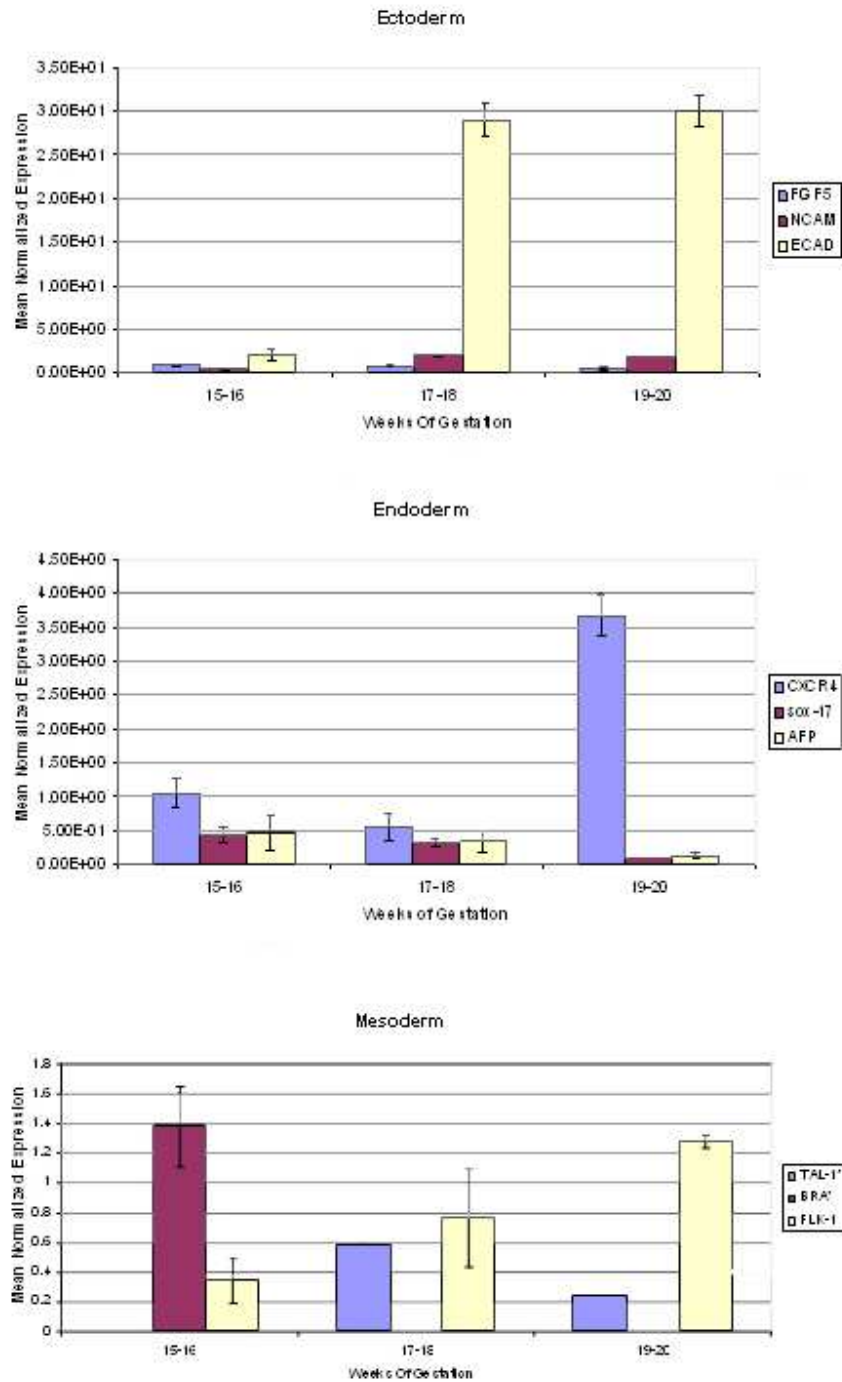


Figure 4 - Real Time PCR for Mesoderm, Endoderm and Ectoderm markers Expression of markers for the three germ layers. Quantitative analysis of markers expression shows an increase of E-Cadherin (Ectoderm), Flk-1 (Mesoderm) and Cxcr-4 (Endoderm). While ectodermal markers FGF-5 and NCAM are constant over the time, endodermal and mesodermal markers are decreasing their expression in older samples.

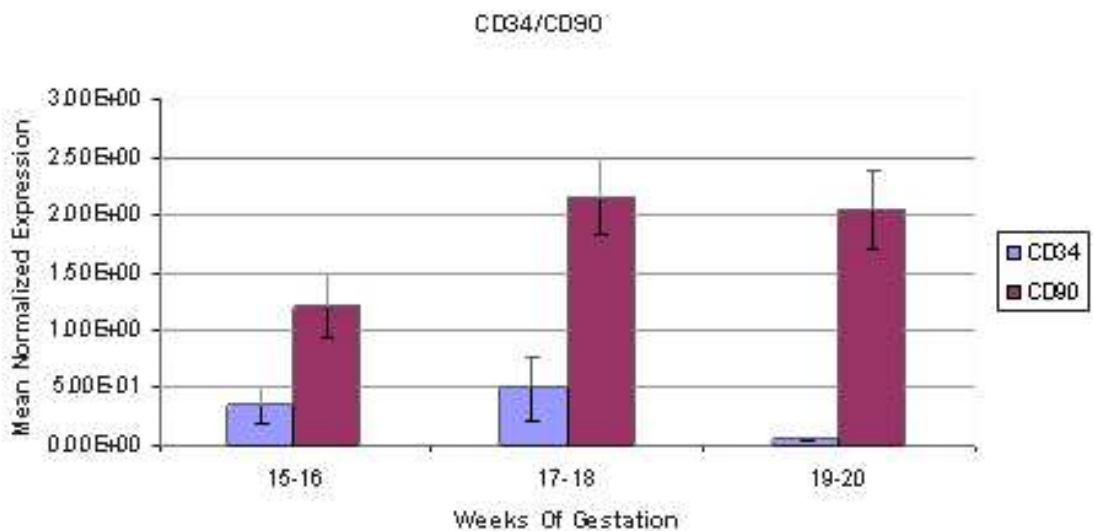
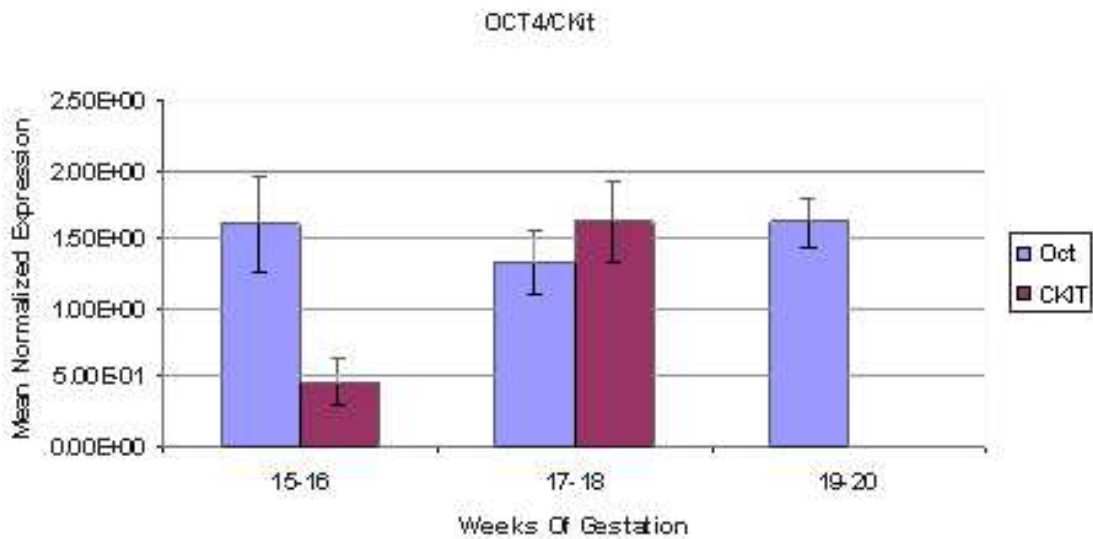


Figure 5 – Real Time PCR for pluripotency hematopoietic and mesenchymal markers. Expression of OCT-4 is not presenting any significant variation over the time while Ckit increases between 17-18 weeks and disappears at 19-20 weeks of gestation. Hematopoietic marker CD34 dramatically decreases as well at 19-20 weeks while CD90, marker for mesenchymal cells, is highly expressed in all the samples evaluated.

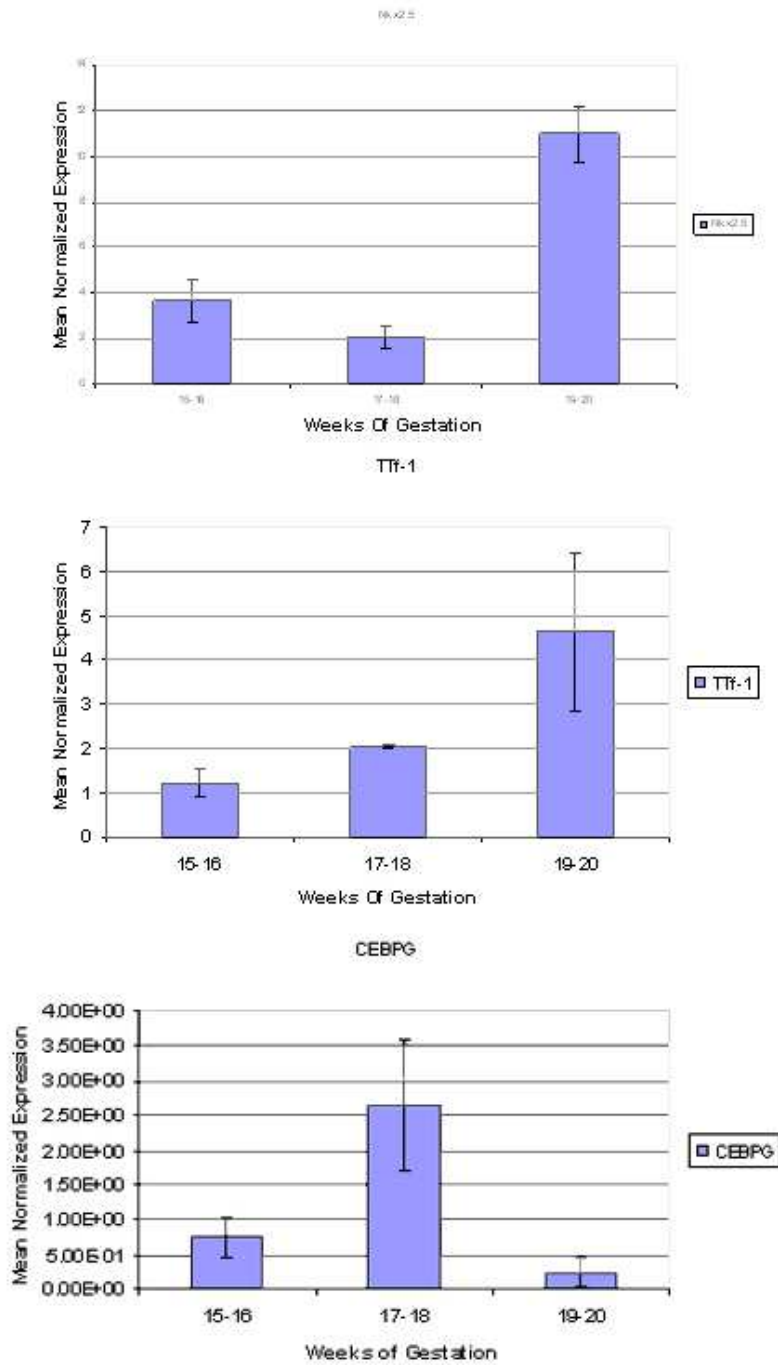


Figure 6 – Real Time PCR for Progenitor markers (Nkx2.5, TTF-1, CEBPG). Expression of Nkx2.5, early cardiac marker, and TTF-1, marker for lung differentiation increases at 19-20 weeks. CEBPG showed an increase between 17-18 weeks to return then to an expression comparable with the 15-16 weeks trend. PDX-1 is not reported. No data were retrieved in the samples analyzed.

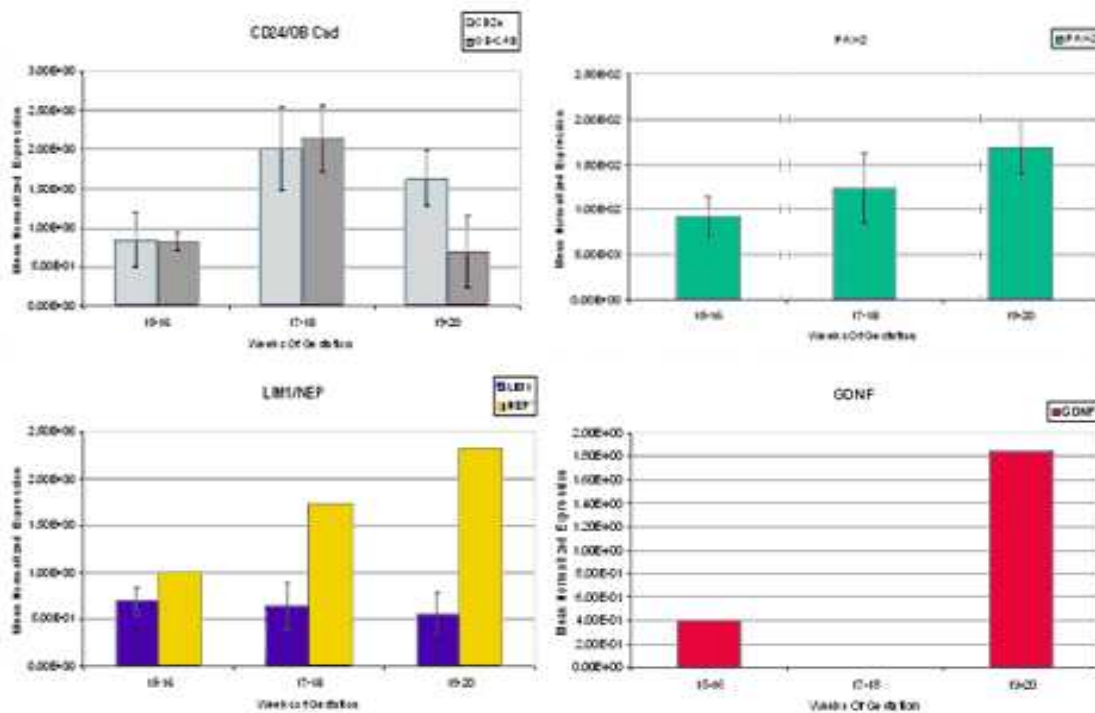


Figure 7 – Real Time PCR for Metanephric Mesenchyme markers in total amniotic fluid population. CD24 and OB-Cadherin, markers of the uninduced Metanephric Mesenchyme are increasing at 17-18 weeks. OB Cadherin is then decreasing to the previous level while CD24 maintain its high expression. Pax-2 shows a trend of increase over time like Nephryn, podocytes marker. LIM-1 maintains constant its expression. GDNF was detected in only two samples but shows a strong increase in the expression at 19-20 weeks of gestation.

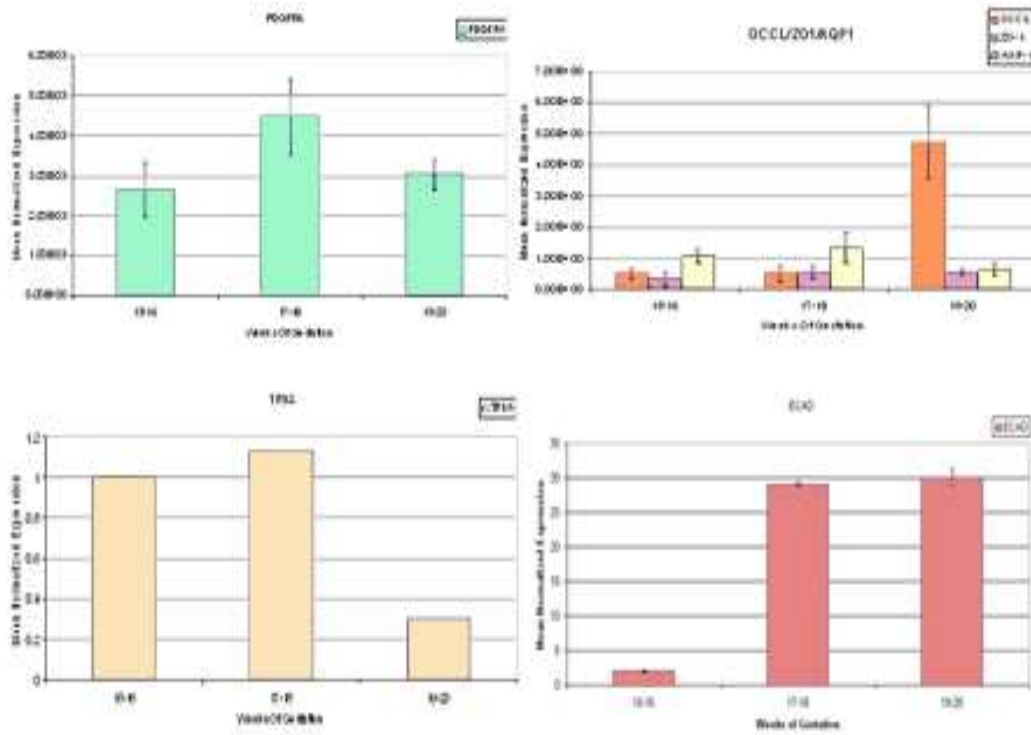


Figure 8- Real Time PCR for kidney markers in total amniotic fluid population. Expression of PDGFRα doesn't show a significant variation over the time while TrkA expression decreases at 19-20 weeks. Occludin expression increases at 19-20 weeks while AQP-1 and ZO-1 are constant over the time.

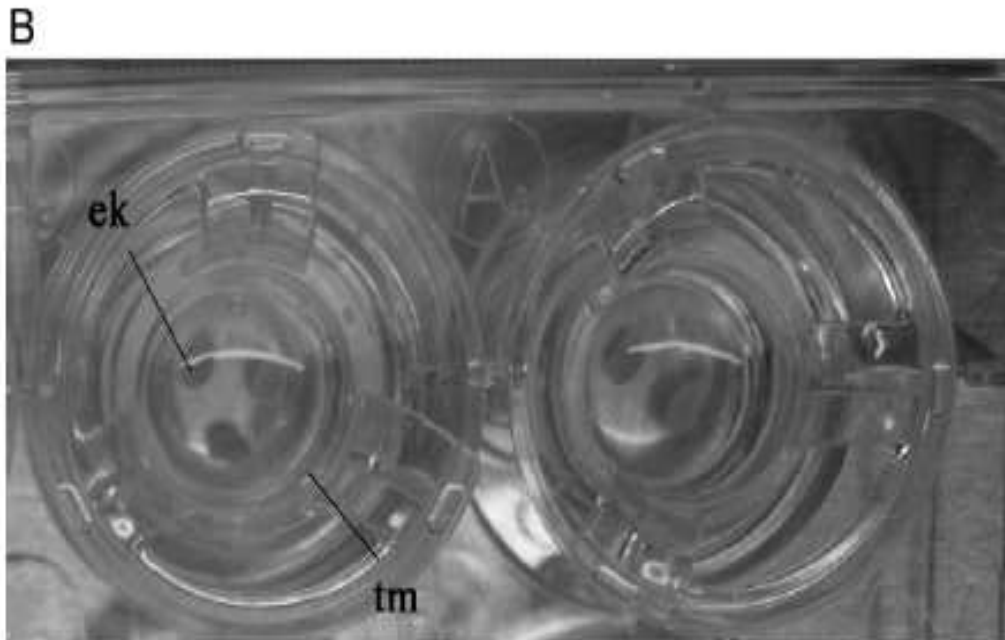
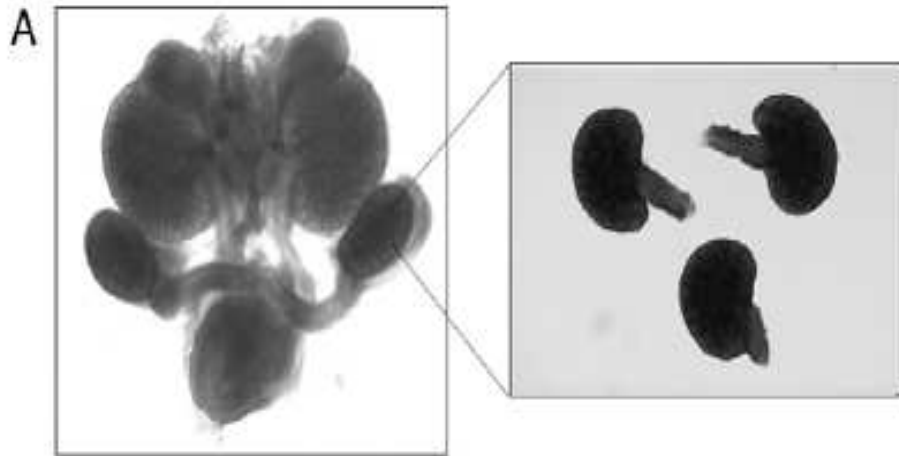


Figure 9 A-B (a) Genitourinary tract of mouse embryo from which embryonic kidneys were excised for ex vivo culture. (b) ex vivo culture system consisting of 24-well plate and insert filter (tm), where embryonic kidneys (ek) are cultured

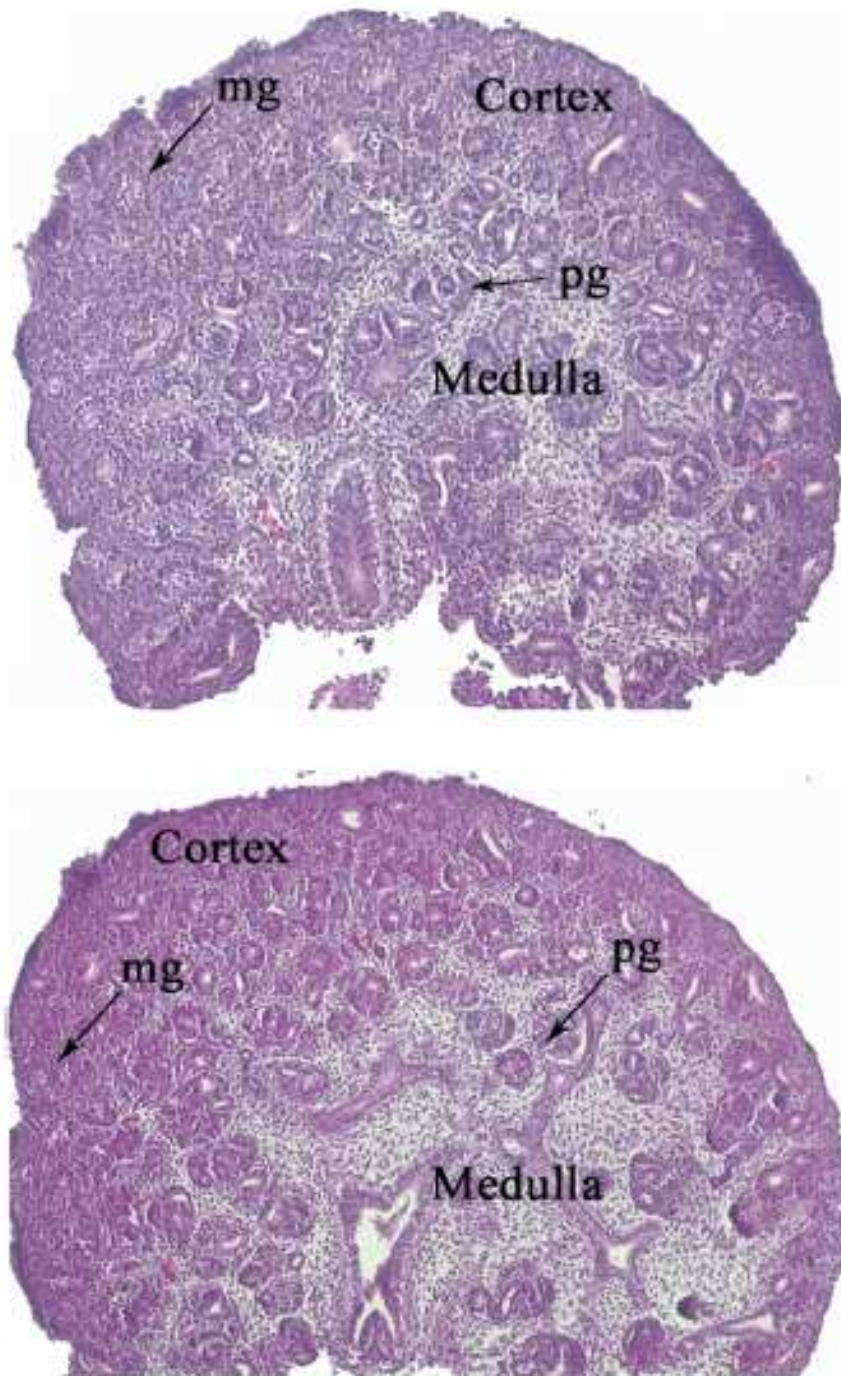


Figure 10 A-B (a) Embryonic kidney at E14 after 3 days of culture. Beyond 3 days cultures kidneys maintain and continue normal nephrogenesis. (b) Renal primordia grow without necrosis and demonstrate normal centrifugal pattern of development with mature glomeruli (mg) in periphery and primordial glomeruli (pg) in the center of embryonic kidney. Reduced from 10x

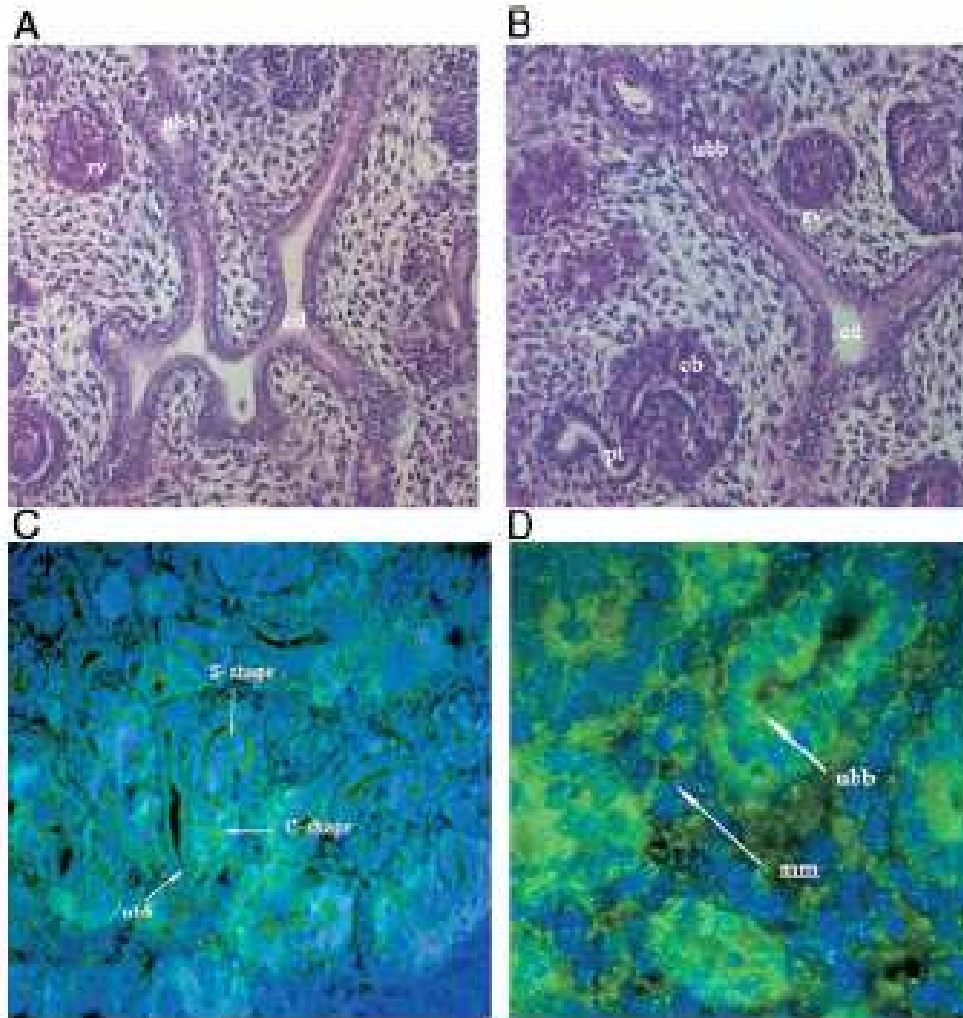


Figure 11 A-B-C-D (a) embryonic kidney at E14 after 3 days of culture. Kidney development in culture was maintained with outstanding quality. Tip of branching UB (ubb) is recognized, connected with developing collecting duct (cd). Renal vesicle (rv) will ultimately give rise to mature nephron. Reduced from x25. (b) embryonic kidney at E14 after 3 days of culture demonstrates different stages of kidney development. Branching UB is fused to collecting duct. Adjacent to collecting duct is renal vesicle. Note mature glomerulus with Bowman's capsule (cb) and portion of proximal tubule (pt) connected to glomerulus. Reduced from x32. (c) immunofluorescent staining for GDNF in E15 embryonic kidney after 5 days of culture. GDNF was expressed by MM (C- and S-shape) surrounding UB tip and also by UB. Reduced from x10. (d) immunofluorescent detection of Pax-2 in E15 embryonic kidney after 5 days of culture. Pax 2 was expressed in branching UB and in adjacent MM (mm). Reduced from x40.

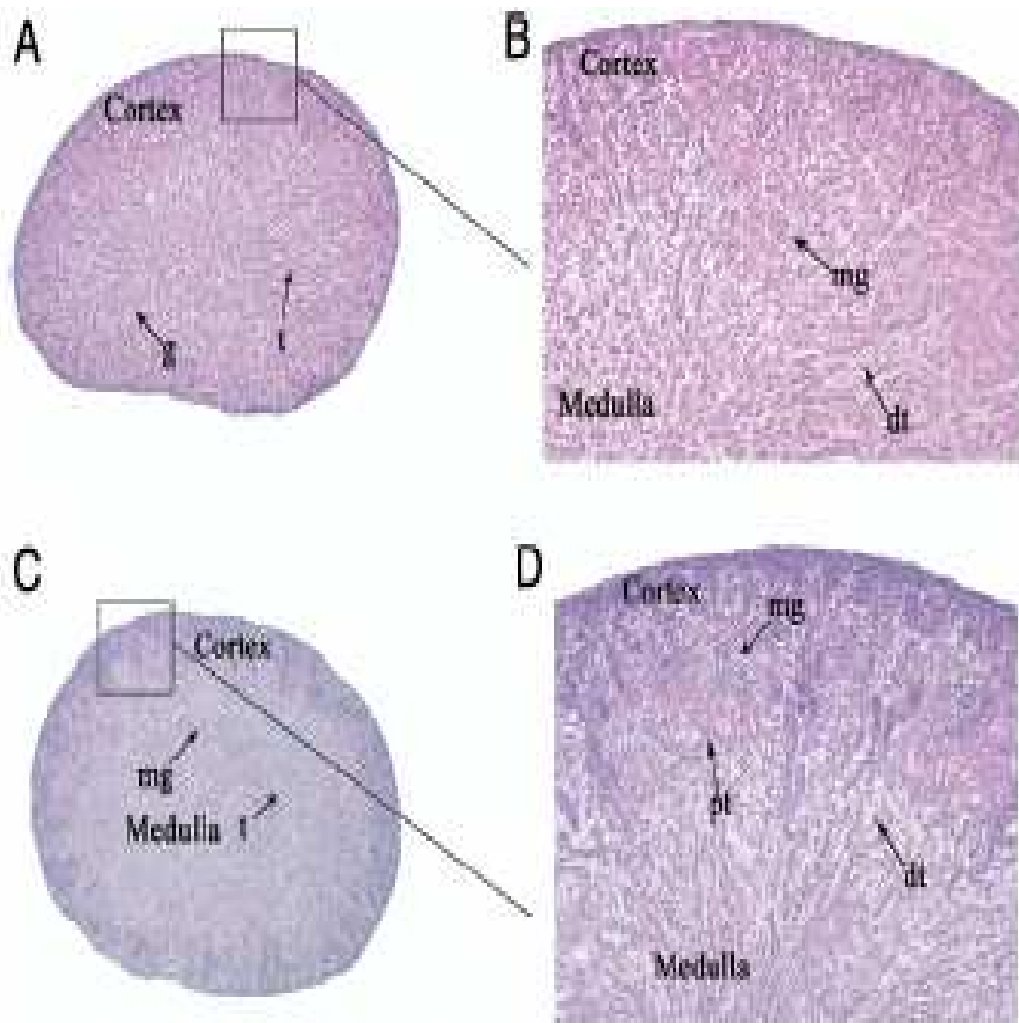


Figure 12 A-B-C-D (a) embryonic kidney at E17 after 10 days of culture. Long-term culture of embryonic kidney provided distinction between medulla and cortex. Glomeruli (g) and tubular structures (t) were well preserved with time and moderate amount of apoptotic cells was noted. Reduced x4. (b) higher magnification reveals mature glomeruli (mg), complete proximal and distal tubules (dt) at the center of the medulla. Reduced from x10. (c and d) another example of long term culture (up to 10 days) of embryonic kidney at E16. Necrosis was present at only small portion of organ periphery, while glomeruli and tubules were well preserved. Pt, proximal tubules. Reduced from x5 (c) and x8 (d)



Figure 13 Immunostaining for apoptosis. Observed pattern is similar to that in normal renal development with more cells at periphery undergoing programmed cell death. Reduced from x20.

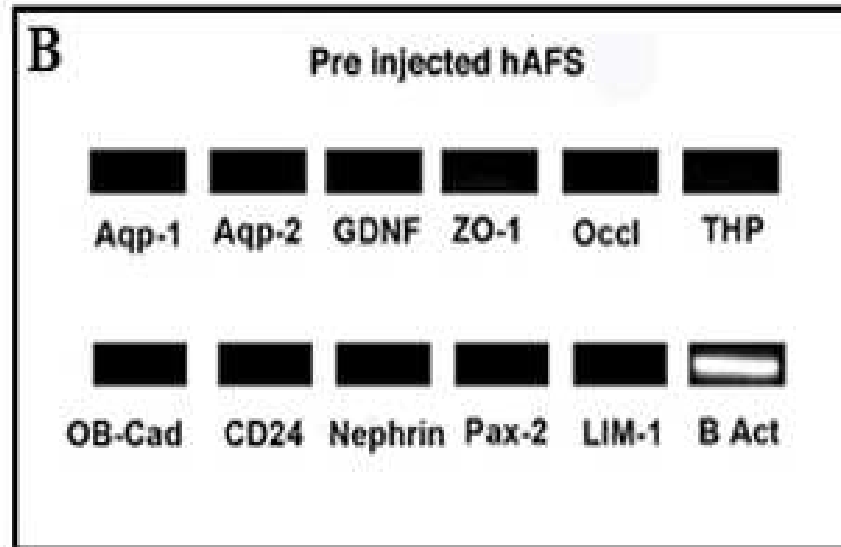


Figure 14 A-B – hAFSC analysis before the injection. AFSC were investigated for morphology (FIG 9A), expression of renal markers such as Aqp-1 and 2 GDNF, ZO-1, Occludin, THP, OB-Cadherin, CD24, Neph rin, Pax-2 and LIM-1 resulting negative by RT-PCR (B);

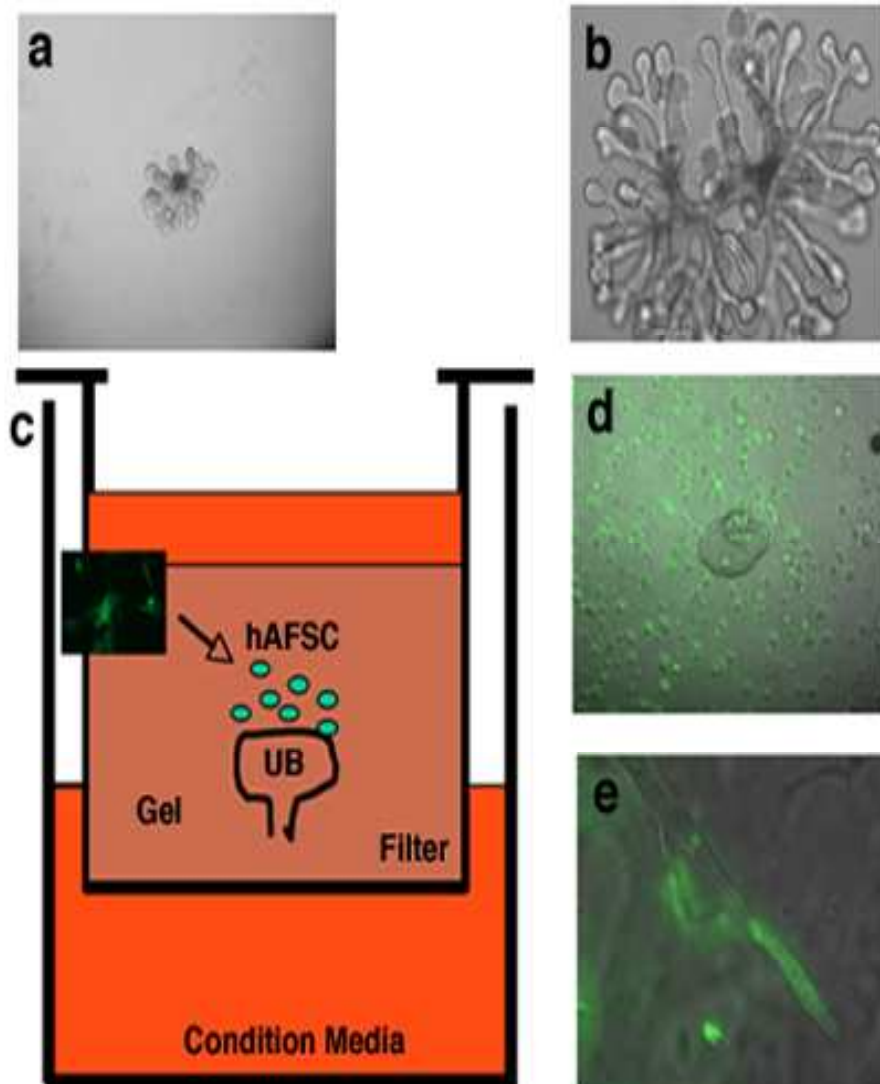


Figure 2. **a.** UB isolated from E13.5 rat embryo and cultured for 24 hours viewed under light microscopy(10x). **b.** UB after 5 days of culture exhibiting multiple branching under light microscopy (10x). **c.** Schematic drawing of the co-culture system: a polycarbonate filter is placed inside a 24 transwell petri dish containing condition media with GDNF and FGF1, serum and antibiotics. Undifferentiated hAFSC are placed close to the branching UB tips. **d.** Fluorescent image of an isolated UB (10x) with GFP labeled hAFSC in contact within the co-culture system at day 0. **e.** Formation of fluorescent tubular structures (40x) are derived from GFP labeled hAFSC after 5 days in culture.

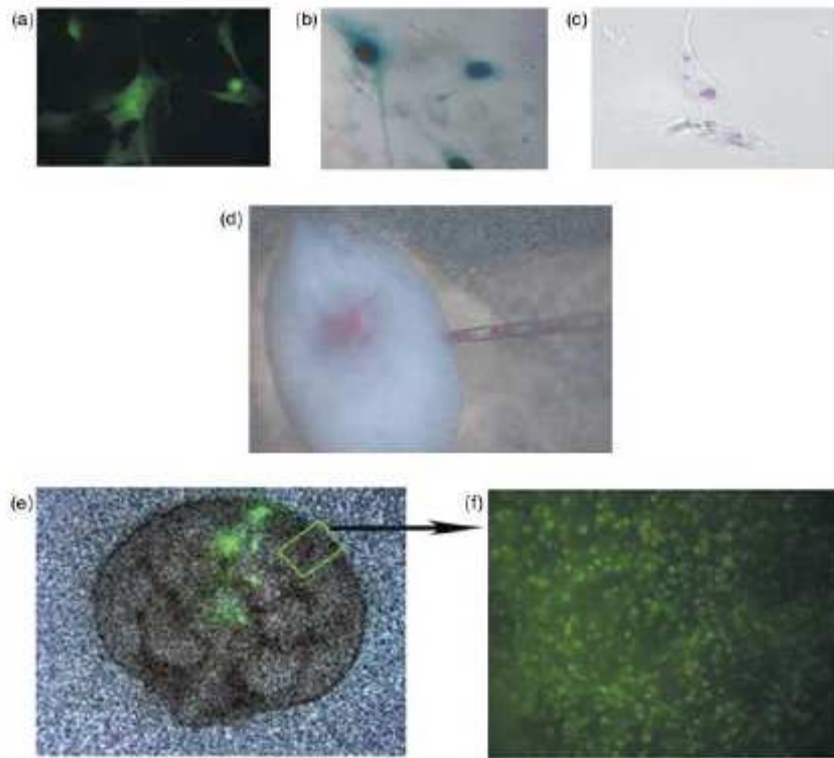


Figure 16 A-B-C-D-E Microinjection of labeled amniotic fluid stem cells, pre-injected stem cells, the injection in process and post-injection. (a) hAFSC transfected with retrovirus carrying the sequence for GFP and β -galactosidase under fluorescent microscopy (x40). (b) Lac-Z nuclear staining of hAFSCs (x40). (c) hAFSC labeled pink for light microscopy with cell surface marker CM-Dil (x40). (d) Microinjection of hAFSC labeled with CM-Dil direct vision (x4) into the centre of the embryonic kidney. (e) GFP labeled cells shown in the embryonic kidney by fluoroscopy at day 0 of injection (x4). (f) Live imaging, at 4h intervals, of the embryonic kidney after 4 days of culture demonstrating GFP labeled hAFSC multiplying and spreading throughout the entire organ from the centre to the periphery (x40, see the supplementary video online: <http://www.blackwell-synergy.com/doi/abs/10.1111/j.1365-2184.2007.00478.x>). hAFSCs human amniotic fluid stem cells, GFP green fluorescent protein.

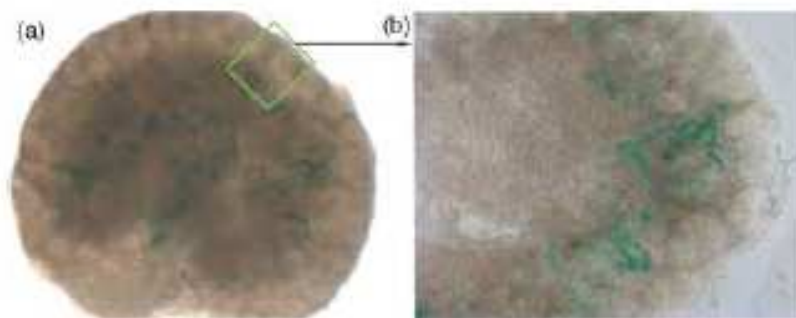


Figure 17 A-B Migration pattern of hAFSC in developing embryonic kidney, histology of sectioned kidneys post-injection of stem cells. (a) Lac-Z staining confirming the presence of hAFSC after 3 days in culture (x6). (b) Lac-Z+ hAFSC migrated to the periphery of the embryonic kidney after injection into the middle of the organ (x8).

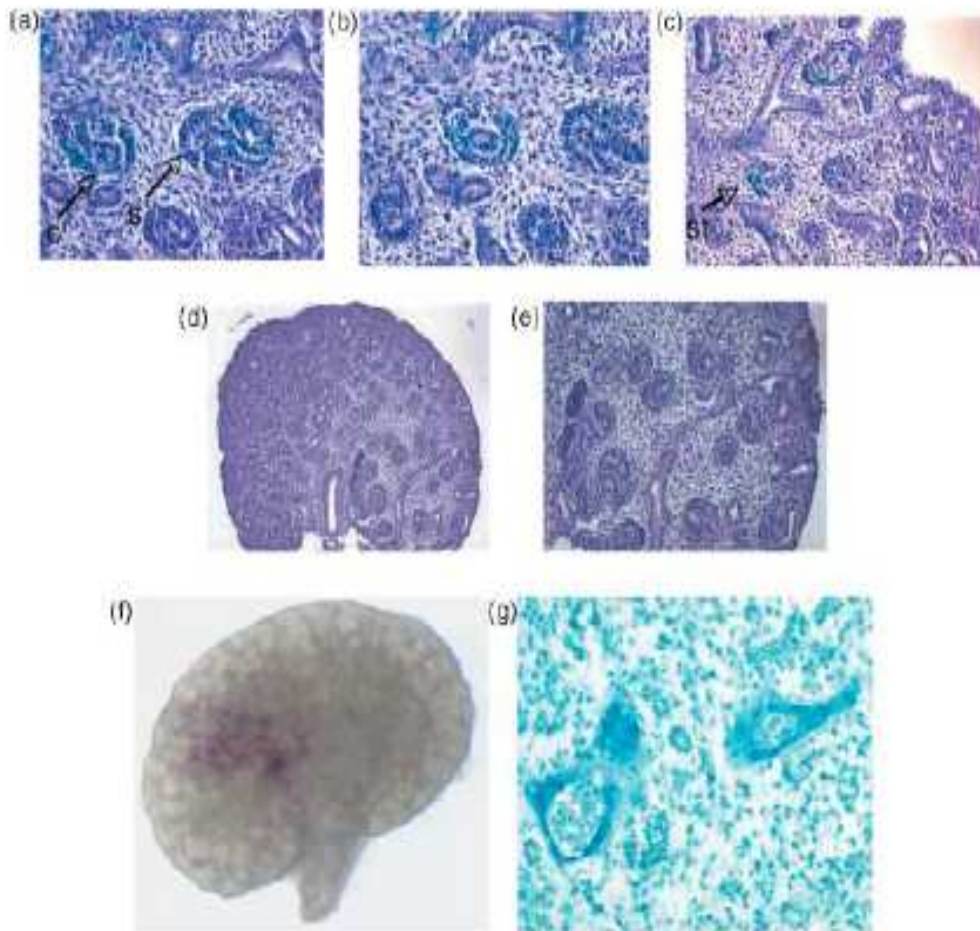


Figure 18 A-B-C-D-E-F-G Structural differentiation of amniotic fluid stem cells within developing embryonic kidneys demonstrating integration of stem cells. (a) H&E staining after Lac-Z staining revealing presence of hAFSC in C- and S-shaped bodies of the embryonic kidney (x40) (arrows). (b) Lac-Z+ hAFSCs within the stroma of the developing kidney after H&E staining (x40). (c) Lac-Z+ hAFSCs within renal vesicles of the developing kidney after H&E staining (x30) (arrow). (d-e) Controls with no detected Lac-Z staining (x10 and x16). (f) hAFSCs labeled with CM-Dil 1 day after injection (x10). (g) hAFSCs labeled with CM-Dil, that appears blue with light microscopy after the toluidine treatment, detected in renal primordia (C- and S-shaped bodies) and in the stroma after 5 days of culture within developing tubular nephrons of the embryonic kidney (x40). H&E, haematoxylin and eosin, St stroma.

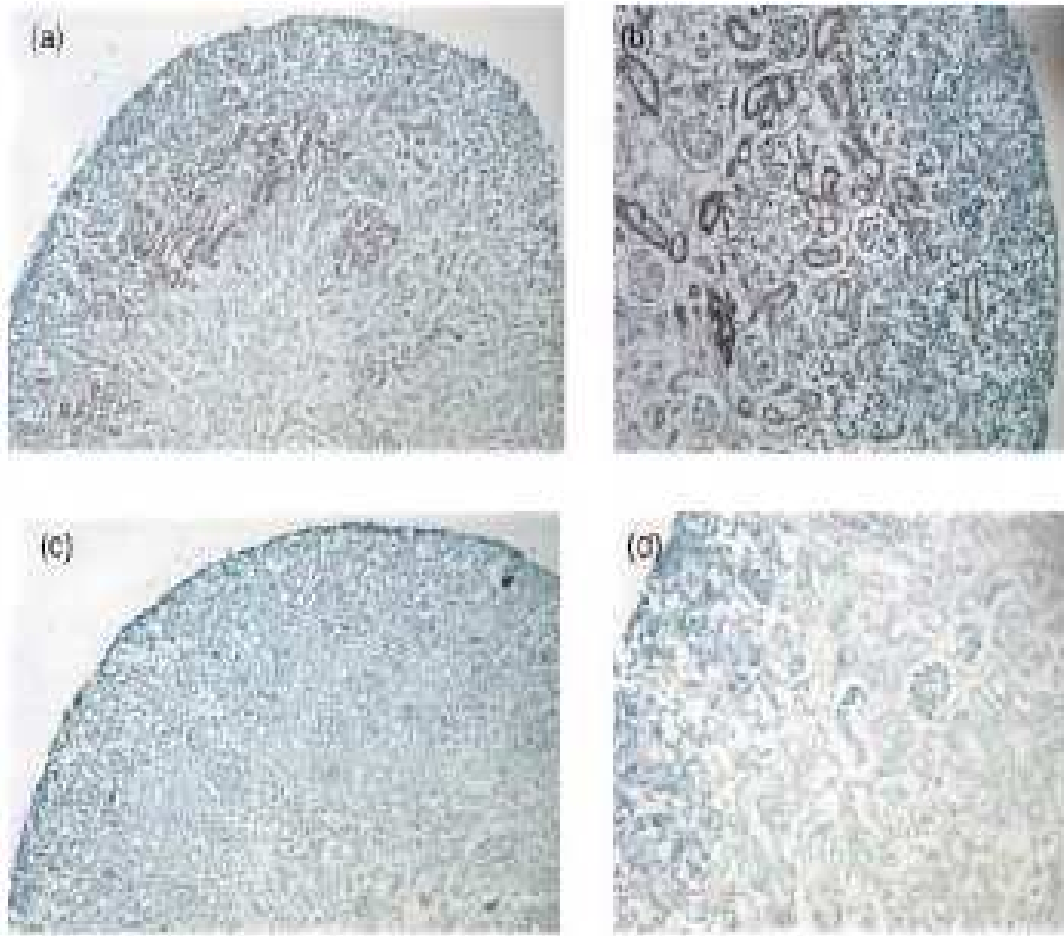


Figure 19 A-B-C-D Chromogenic in situ hybridization (CISH) of injected amniotic fluid stem cells, integration of stem cells into the cultured developing kidneys. (a) CISH for Y chromosome of hAFSC also confirmed integration into embryonic kidney structures (x20). (b) Primordial tubular nephrons stained positively with CISH confirming integration of hAFSCs into these structures. (c) Controls demonstrated no positive reaction with CISH (x20). (d) CISH controls with no positive stain (x30).

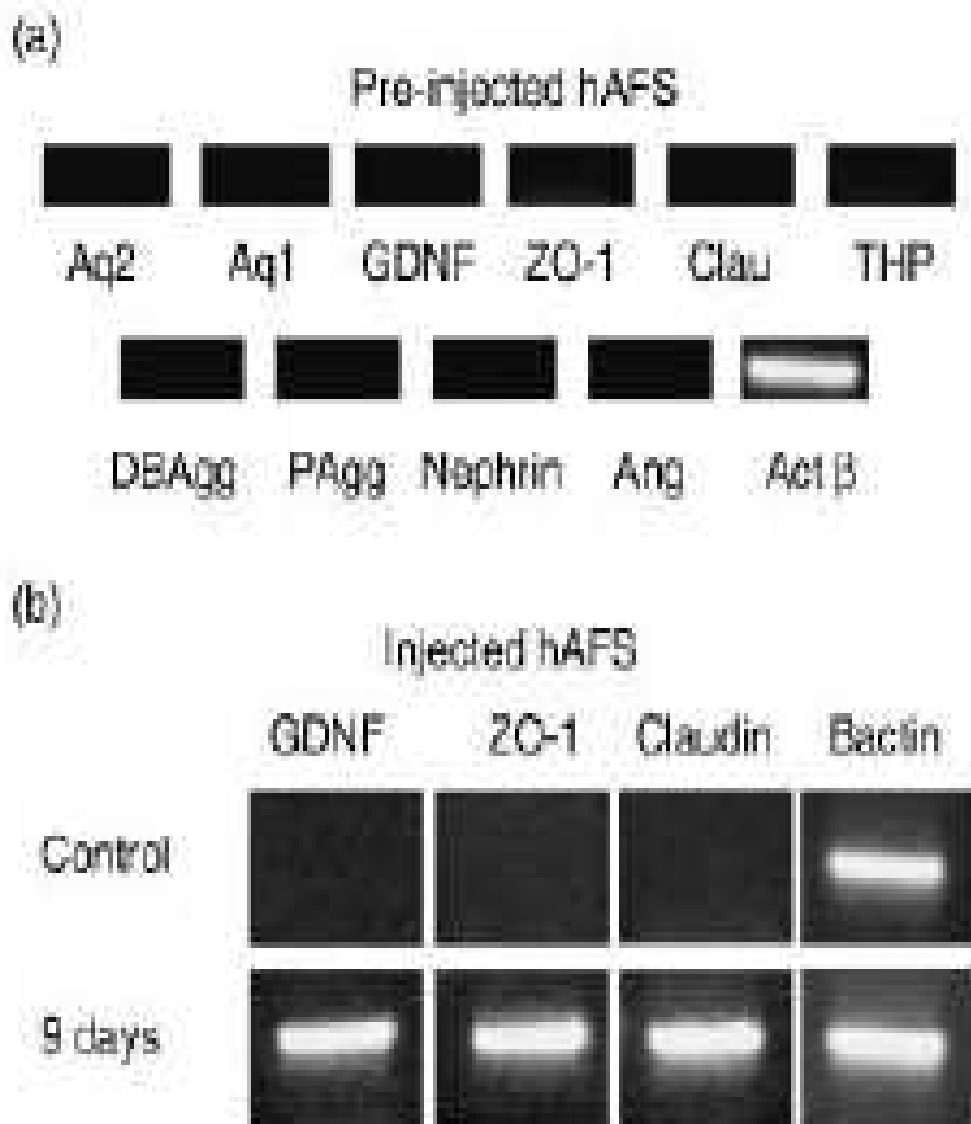


Figure 20 A-B Molecular evidence of primordial kidney differentiation from amniotic fluid stem cells, RT-PCR markers demonstrating expression of renal specific markers pre- and post-injection and culture. (a) RT-PCR of hAFSCs prior to injection are negative for most kidney markers. (b) hAFSCs, 9 days after injection into embryonic kidneys, demonstrate early kidney gene expression markers, zona occludens-1 (ZO-1, 760bp), glial-derived neurotrophic factor (GDNF, 630pb), and claudin (480bp), compared to no expression of kidney markers in controls (hAFSCc prior to injection). RT-PCR, reverse transcription-polymerase chain reaction.

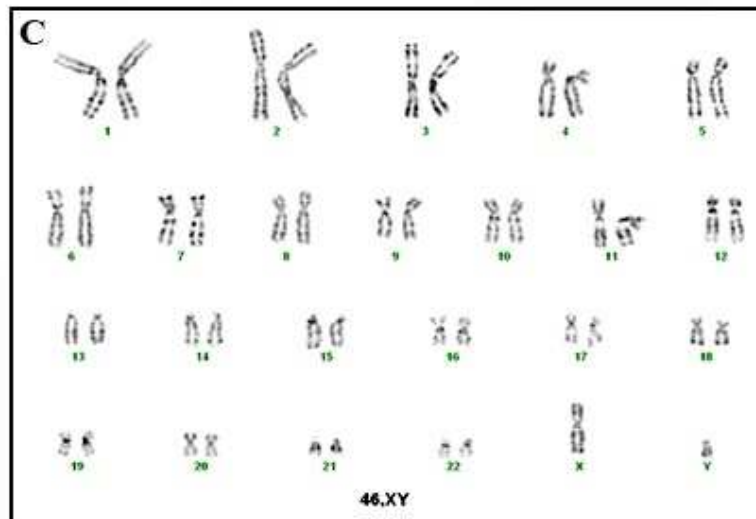
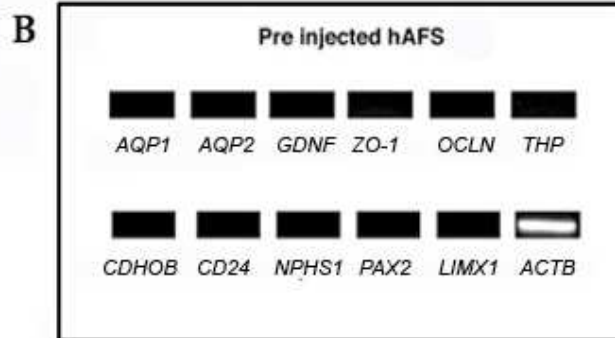
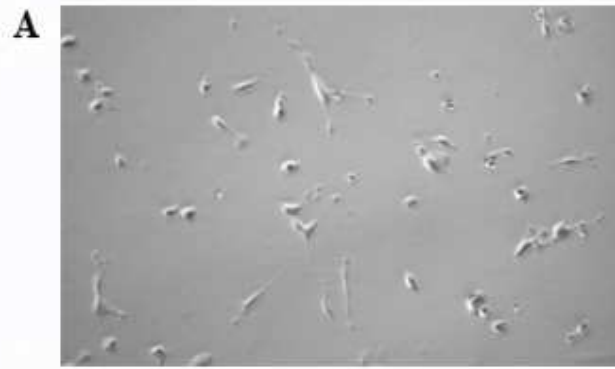


Figure 21. A. Morphology of hAFSC population. After 40 passages in culture under bright field the cells present a fibroblastoid appearance (10x). **B. RT-PCR of hAFSC before the injection.** As shown in the picture, no earlier and mature kidney markers are expressed. ACTB is used as housekeeping gene. **C. Karyotype of hAFSC after 38 passages.** As shown in the picture the cells do not present any abnormality and have a normal karyotype.

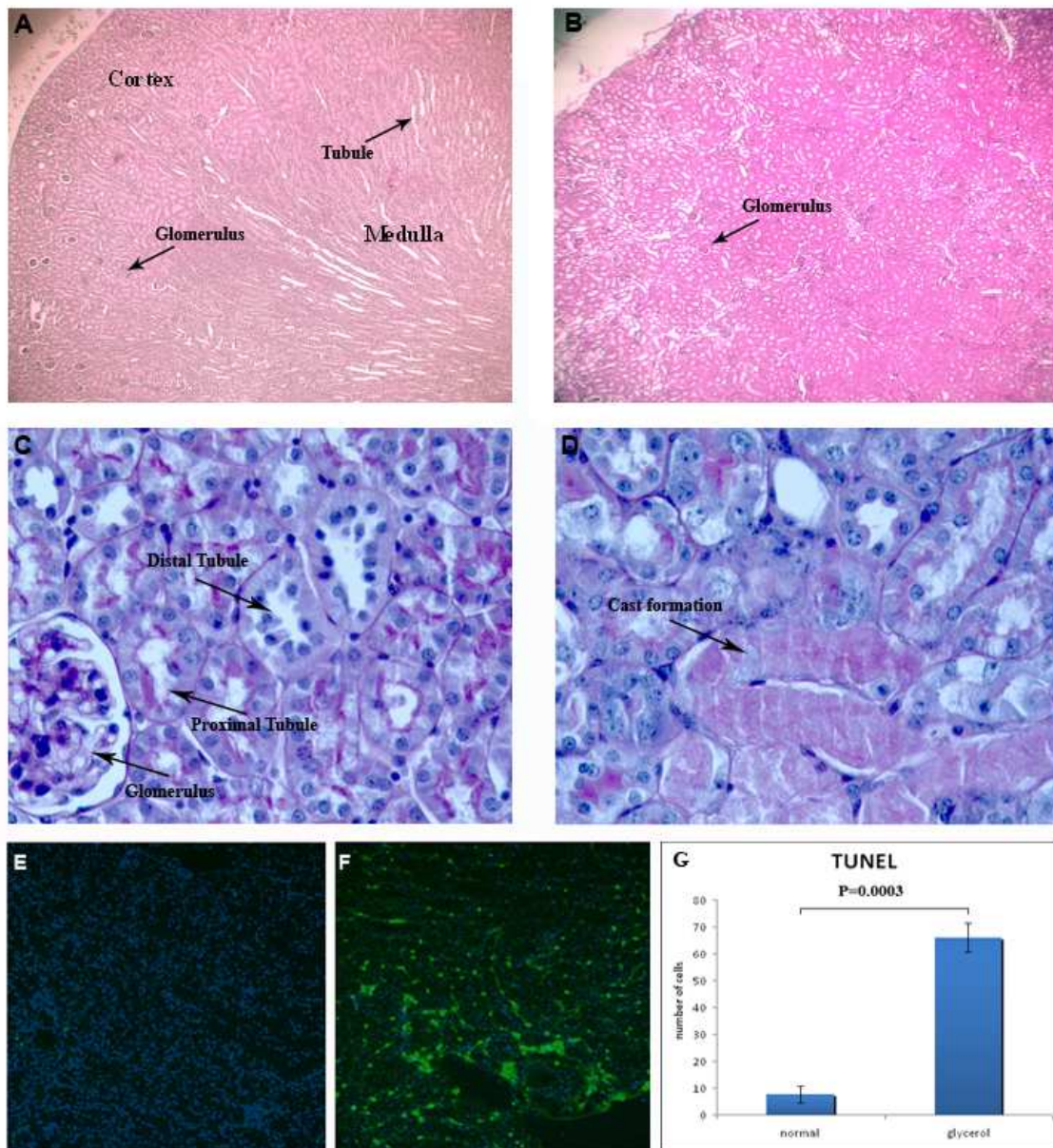


Figure 22. A. Histological section (H&E) of a nu/nu mouse kidney. Tubules and glomeruli, indicated by the arrow, present normal morphology (10x). **B. Histological section (H&E) of a nu/nu mouse kidney after 3 days of glycerol-rhabdomyolysis-induced-ATN.** It is not possible to distinguish between the medulla and the cortex. The glomeruli are still present (arrow) and not damaged, while the tubules are damaged (10x). **C. PAS staining of a nu/nu mouse kidney when compared with a nu/nu mouse kidney after 3 days of glycerol-rhabdomyolysis-induced ATN where the destruction of the brush borders, intraluminal cast formation and general disorganization of the kidney structures is evident (arrow, 40x) (D).** **E. TUNEL staining of a nu/nu mouse kidney.** The level of apoptotic cells is very low, when compared with a TUNEL staining of a nu/nu mouse kidney after 3 days of glycerol-induced ATN (F), (10x). **G. Graph representing the effect of glycerol injections in kidney cells apoptosis (positive apoptotic nuclei per 300 nuclei) compared with untreated controls.** Values are mean \pm SD ($p=0.0003$)

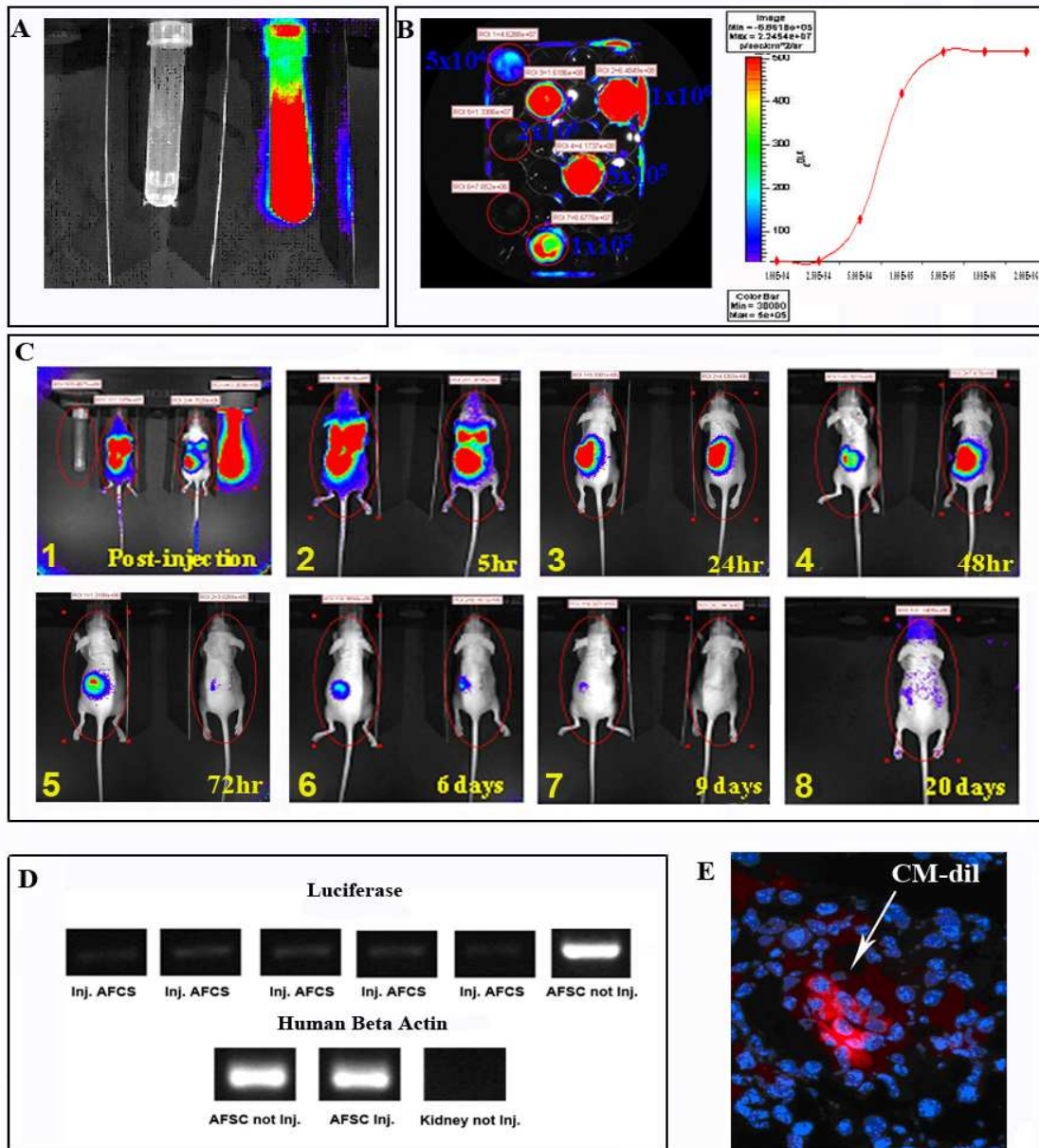


Figure 23. In vitro evaluation of luciferase expression in transduced hAFSC over the population doublings (a) and determination of limit starting point of number of cells that exhibits luciferase signal under bioluminescence (b). C. In vivo experiment showing bioluminescent detection of hAFSC after injection into a damaged nu/nu mouse kidney over a period of 21 days. D. RT-PCR demonstrated the presence of the luciferase sequence in injected kidneys, compared with the cells before injection (positive control) and in un-injected kidney (negative control). ACTB was used as housekeeping gene. E. Immuno-fluorescence staining of injected kidney with hAFSC after 3 weeks. The red fluorescence (arrow) confirms the presence of hAFSC expressing luciferase. The nuclei are stained with DAPI (20x)

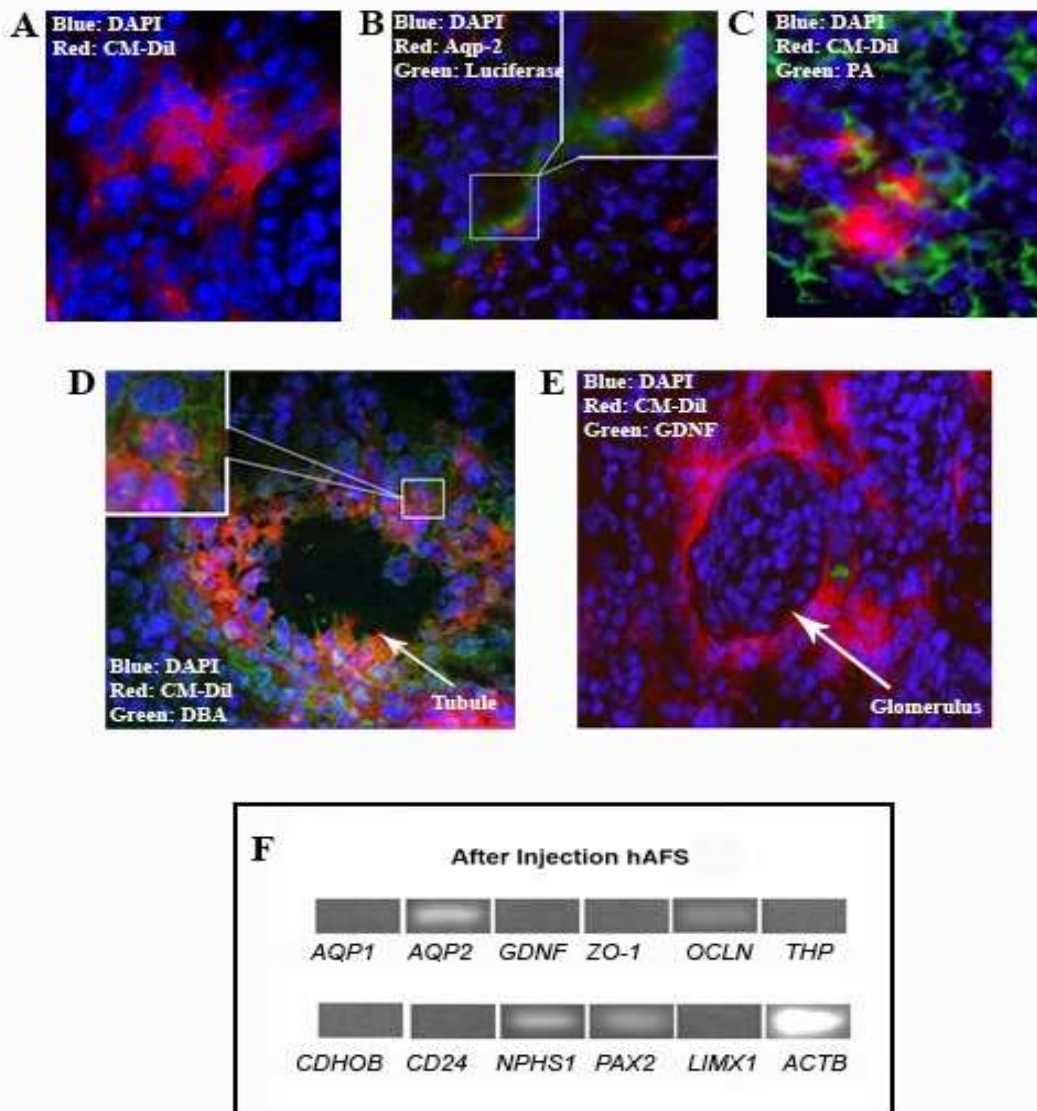


Figure 24. **A.** Frozen section of a kidney injected with hAFSC after 1 week. The cells are evident as red fluorescence of the surface marker CM-Dil. The nuclei are stained with DAPI (30x). **B.** Double Immuno-fluorescence staining of injected kidney with hAFSC on the same cells expressing both Aqp2 and luciferase of the markers in a tubule (arrow), after 3 weeks. The nuclei are stained with DAPI. (30x). It is noticeable that CM-Dil-labelled-hAFSC locate in proximity of the tubular structure after 3 weeks on injection expressing Peanut Agglutinin (**C**) and Dolichus Biflorus Agglutinin (arrow) (**D**); hAFSC locate also in close proximity of the glomerular structure expressing Glial Derived Neurotrophic Factor by hAFSC (arrow) (**E**). The nuclei are stained with DAPI (40x). **F.** RT-PCR of injected hAFSC after 3 weeks. The cells expressed NPHS1, AQP2, PAX2, OCLN, ACTB is used as a housekeeping gene.

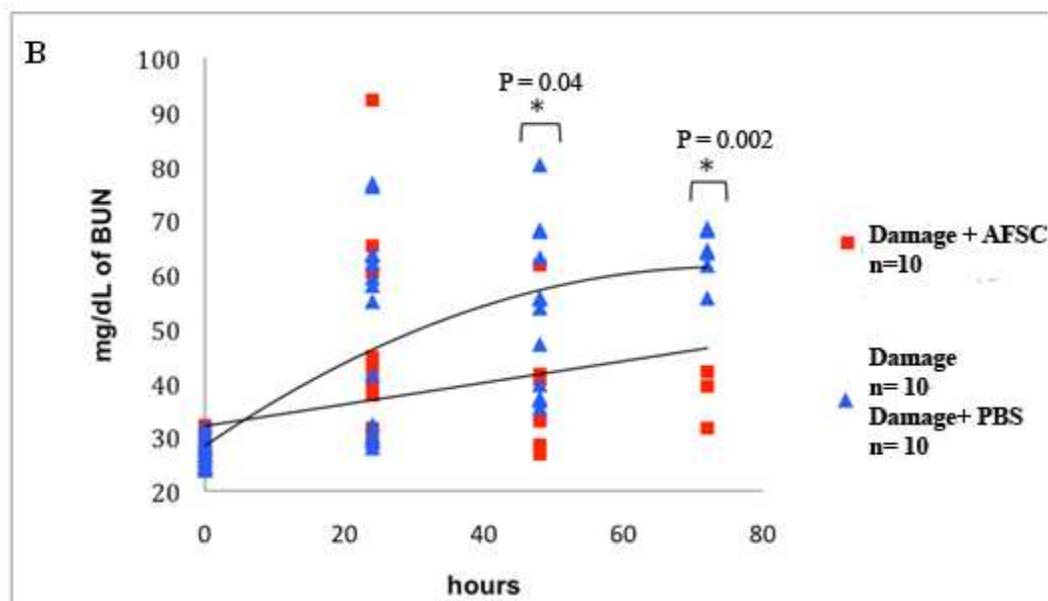
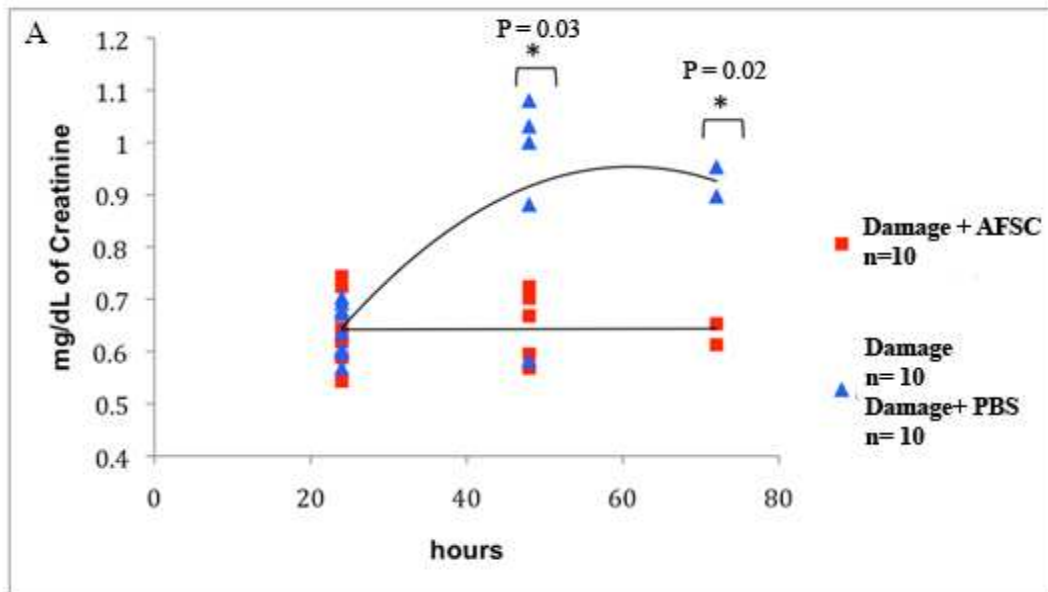


Figure 25. In these graphs is shown the difference in levels of blood creatinine (A) and BUN (B) between two groups of *nu/nu* mice over a period of 72 hours. The blue triangles represent mice that underwent only intramuscular glycerol injection and the mice that underwent intramuscular glycerol injection plus PBS injection into the kidneys. The red squares represent the mice that underwent intramuscular glycerol injection plus administration of hAFSC into the kidneys. Values are mean \pm SD (creatinine: 48 hours: $p=0.03$; 72 hours: $p=0.02$; BUN: 48 hours: $p=0.04$; 72 hours: $p=0.002$).

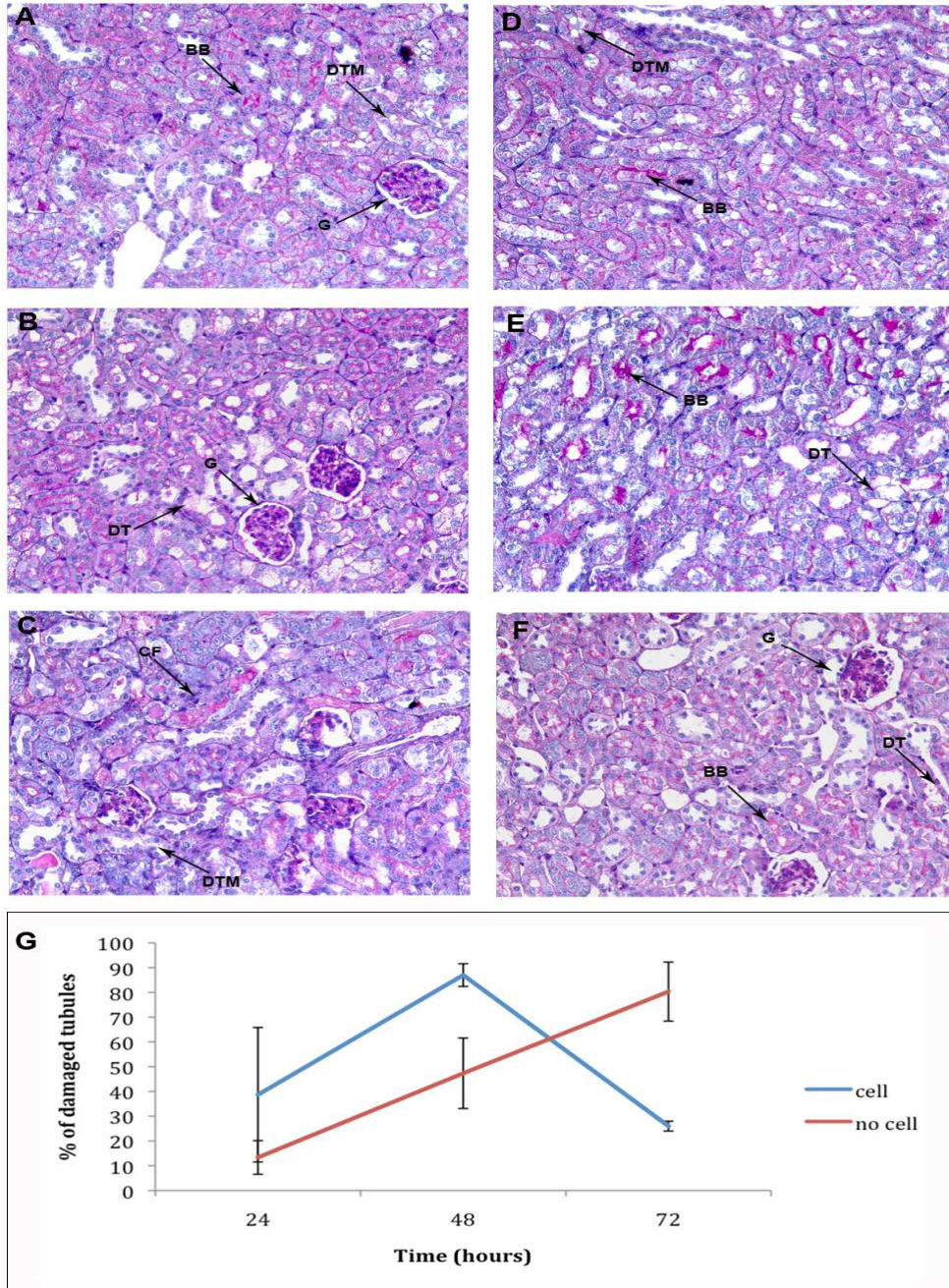


Figure 26. In these figures it is shown the PAS-Staining of kidney sections of mice treated only with injection of glycerol over the course time of 24 hours (A), 48 hours (B) and 72 hours (C) when compared with mice treated with injection of glycerol and hAFSC at 24 hours (D), 48 hours (E) and 72 hours (F) after injections. In the mice treated only with glycerol the level of disruption of brush border (BB), the desegregation of the tubular membrane (DTM) are cast formation (CF) increased over time while the injection of hAFSC preserved the morphology of the tubular structures after they been damaged by glycerol injections. The graph represents the percentage of damage tubules per total number of tubules in the sections (G). Values are mean \pm SD. (48 hours: $p=0.03$; 72 hours: $p=0.01$).

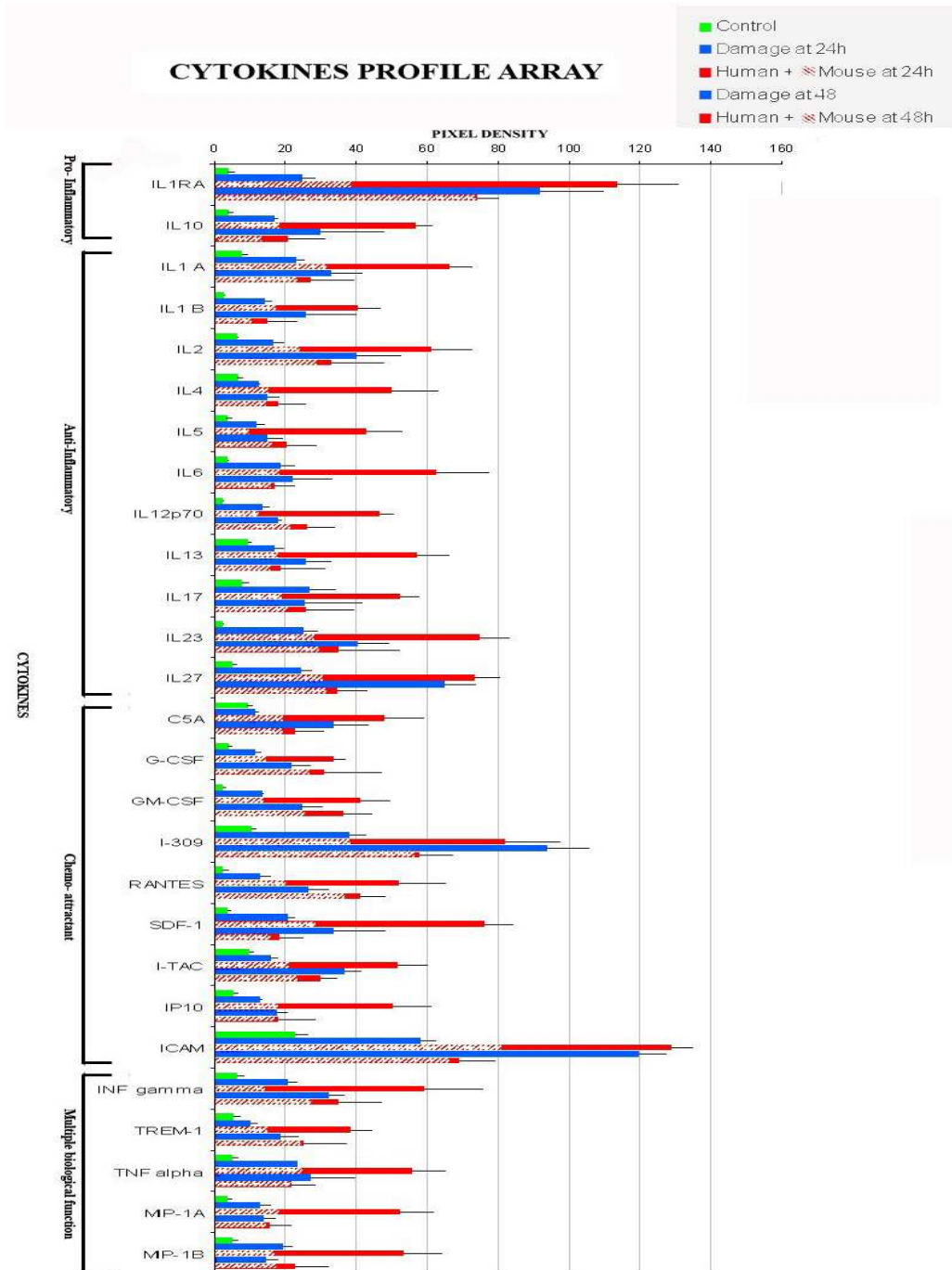


Figure 27. This suite of bar graphs shows the profile of mouse and human cytokines that are expressed in mouse kidney in control mice (green), in mice with glycerol-induced-rhabdomyolysis ATN (blue) versus mice with injection into the kidney of hAFSC simultaneous with the intramuscular glycerol injection to induce ATN (mouse derived cytokines shown as red hatched bars, human cytokines as red bars). Values are mean \pm SD. The cytokines were divided into 4 broad functional groups based on their principal biological activity during inflammation: 1. Anti-inflammatory, 2. Pro-inflammatory, 3. Chemoattractants, 4. Multiple biological effects. The profile of cytokines expressed in whole mouse kidney was evaluated at 24h and at 48h.

Gene	Primer Sequence (5'→3')	Size (bp)	Annealing Temperature
Nephrin, <i>NPHS1</i>	aca cgg agc aca cat acc ac gga ttg gag agg agc aga ag	570	59
Zona Occludens-1, <i>ZO1</i>	agg aga ggt gtt ccg tgt tg gct ggt ttt gct gtt gtt ga	760	59
Glial Derived Neurotrophic Factor, <i>GDNF</i>	tat ggg atg tcg tgg ctg t aca cct ttt agc gga atg ctt	630	58
Aquaporin-1, <i>AQP1</i>	cac ctc ctc cct gac tgg ggt tgc tga agt tgt gtg tga	290	58
Aquaporin-2, <i>AQP2</i>	gat cac gcc agc aga cat c ggg cag gat tca tag agc ag	240	59
Tam-Horsfall-Protein, <i>THP</i>	tag acg agg act gca aat cg gtc ccg gtt gtc tct gtc at	220	59
OB-Cadherin, <i>CDHOB</i>	cactgtctttgcagcagaaatc tacaatgaccaaggagaatgacg	430	55
<i>CD24</i>	acc cag cat cct gct aga c ctt aag agt aga gat gca gaa	290	59
LIM1, <i>LIMX1</i>	aag agc gag gat gaa gat gc tca gga ggc gaa gtagga ac	620	59
Occludin, <i>OCLN</i>	gcc ctc gca acc caa att tta tca ttc act ttg cca ttg ga	430	58
PAX-2, <i>PAX2</i>	aac gac aga acc cga cta tgt t agg atg gag gga cca act gc	740	59
Beta-actin, <i>ACTB</i>	aga aaa tct ggc acc aca cc ctc ctt aat gtc acg cac ga	390	55
Luciferase	agg agc ctt cag gat tac aag att caa agt gta ctt aat ca gaga ctt cag gcg ggt caa c	500	58

Figure 28: List of the human primers, the size of the products and the annealing temperature used in the experiments

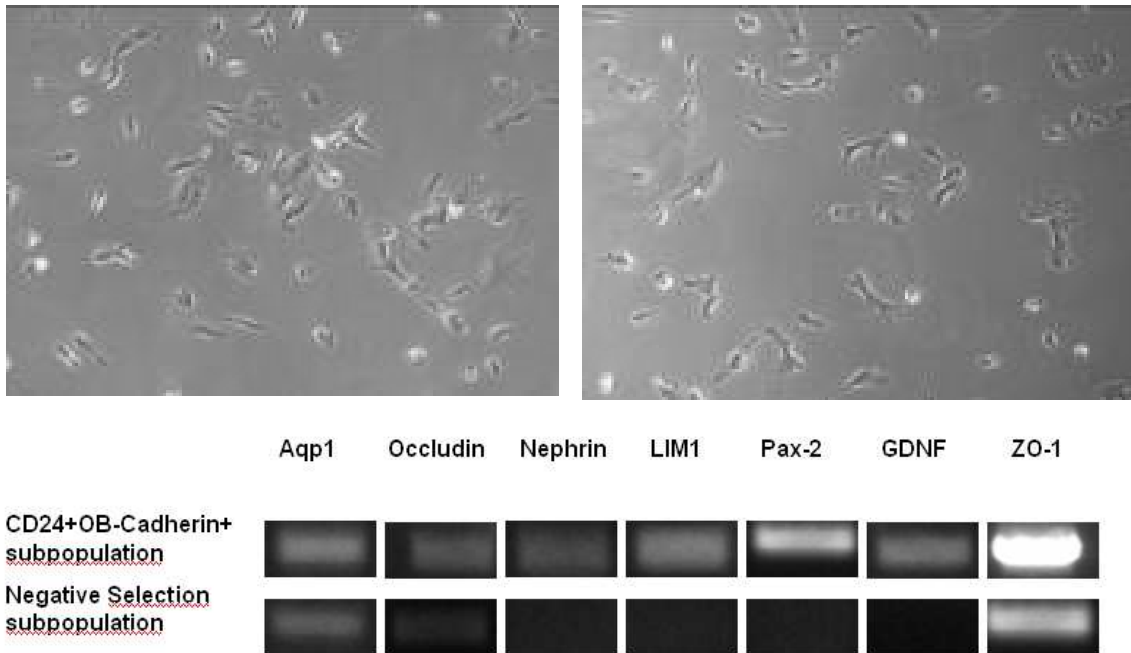


Figure 29 A-B – Morphology and Characterization of MMDC cells. A Morphology of the MMDC selection. (x20) B- RT-PCR of MMDC population compared with a CD24 Negative OB Cadherin negative selection. Expression of renal markers in the double positive selection, compared with the negative results for the negative selection, confirm the successful immunoseparation of cells with renal traits from the whole amniotic fluid population.

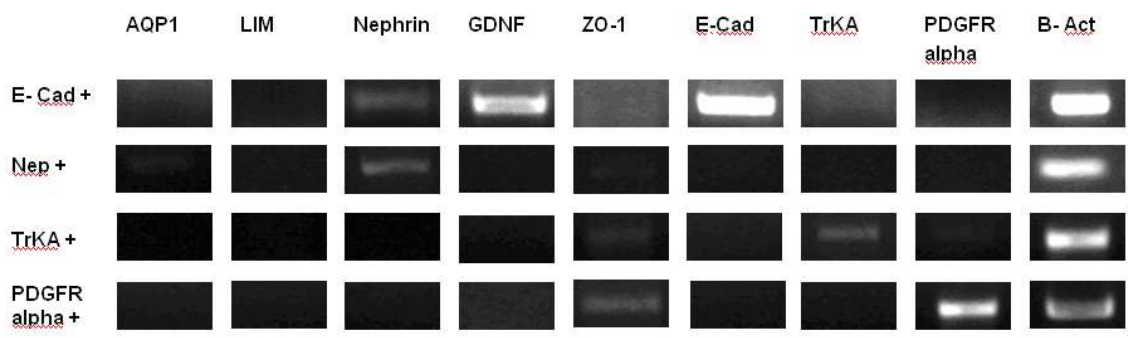


Figure 30 – RT-PCR of CD24+OB-Cadherin+ derived subpopulations (AKPC). Patterns of expression are showing that the selection retrieved four different populations with diverse characteristics.

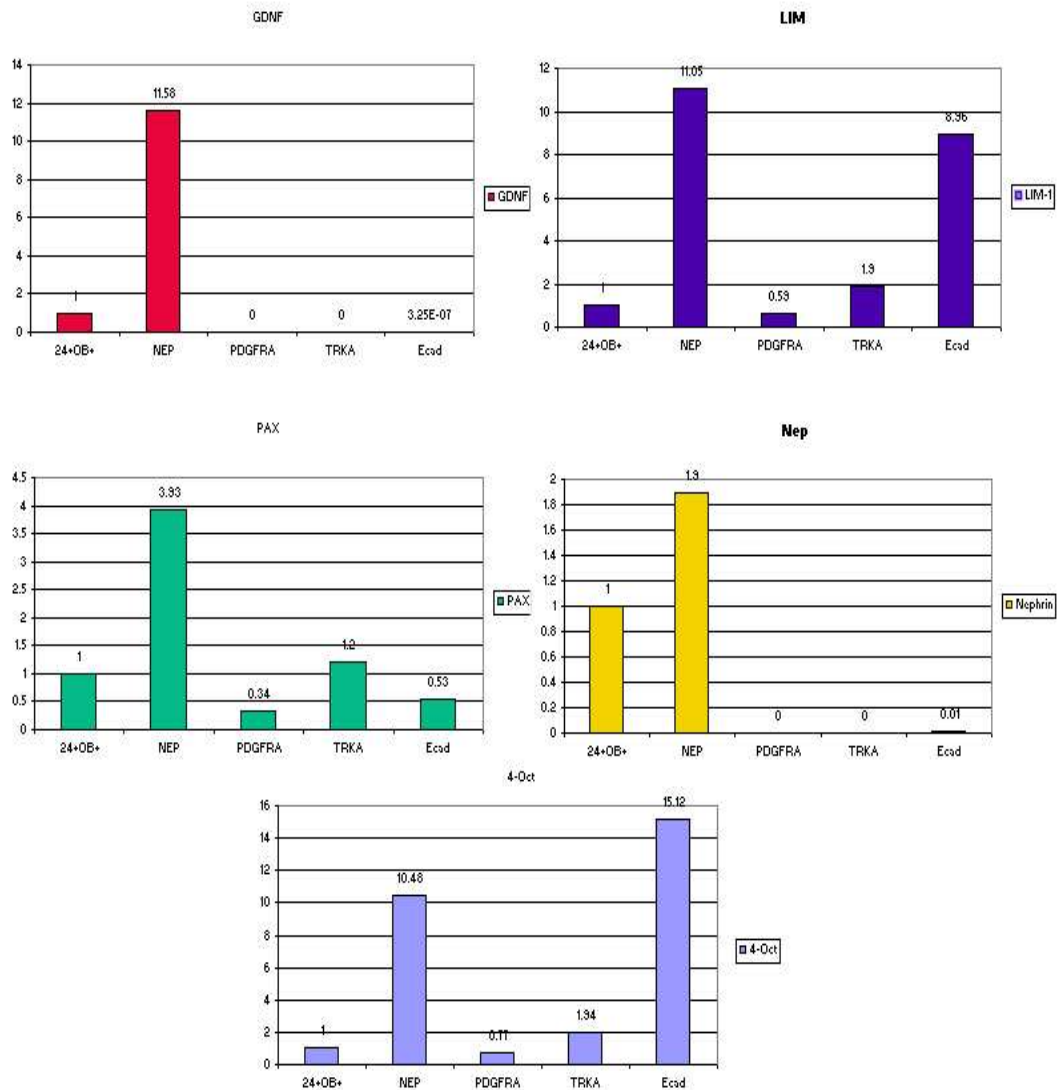


Figure 31 - Real Time PCR for AKPC populations. Expression of GDNF was found in the main population (AKPC) and in the Nephrin+ selection. LIM-1 was expressed by all the populations with a strong expression in Nephrin+ and E-Cadherin+ AKPC cells. PAX-2 was expressed highly by Nephrin+ cells but was present in all the selections. Nephrin was found expressed in the Nephrin population while OCT-4, highly expressed in Nephrin+ and E-Cadherin+ AKPC cells, was expressed broadly.

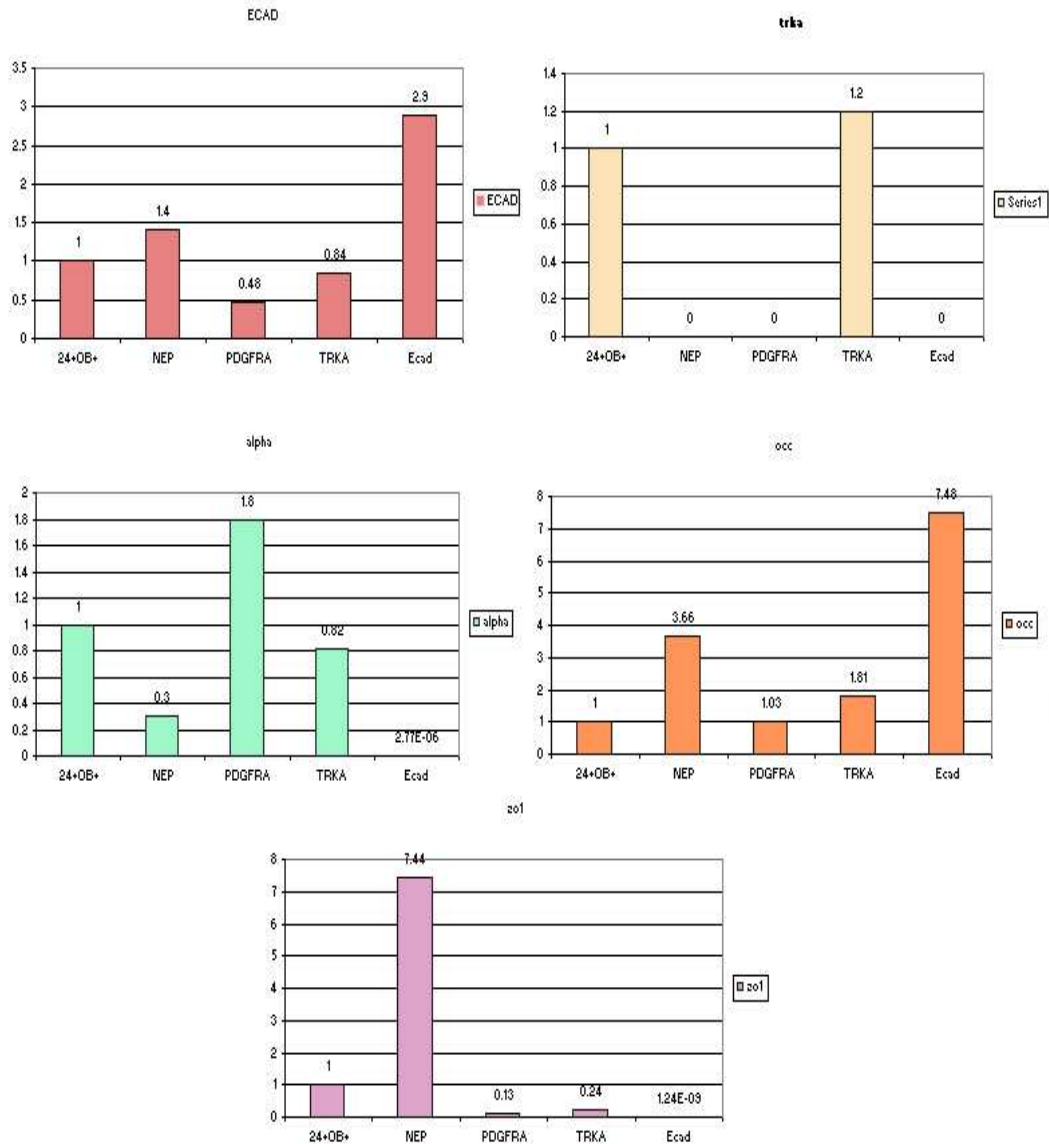


Figure 32-- Real Time PCR for AKPC populations. Expression of E-Cadherin was found in all the samples, indicating E-Cadherin as a marker not specific for MET cells. TrKA was expressed solely by TrKA+ AKPC cells. PDGFR Alpha was expressed strongly by PDGFR Alpha selection, underexpressed in Nephrin+ and TrKA cells and barely detectable in E-Cadherin+ cells. Occludin was highly expressed by E-Cadherin and in minor degree by Nephrin+ AKPC and was present in PDGFR Alpha+ and TrKA+ cells. ZO-1, molecule usually paired with nephrin within podocytes, was highly expressed in Nephrin+ selection and was barely expressed in the other populations.